AD_____

THREE-DIMENSIONAL COMPUTER GRAPHICS
BRAIN-MAPPING PROJECT

Annual/Final Report

Robert B. Livingston, M.D.

March 24, 1988

Supported by

U.S. ARMY MEDICAL RESEARCH AND DEVELOPMENT COMMAND
Fort Detrick, Frederick, Maryland 21701-5012

Contract No. DAMD17-86-C-6093

University of California, San Diego
La Jolla, CA 92093

Approved for public release; distribution unlimited.

The views, opinions and/or findings contained in this report
are those of the author and should not be construed as an
official Department of the Army position, policy or decision
unless so designated by other documentation.

REPORT DOCUMENTATION PAGE

Form Approved
OMB No 0704-0188
Exp. Date Jun 30, 1986

1a. REPORT SECURITY CLASSIFICATION	1b. RESTRICTIVE MARKINGS
Unclassified	

2a. SECURITY CLASSIFICATION AUTHORITY	3. DISTRIBUTION/AVAILABILITY OF REPORT
2b. DECLASSIFICATION/DOWNGRADING SCHEDULE	Approved for public release; distribution unlimited

4. PERFORMING ORGANIZATION REPORT NUMBER(S)	5. MONITORING ORGANIZATION REPORT NUMBER(S)

6a. NAME OF PERFORMING ORGANIZATION	6b. OFFICE SYMBOL (If applicable)	7a. NAME OF MONITORING ORGANIZATION
The University of California, San Diego		

6c. ADDRESS (City, State, and ZIP Code)	7b. ADDRESS (City, State, and ZIP Code)
La Jolla, California 92093	

8a. NAME OF FUNDING/SPONSORING ORGANIZATION US Army Medical Research & Development Command	8b. OFFICE SYMBOL (If applicable)	9. PROCUREMENT INSTRUMENT IDENTIFICATION NUMBER
		DAMD17-86-C-6093

8c. ADDRESS (City, State, and ZIP Code)	10. SOURCE OF FUNDING NUMBERS			
	PROGRAM ELEMENT NO.	PROJECT NO.	TASK NO.	WORK UNIT ACCESSION NO.
Fort Detrick, Frederick, Maryland 21701-5012				

11. TITLE (Include Security Classification)

(U) Three-Dimensional Computer Graphics Brain-Mapping Project

12. PERSONAL AUTHOR(S)
Robert B. Livingston, M.D.

13a. TYPE OF REPORT	13b. TIME COVERED	14. DATE OF REPORT (Year, Month, Day)	15. PAGE COUNT
Annual/Final	FROM 3/10/86 TO 12/24/87	1988 March 24	140

16. SUPPLEMENTARY NOTATION

Annual covers period of time March 10, 1987 – December 24, 1987

17.	COSATI CODES		18. SUBJECT TERMS (Continue on reverse if necessary and identify by block number)
FIELD	GROUP	SUB-GROUP	Keywords – Brain Mapping, Neuroanatomy, Computer Graphics.
			Image Processing, Data bases, anatomical models (AT)

19. ABSTRACT (Continue on reverse if necessary and identify by block number)

In response to the AMCRDC Broad Agency Announcement, we assembled a core group at UCSD and the Scripps Clinic and Research Foundation, which, together with participating national advisors, could solve problems that stand in the way of engaging computer graphics and database management more effectively in the solution of neurosciences problems. Labor-intensive, data-laden problems abound for image acquisition, image editing and manipulation, data storage and retrieval, 2-D and 3-D reconstructions, and the display and analysis of whole animal and human brains at microscopic levels of detail. We aimed at improving the interface between neuroanatomy and computer graphics systems so that the groundwork for accurate quantitative morphology will be satisfactory from the neurosciences viewpoint in proceeding to achieve whole brain reconstructions. We have succeeded in developing sound methods for preparing whole brains for sectioning and microscopic analysis, with controls for reducing brain distortions in three dimensions and for correcting the inevitable distortions that accompany slicing brain tissue at microscopic intervals, for combining structure/function data, and for beginning an analysis of whole brain tissue sections at microscopic levels of detail.

20. DISTRIBUTION/AVAILABILITY OF ABSTRACT	21. ABSTRACT SECURITY CLASSIFICATION
☐ UNCLASSIFIED/UNLIMITED ☒ SAME AS RPT ☐ DTIC USERS	Unclassified

22a. NAME OF RESPONSIBLE INDIVIDUAL	22b. TELEPHONE (Include Area Code)	22c. OFFICE SYMBOL
Mary Frances Bostian	301-663-7325	SGRD-RMI-S

DD FORM 1473, 84 MAR

83 APR edition may be used until exhausted.
All other editions are obsolete.

Table of Contents

DTIC
COPY
INSPECTED
6

on For

A&I

ed

ition

Distribution/

Availability Codes

Avail and/or

Dist   Special

A-1

4

INTRODUCTION

The central aim of the Brain Mapping Project is to con-
tribute to the solution of an exceedingly important and
refractory problem: how to go from a whole human brain to an
accurate computer graphics representation of its three
dimensional structure/function organization at microscopic
levels of detail.

To comprehend how human brains govern multi-factorial
processes like sensory processing, decision making, and
behavior, it is necessary to be able to analyze and to com-
pare brain structure/function relations in whole human
brains.

Brain structure and function are two sides of the same
coin. Yet little is known about brain structure/function
relations except piecemeal, in small-scale and scattered
circuits. Brain functions, however, are globally
integrated: this mandates integration of innumerable lower
order integrative processes.

"Mapping" the human brain is further complicated by the
fact that there are gross morphological differences among
individual human brains. Techniques such as we are develop-
ing are essential to begin acquiring normative data that can
reflect the range of differences in gross and microscopic
neuroanatomical form and function among so-called "normal"
individuals. Establishment of such a database requires
accurate mapping and comparison of a great many brains.
This is a technically and quantitatively formidable task for
which there presently exists no adequate conceptual frame-
work and no sufficiently competent hardware or software to
acquire, manipulate, display and analyze the necessary
images.

Whole human brain structure/function representations
have not been feasible heretofore because of the enormously
labor-intensive, computation-intensive requirements of the
task. There are five major challenges: (1) acquisition and
identification of data that are desirable for three dimen-
sional whole brain mapping; (2) intelligible and efficient
management of the massive amounts of data (measured in giga-
and tera-bytes) necessary to represent whole human brains at
microscopic levels of detail; (3) morphometric manipulations
necessary to de-deform microscopically thin whole brain tis-
sue sections--which are inevitably deformed in the process
of sectioning--to conform to their pre-sectioned form, and
to re-de-deform sequences of sectional images to conform to
three dimensional requirements, some of which are not deter-
minable two dimensionally; (4) display, comparison and
analysis of brain mapping data including statistical
analysis; (5) creation and maintenance of a widely sharable

neurosciences database that includes neuro-anatomy, -phy-
siology, -pharmacology, -pathology, -psychophysics and
-psychological correlates of normal and abnormal brain
organization.

The Brain Mapping Project addresses how to overcome to
a modest degree the first of these five challenges, while
paying due regard to the requirements imposed by the other
four challenges on the first.

INTRODUCTORY COMMENTS:
THE IMPORTANCE OF THREE-DIMENSIONAL COMPUTER
GRAPHICS DISPLAY AND ANALYSIS TO UNDERSTANDING
THE INTEGRATIVE ACTIONS OF THE HUMAN BRAIN

The purpose of this section is to present a few heuris-
tic reflections which argue that to understand integrative
action of the nervous system, the brain must be investigated
as a whole. The nervous system is continuously integrative
for the body as a whole. [Details of these reflections are
found in twelve chapters on Neurophysiology in Best and
Taylor's Physiological Basis of Medical Practice, Eleventh
Edition, edited by John B. West, pages 969-1312, 1985,
authored by the Principal Investigator.] If the reader is
already convinced, or wishes to sally forth without convic-
tion, he/she should proceed to the section called "Scope of
Work," which documents the ways in which the Brain Mapping
Project has responded to the detailed requirements of the
U.S. Army Medical Corps Research and Development Command
Contract DAMD17-86-C-6093. These "reflections" are entered
here because, if one isn't convinced of the urgent need to
examine structure/function relations of the nervous system
as-a-whole to be able to comprehend human perception, judg-
ment, and behavior, there is no need to make such an
extraordinarily difficult research and development effort.

The nervous system integrates visceral activity, cons-
ciousness, perception, memory and behavior. Remove any part
of the brain and the remainder continues pursuing overall
integration. When Sherrington wrote The Integrative Action
of the Nervous System, in 1906, in accordance with contem-
porary insight, he assumed that the nervous system is
informed by message passing, a cognate operation which, in a
Cartesian sense, can be disassembled and reassembled, like
clockwork parts. Although that view has a popular appeal,
it is more appropriate at present to consider motor and sen-
sory systems as functioning adaptively together as a coordi-
nated selective system in the pursuit of a dynamic integra-
tion of both short- and long-range central satisfactions.

The brain uses massive parallel processing, "degen-
erate" mapping of body parts on brain parts, and mapping of

environmental features and events on brain parts via body
parts. Degenerate refers to structurally/functionally abun-
dantly overlapping processes, functionally closely
equivalent, but neither structurally nor functionally
strictly redundant.

Central responses to external objects and events pass
via parallel channels to multiple internal mappings, and
these communicate reentrantly with one another. This organ-
izes what Edelman (1987) calls "global maps," that
interweave central combinations of endowed and acquired
capabilities. Global maps, according to Edelman provide
continuous dynamic programs which integrate and govern
experience and performance. Both perception and behavior
are thus creative functions, destined to follow internal
needs. Furthermore, the shaping of brain maps is mainly by
population selection. Various mapping systems: motor,
sensori-motor, sensory, limbic, etc., connect reentrantly
with other mapping systems, including what are thought of as
association areas, often reciprocally, back and forth,
establishing reentrant mapping which provides for a global
or gestalt organization of brain functions.

Initial mapping as well as reentrant mapping is capable
of considerable adjustment when the body changes or when
presumably corresponding maps get out of alignment. Global
mapping appears to facilitate perceptual generalization and
categorization and may be fundamental to conventional learn-
ing.

Selection of secondary repertoires is based on sys-
tematic conditioning of partially overlapping large domains
of synaptic populations. On this foundation, conventional
learning and social interactions are organized. Social
interactions contribute to information processing which
enhances conventional learning and possesses the advantage
of social transmission.

To comprehend integrative actions of the human brain
adequately, we need access to accurate three-dimensional
computer graphics display and analysis of whole brains.
Adult brains exhibit extraordinary variations at gross as
well as microscopic levels of detail. Relatively surprising
is the extent of variation in gross morphology; anyone who
teaches a course in gross neuroanatomy can vouch for this
observation. We tend to assume more uniformity in gross
neuroanatomy than our experience actually warrants because
of the repetition of diagrammatic images carried over from
the nineteenth century, and also because our observations
during dissection and surgery are ordinarily both partial
and non-quantitative. Quantitative neuroanatomical analysis
is ordinarily confined to small tissue blocks which are
dislocated from overall organization of the brain.

We have sliced at microscopically thin intervals and carefully reviewed serial cinemorphology sequences through more than seventy whole human brains. We found each brain to be unique at the level of gross neuroanatomy. There are major differences in gyral formations on the surfaces of each hemisphere, including multiple asymmetries between the two hemispheres in addition to those identified recently by Geshwind and Levitsky (1968) and Gazzaniga (1970) in areas of speech and language representation.

There are also conspicuous differences and asymmetries in the dimensions of subcortical structures, in the gross morphology of thalamus, hypothalamus, basal ganglia and cortical and subcortical organization of the cerebellum. These are not trifling differences but range in scale among individual anatomical parts from ten to a hundred percent of volumes, and manifest distinctiveness in shapes that enable easy familiarity in specimen recognition: "This is the brain with a relatively squared-off thalamus, not so smoothly rounded as as in most other brains;" "This is the brain with a two-to-one L/R asymmetry in volumes of heads of the caudate;" "This is the brain with extraordinarily large dentate nuclei in the cerebellum;" etc.

In a 28-minute composite motion picture film, produced in 1976, The Human Brain: A Dynamic View of Its Structures and Organization, we demonstrated gross neuroanatomical differences in seven of these specimens and showed one specimen in its entire cinemorphology sequence. Images of that specimen were then employed in the creation of a dynamic three-dimensional computer graphic display which exhibited twenty neuroanatomical structures moving in their correct relative orientations in three-space, and portrayed their participation in different composite functional systems.

From these experiences we became convinced that development of a "normative data bank" for gross human brain neuroanatomy will require very sophisticated specimen selection, slicing, imaging, digitizing, and quantitative morphometric and statistical analysis. We have no notion which of the seventy human brains we have sliced or what kind of an amalgam of them might be suitable to establish a "standard human brain" although several groups have used our morphological data as their standard for PET-scanning localization, and other purposes.

In the past couple of decades it has become possible to "map" neural circuits that have distinctive neurotransmitter patterns. Some neurons utilize more than one neurotransmitter and some exhibit changes in neurotransmitter during the course of development.

Some neurotransmitter-specific circuits have been

identified with certain disease categories--parkinsonism,
schizophrenia, Alzheimer's disease, manic-depressive disord-
ers, tardive dyskinesia, etc. They have been associated
with dopamine, norepinephrine, serotonin, enkephalin and
other naturally-occurring opioid products, and a large
number of distinctive oligopeptides. Certain behavior pat-
terns have also been identified with monoamine transmitters
and modulators: exploratory pursuit (dopamine), active
avoidance (serotonin), resistance to extinction (norep-
inephrine), and the like. Many of these circuits are dis-
tinctively and diversely far-reaching and complicated in
their distributions. Obviously, neuropharmacological pat-
terns are likewise neuroanatomically specifically and ela-
borately distributed.

Finally, neurological studies find, for example, that
such phenomena as directed attention and unilateral neglect
have multiple, distributed, interdependent functional local-
izations. Mesulam (1981) observed that unilateral neglect
reflects disturbances in the spatial distribution of
directed attention. Four cerebral regions constitute an
integrated network for the guidance of directed attention
into extrapersonal space: a frontal component coordinates
motor programs for bodily and gestural exploration, and for
eye-scanning and fixation; a posterior parietal component
provides an internal sensory map and apparently varies the
dimensions of the map for specific portions of the external
world; a reticular component generates the level of arousal
and vigilance; and a limbic component in the cingulate gyrus
conveys motivational valence. Lesions in only one locality
in this network yield partial unilateral neglect syndromes.
There is asymmetry here, too, in that unilateral neglect
syndromes are more frequent and severe following disorders
in the right hemisphere.

It is therefore becoming increasingly obvious that the
nervous system needs to be examined, structurally and func-
tionally, in its entirety. The interdependence of parts and
functions cannot be adequately appreciated unless there is
knowledge of the relative dimensions, specific connections,
neurotransmitters and other agents which exist in relation-
ship with one another in terms of feed-back, feed-forward,
reciprocity and linked sequential circuitry.

The Importance of a Comprehensive Neurosciences Database

Assuming that a normative database is established for
display and analysis of the human brain at, say, 40 microns
cubic resolution, and similar standards are created for com-
mon laboratory animals, then the structure/function data
from a wide variety of laboratory and clinical research
sources can be evaluated and introduced into the maps, or
filed with reference to specific 3-D parts of established

whole brain maps. By such means, structure/function rela-
tions can be accumulated and assembled in relation to whole
brain maps in a disciplined and instructive fashion.

Not everyone would need to have the sophisticated
equipment necessary to acquire whole brain maps at micros-
copic levels of detail. Rather, optical discs could be used
to transport three-dimensional maps and "standard atlases"
to practically all neuroscientists.   This would encourage
collaborative sharing of data, accelerate the accumulation
of structure-function-literature correlations and documenta-
tion, and improve the teaching of neuroanatomy and the
application of three-dimensional computer graphics data for
display and analysis.   By this means, data could be made
available to clinical neurosciences research and patient
care.   This will be useful for controlling spatial localiza-
tion and comparing normal parameters in a variety of scan-
ning procedures and will contribute to both research and
clinical neuroanatomical interpretations.

There is no question that it is highly desirable to
pool information on neurotransmitters, connectivity, electr-
ical phenomena and morphological plasticity in adequate
recognition of the great amount of high quality work that is
being accumulated.   In significant respects three-
dimensional graphics will contribute to a database that is
complementary and supplementary to other forms of neurosci-
ences communication and sharing.

BACKGROUND REFERENCES CITED IN INTRODUCTION

Edelman, Gerald M., Neural Darwinism: The theory of neuronal
group selection, New York, Basic Books, 1987.

Gazzaniga, M., The Bisected Brain, New York, Appleton-
Century-Crofts, 1970.

Geschwind, N. and W. Levitsky, Human brain; left-right asym-
metries in temporal speech region, Science 161: 186-187,
1968.

Mesulam, M-M. A cortical network for directed attention and
unilateral neglect, Annals Neurol., 10:

Sherrington, Charles, The integrative action of the nervous
system, New York, Charles Scribner, 1906.

*   *   *

RATIONALE, EXPERIMENTAL METHODS, RESULTS, AND DISCUSSION
FOLLOW SECTION-BY-SECTION IN THE "SCOPE OF WORK"

S C O P E   O F   W O R K

1.   DEVELOP AND IMPROVE BRAIN MAPPING TECHNOLOGY/METHODOLOGY

Between 1967 and 1976, UCSD developed Cinemorphology. This involves photography, in registration, of each successive surface of whole human brains sectioned at microscopically thin intervals. Qualitative examination of seventy such Cinemorphology sequences, all from "normal" adult brains, showed each of them to be unique. They differed conspicuously one from another in various gross neuroanatomical components. Neurosciences peeked into a box labeled "Endophrenology."

In 1975-76, one of these brains was hand digitized. It was then reconstructed three dimensionally, using an Evans and Sutherland Picture System 2. This provided a dynamic three dimensional display of the whole brain. The digitization had to be done by hand, however, and therefore the three dimensional reconstruction was achievable only at macroscopic z-level intervals (1.1mm).

To permit the analysis of enough brains in enough detail to answer interesting scientific questions, it is necessary to overcome the time and labor consumed by hand digitization. There is no existing alternative to developing efficient systems for image acquisition, three dimensional reconstruction, and computer graphics display and analysis.

We are convinced that within a few years computer graphics technology directed toward this goal will prove tremendously powerful as well as labor-saving. Computers will bring new objectivity and sharability to neuroanatomical interpretations. They will also enable database developments that combine structure/function and source information. This will revolutionize the quality and applicability of neurosciences research. Of course, similar computer techniques for combining structure/function/information can be applied to all of biology. New analytic and synthetic power will become available for the investigation of evolution, development and disease.

We believe three dimensional reconstruction of whole brains must conform as closely as possible to the three-space organization of the same brains when they were functionally intact. With support through this Contract, we developed innovative methods for preparing rat, monkey and human brains and tissues: they provide (1) accurate spatial integrity for whole brain 3-D reconstruction, and (2) specific localization of structure/function relations.

The Brain Mapping Project (BMP) organized collaboration between UCSD and the Scripps Clinic and Research Foundation (SCRF), with the latter group operating under the leadership of Floyd E. Bloom.

The BMP benefitted greatly from scheduled contributions in La Jolla and continuing remote consultations by three National Co-Directors: Dean Hillman from New York University; Larry Stensaas from the University of Utah; and Arthur Toga formerly from Washington University at Saint Louis, now from UCLA; and by a European Consultant, Wolfgang Rauschning from the University of Uppsala.

The BMP also gratefully appreciates the engineering and computer science advice provided at the beginning of the Project by Wesley Clark, BMP's "Dutch Uncle Engineer" from New York City, and Jerome Cox and Charles Molnar, both from Washington University at Saint Louis. They provided extremely cogent advice during the period when the Army was asking UCSD to lead a national program to construct a prototype computer system within four years that is capable of mapping in three dimensions and displaying the entire human brain at microscopic levels of detail. When that prospect was abandoned by the Army, the need for organizing engineering and computer science talent relaxed in urgency.

The BMP hosted a four-day National Task Definition Workshop which assembled experts in fields of computer science, engineering, database management and neurosciences (See List of Workshop Participants in Appendix A). The Workshop evaluated technical opportunities and provided guidelines for a collaborative, multi-university National Brain Mapping Program.

This "Final Report" describes BMP considerations relating to acquisition of equipment, research and development in quantitative morphology, and systematic fulfillment of the four-part "Scope of Work" required under Contract with the U.S. Army Medical Corps Research and Development Command. The Report is also written with the objective of specifying some of the most important brain mapping contributions, for the benefit of future brain mapping enterprise.

The BMP wishes to express very sincere appreciation for the generous support of the U.S. Army Medical Corps Research and Development Command, and particularly for the thoughtful personal attention given the BMP by many Officers and Staff of the USAMCRDC.

13

1.1. Improve Accuracy and Speed of Histological Data Acquisition

(a) Computer-Assisted Cryomicrotomy and Registration Control Image Acquisition

(i) Selection of Major Items of Equipment

Criteria for selection of major items of equipment have been identified in Quarterly Reports. Here we consider equipment selection in the context of contributions to general strategies for brain mapping.

For computing purposes we selected two DEC VAXstation II/GPX Graphics Workstations composed of a MicroVax II processor and advanced graphics capabilities. A medical student, Sheldon Furst, who had installed DEC equipment professionally, skillfully organized the BMP computing environment. This enabled double team pursuits in parallel at SCRF and UCSD, for image acquisition, software development, and neurohistological analysis. The two systems were linked telephonically to support complementary research activities being pursued simultaneously by investigators working in separate buildings. Similar networking could be used on a larger scale for national coordination of collaborative brain mapping progress.

Warren Young and Phil Mercurio analyzed four image acquisition hardware-software systems, including Kontron/Zeiss IBAS 2; Gould IP 8500; Recognition Concepts Trapix 5500; and MegaVision 1024 XM. Discussions were held with high-level technical personnel from each vendor and hands-on experience was obtained. MegaVision was selected as the system within our price range best qualified for brain mapping purposes.

MegaVision systems under control of MicroVAXes were installed for brain mapping purposes in the two settings. The MegaVision at SCRF is primarily engaged in localization of specifically labeled neurotransmitters and other functionally significant brain components in the three-space of monkey brains. The MegaVision at UCSD is primarily engaged in image acquisition of Registration Control Images (RCIs) from the surface of brain blocks, and in two dimensional reconstruction of whole tissue section composite images obtained by means of a new Tissue Section Image Microscope, the TSI Microscope.

We estimated the comparative accuracy and speed of several data acquisition instruments and components. These included film and digital cameras for image acquisition through microscope columns, for imaging the cut surface of whole brain blocks, and for imaging neuroanatomical slides on light boxes. Don McEachron at Drexel University

established criteria for testing cameras, helped in the selection of types of cameras and tested specifications and performance of the Circon CCD camera and MegaVision vidicon-type camera utilized in the Project.

We compared and analyzed equipment specifications and tested other hardware including different assemblies of microtomes, cameras, microscopes, stages, condensors, nose-pieces, drawing tubes, oculars, objectives, optical filters, image intensifiers, fluorescent and other light sources, etc.

Harvey Karten, John Morrison, and Charles Wurtz con-scientiously investigated designs and specifications, ran tests and selected three research microscopes. These reflect a conscientious BMP effort to establish neurological structure/function relations and to acquire digital images for quantitative two and three dimensional brain mapping.

A Zeiss Axiophot Widefield Research Microscope, with a Maerzhauser computer-driven stage, mainly for BMP research by John Morrison, Floyd Bloom, Warren Young and their col-leagues, has been devoted to quantitative three dimensional brain tissue mapping of neurotransmitters such as somatosta-tin, substance p, dopamine, norepinephrine, and other impor-tant stereospecific molecules in monkey cortex. These stu-dies have been made possible by the use of EMMA, a powerful software development by Warren Young that enables efficient computer-aided quantitative morphological display and analysis.

A Leitz Orthoplan II Microscope, including equipment for epifluorescence, with Nomarski optics and a Maerzhauser stage, modified for visualization with three different fluorescent module cubes, interchangeable stages, a video port and microdensitometry, has been utilized by Harvey Kar-ten and his colleagues for quantitative spatial analysis of the architecture and biochemical diversity of cell popula-tions in the retina--the most accessible part of the brain.

This microscope is equipped with an OPELCO image inten-sifier which permits the examination of single tissue sec-tions stained with three different fluorophores. The output of the image intensifier is captured by means of a CCD Cohu solid state camera, and the image is directly copied onto a Mitsubishi video copy processor, permitting the acquisition of images rapidly enough to prevent loss of data due to decay of fluorescent sources in the tissue. Alternatively, the image can be piped to a microcomputer which has a dedi-cated frame grabber for digital image processing. This allows Karten and his colleagues to capture alternative images showing the pattern of receptor staining for each fluorophore. From this, clarification of the relationships between cholinergic amacrine cells in the retina and neurons

15

which contain nicotinic acetylcholine receptors was esta-
blished.

A Tissue Section Imaging Microscope (TSI Microscope)
was designed by Charles Wurtz in collaboration with William
McBain of Pacific Precision Laboratories (See Figure 1b).
The TSI Microscope presents a very large computer-driven
stage for "mosaic mapping" or "strip mapping" of whole brain
tissue sections. Images are acquired in strips or squares
and composed into a single large synthetic image which com-
bines the strips or squares in exact order so as to create a
large synthetic image that combines the strips or squares
into a "seamless" image of large regions or the entirety of
whole brain tissue sections. Computer control of camera and
stage allows for either "strip map" or "mosaic map" options.

Mark Shin wrote an easy mosaic program that permits
automatic TSI acquisition and reconstitution for 2x, 4x, 10x
and 20x magnifications to secure synthetic images up to 16
Mb in detail. This permits whole rat brain TSIs to be
obtained at each of the three lower magnifications. The
images are stored in memory with indicators of where they
fit into the magnified, reconstituted TSI.

Compression of the synthetic TSI images is necessary
for display of the images on limited graphics systems. This
technology can be expanded with larger memory and more
powerful graphics management computers and it promises to
provide a radically new opportunity for neurohistological
study. When robust warping machines become available, the
large synthetic TSI can be subjected to automatic de-
deformation to compel the inevitably distorted thin tissue
section to conform to the registration control image (RCI).

(ii) Research for Registration Control Imaging

It was necessary to establish a system for obtaining
Registration Control Images (RCIs) from each successive cut
surface of whole brain blocks undergoing serial sectioning.
The LKB giant cryomicrotome was selected as the most rugged,
accurate and and versatile programmable microtome (See Fig-
ure 1a). The MegaVision system was installed and software
programs were designed expressly to facilitate imaging the
cut surface of whole brain blocks.

A scaffold was built to fasten the MegaVision vidicon-
type camera joined to a Tamron 70-210mm macro-zoom lens and
special Examatron lamps in a precisely fixed relationship to
the angle and distance of the cutting plane of the microtome
(See Figure 2). The scaffolding was mounted on the pillars
on which the microtome knife is supported so that as the
knife descends the camera and lights maintain an exact and
fixed relationship to the block surface. Cynthia Lemere
constructed a tailored black shroud to protect the specimen

surface from spurious light reflections within the cryomicrotome. Spectral sensitivity of the cameras was tested carefully before their selection and tested again in situ in the environment of image acquisition (See Figure 3).

Whole rat brains, perfused, stained and embedded in CMC by Lemere, destined for acquisition of RCIs, were sectioned in the LKB cryomicrotome at -30°C with a 35° angle to the knife. Section thickness was 5μm, with RCIs acquired at 40μm intervals. Later, methylene blue-stained albumin-gelatin embedded rat brains were used for RCI acquisition and for extensive operator experience with tissue section removal. These brains were sectioned at -10°C with a lower knife angle setting. Section thickness was 50μm, with RCIs acquired at 200μm intervals. The cutting was smoother and the tissue section integrity was better with the second set of sectioning parameters.

(b) MegaVision Image Acquisition, Editing, Contouring, and Storage

Sectioning and image acquisition software created and adapted to the MegaVision by Warren Young is called SLICE. This software package provides an easy interface for users operating the MegaVision system under UNIX control. Commands are specific to RCI acquisition (See Figure 4).

Version I of SLICE provided a primitive repertoire for image processing and proved successful for acquisition of images from the blockface at selected intervals during automatic cryomicrotome slicing. Version I was used to develop and refine procedures and it provided the first computer-aided automatic acquisition of digitized blockface images. SLICE was also important as a test for μMIPS, showing that μMIPS has been designed by Warren Young and Mark Shin so that innovative applications can be easily and flexibly constructed to enable progress toward specialized image processing objectives.**

**Footnote: μMIPS refers to UNIX Multiuser Image Processing Software. μMIPS constitutes a series of command programs designed to control the image processing environment, including any number of users or 1024XM (MegaVision) systems, and the Maerzhauser stage on any number of microscopes. μMIPS is implemented as an applications software and is now implemented on three separate operations contexts. The programs are UNIX-based, therefore highly flexible and callable from nearly any level of the UNIX software hierarchy. The internal structuring of the programs is written so that embellishments do not involve extensive rewriting of the code.

SLICE now includes methods for automatic filenaming of images, automatic correction of non-uniform shading across the image field, and automatic processing of images through a variety of user-selected sequences available through the MegaVision system.

Analysis of blockface images (RCIs) and Tissue Section Images (TSIs) is achieved by a series of routines called MAPPER. The MAPPER sequence represents a cascade of procedures to generate boundary contours from gray level digitized images. Contours consist of coordinates that characterize a series of linked points having vector dimensions that are defined according to the gray level values of neighboring points. Contours can be labeled to identify a set of coordinates that circumscribe any relatively differentiable object in a given section.

The sequence of MAPPER operations uses MegaVision routines to optimize contrast in the image and then define the edges (See Figure 5). One of first operations subtracts an image of the background taken without the specimen. This eliminates some unevenness of illumination inherent in the cryomicrotome environment. The process includes image normalization which reschedules density values from low contrast images so that they can span the full 256 gray level range.

Once the blockface image has been normalized, edge detection and thresholding routines are run. The threshold is then mapped to a binary overlay channel to compare threshold level with boundaries of structures represented in the image. MAPPER offers an option which allows editing of the image after thresholding and before contouring.

An edge detector is applied to the binary image to generate a set of vectors that characterize the boundary. This edge follower tracks the boundary from an arbitrarily selected point to extract a serial set of pixel coordinates that comprise the contour (See Figure 6).

(c) Additional Specialized Software Developments
for Contouring Neurohistological Structures

Our goal is to design and implement edge-detection and boundary extraction software that will define contours that have substantial neuroanatomical interest, among the subtle and confusing patterns reflected from the cut surfaces of whole brain blocks, and as seen by TSI Microscope transmission through tissue sections.

We find that with present histological and software techniques, there is precious little neuroanatomical material that is amenable to "unambiguous contouring." Not surprisingly, as has been learned through studies of

18

artificial intelligence, some things that seem incredibly obvious to human observers are loaded with ambiguities when it comes to machine segmentation. An old "Rule for Schedul- ing Software Development" has been reinforced: "No matter how long it is predicted that software development will require, it will actually take twice that long."

MAPPER contouring remains to date the most applicable software. BRAINMATE was developed at UCSD by Donal Hurley, of Ireland. It is specialized for neuroanatomical tissue analysis and is based on CELLMATE, developed earlier by Hur- ley at New York University, under the guidance of Dean Hill- man. CELLMATE enables an operator to contour neurons for two and three dimensional reconstructions. BRAINMATE enables an operator to trace neuroanatomical boundaries onto the digital image of a tissue section. BRAINMATE is also employed for correcting and amending machine-generated con- tours.

A number of innovative approaches to the software extraction of image boundaries have been undertaken and vigorously explored and improved during the period of the Contract. Developments in boundary detection software include a series of novel and evolving algorithms known as ROTATING BAR, FACET-MODEL, HARALICK, and CONTOUR FOLLOWER. Shankar Chatterjee provided considerable understanding of the art of computer graphics image interpretation and gen- eral guidance for these software developments.

Detection of subtle neuroanatomical boundaries within widely variable pixel densities manifested in digital images of whole brain blockfaces remains a profoundly difficult image analysis problem. A roughly approximated rapid edge- detection and boundary generation program is available in the standard software provided by MegaVision. However, it suffers from many inaccuracies and inadequacies and is not robust against laboratory actualities, including factors such as non-uniform illumination across the image field and electrically noisy circumstances that accompany image col- lection.

ROTATING BAR and FACET-MODEL are edge detectors that use local intensity derivatives to discover edges, assuming that an edge is nothing more than a chain of relatively con- sistent local variations in pixel intensity (See Figure 7). Both algorithms are implemented in C language under the MicroVax UNIX operating system. Both algorithms generate an "edgel" file that contains edge magnitudes and edge direc- tions for each pixel in the image. This information is then used by an "intelligent" CONTOUR FOLLOWER to produce a con- tour file in vector format, where the contour lists are described in terms of three spatial values.

The main design problem in CONTOUR FOLLOWER is the

successor function, which at any given point along the con-
tour selects the function that is most likely to prolong an
existing contour. The choice is guided by the magnitude and
direction associated with each edge pixel, and by such
parameters as the look-ahead depth, tolerance in direction,
and closest permitted distance to neighboring contour data.

Work is currently in progress to design a refined
edge-detector (single pixel-width edges) that will detect
all points on the boundary accurately and pass them to a 3-D
graphics routine which will generate the three dimensional
reconstruction display. We are continuing research on
edge-detection algorithms that will be sufficiently robust
to detect edges within both high and low contrast gray level
ranges.

(d) Three Dimensional Reconstructions From Registration
Control Images

Registration Control Images (RCIs) are images taken
from the cut surface of a brain block. They are images of
the as yet undistorted plane of the tissue section which is
the next one to be removed by the cryomicrotome. Since the
microtome considerably deforms the microscopically thin tis-
sue section during the process of cutting, it is necessary
to have a corresponding Registration Control Image (RCI) for
de-deforming the synthetic image made from the distorted
thin tissue section, the Tissue Section Image (TSI).

RCIs do not have much blockface contrast and the gray
levels do not contrast sufficiently for sharp digital image
analysis. Nevertheless, they do contain considerable infor-
mation, enough to be able to define a number of landmarks,
which are then used as an RCI "x, y, Truth Base" to which
homologous landmarks on the TSI are to be matched as the
basis for guiding the algorithm for de-deformation of the
TSI. Methods for both RCIs and TSIs must be pushed to the
optimum for locating and circumscribing data that are of
interest and value to the population of neuroscientists,
neuroanatomists, neurophysiologists, neuropharmacologists,
neuropathologists, and clinicians.

The RCIs, taken off the block surface, as they are now,
are rich and reliable enough in data to enable contouring of
the whole brain for purposes of creating a wireframe
"atlas." The same information can be used, with CONTOUR
VIEW, developed in Philadelphia by Anthony Reynolds, and
specifically adapted by him to run on our system with our
data, to display solid surfaced, shaded images. See Figure
8 for examples of three dimensional wireframe reconstruc-
tions and solid surface renderings.

(e) Three Dimensional Reconstructions from Tissue
Section Images

20

Many neuroscientists would like to obtain a robust software package that requires minimal specialized operator discrimination in the course of mapping whole brain tissue sections. They would then like to create three dimensional reconstructions from such stacked tissue section maps. Such software does not exist, but its potentialities are implicate in the three dimensional reconstruction that has been accomplished from tissue sections by Larry Stensaas. Using serial sections selected by him as the best in the Yakovlev Collection at the Armed Forces Institute of Pathology, Stensaas has personally invested the extraordinary time and effort to discriminate neuroanatomical structures, section-by-section, throughout the brain stem and telencephalon, exclusive of neocortex (See Appendix B for a list of the names of neuroanatomical structures identified and contoured by Stensaas). This means that Stensaas has differentiated almost all the important structures in the whole brain, by hand. More information on Stensass' contribution is presented later in this report.

This is exactly what is hoped can be accomplished in the near future automatically or semi-automatically with the aid of TSI-Microscope-like computer systems. Such software must be adaptable to a wide variety of types of neurological tissues and exotic stain applications (including molecularly stereospecific labels, fluorescent [i.e., transient duration] antibody markers, radioactive tracers to be identified in photographic plates, etc.).

Explicit expectations were expressed during the Task Definition Workshop relating to special kinds of software that could be developed for computer-aided microscopic analysis of neuroanatomical tissues. This expectation includes being able to detect and localize in x, y, z, coordinates, and count specialized neurons, characterize them by class iconically, trace neuroanatomical structural boundaries, and distinguish the borders among different cytoarchitectural regions of cortex.

(f) Comparison Between Registration Control Images (RCIs) and Tissue Section Images (TSIs)

It is essential for purpose of accurate three dimensional whole brain reconstructions, that we compare RCIs, obtained from the blockface, which are taken to be TRUTH Images, with TSIs, obtained as composite mosaics through the TSI Microscope. The two images need to be compared for purposes of correction of deformations that occur to the thin tissue sections during microtomy. Homologous landmarks are located in each image; the RCI landmarks are considered to be undeformed, hence the TSI landmarks must be made to conform to the RCI landmarks. This is necessary for two dimensional "de-deformation" of the TSIs.

21

Even after all the TSIs have been de-deformed in this way, to compell conformation among as many landmarks as can reasonably be identified in the corresponding RCI/TSI pairs, there will still remain three dimensional deformations which will be evident only when the TSIs are assembled into some measure of z-depth tissue or brain reconstruction. Therefore, it is necessary to identify the individually discrepant TSIs and to "re-de-deform" them iteratively, until the entire three dimensional reconstruction is clearly correctly aligned. The re-de-deformation of each discrepant TSI must always be referred for its re-alignment to the corresponding RCI.

For the purpose of both (2-D) de-deformation and (3-D) re-de-deformation, it is essential that the two images (RCI and TSI) overlie one another in a display so that each of the images can be presented independently, in different colors, and that they also can be separately "blinked" on demand. To make a reasonably accurate two dimensional correction, it must be possible to identify a sufficient number of homologous landmarks that can be located on both images. [Although we refer to them as homologous landmarks, they are really the same landmarks, the TSI landmarks being more or less displaced.] The TSI landmarks must be differentially deformable with linear extrapolations among the landmarks in order to match the homologous landmarks of the corresponding RCIs. Then they must be checked visually, by image overlay, for satisfaction of correspondence of the entire TSI to the RCI. Both images need to be examined and the TSIs de-deformed on a high resolution monitor that is not troubled by weak sensors, electric overload, non-linearity, and that shows comparatively little flare.

It is generally agreed that information obtained from the cut surface of a block, the RCIs, aided by prior perfusion of coloring material, should be as detailed as single frame imaging can provide. Our methodological research suggests that in continuation of the Brain Mapping Project we may want to convert RCI acquisition to photographic camera images which can document at least an order of magnitude more information than is presently obtainable by digital systems. RCI information is so desirable and useful that we will probably eventually forego digital imaging of RCIs in favor of large format, fine-grained color photography. Exactly this, in fact, was advocated from the beginning by our Swedish Consultant, Wolfgang Rauschning, who has considerably improved images obtainable for Cinemorphology by introducing superior photography. Photographic images provide an abundance of fiduciary information for comparison purposes in the processes of de-deformation and re-de-deformation of TSIs. Finally, photographic images are familiar and reassuring. They can easily be preserved indefinitely to serve as a stable reference and registration control series for each brain. There may be a further

advantage in being able to have smooth-flowing Cinemorphol-
ogy images of the same brain, to supplement its three dimen-
sional computer graphics reconstruction.

The saving grace is that RCIs themselves are never to
be de-deformed: there is therefore no requirement that they
be digitized. We have shown that digital images can be com-
pared to photographic RCIs by projection means, and homolo-
gous landmarks can be identified on both images and speci-
fied in x, y, space in the RCIs for definition of the
required 2-D de-deformation of the corresponding TSIs.

TSI images can be de-deformed and re-de-deformed as
much as may be required to complete a satisfactory three
dimensional whole brain reconstruction. Note: Reference
control must always be made back to the original RCIs. The
tissue section, of course, has been obtained from that par-
ticular anatomical plane, although, depending on translu-
cency of the specimen, the RCI will detect some structures
that may be discernible beneath the thickness of the tissue
section.

It is our considered opinion that the TSI images should
be as highly detailed as TSI microscopy allows. At the Task
Definition Workshop, Bud Tribble III suggested that 8 bits
per pixel is not enough. He recommended 12, or better, 16
bits. Three colors are considered to be useful and Bud
thought that additional colors, including UV might prove to
have discriminative advantages in the analysis of histologi-
cal materials.

It may prove advantageous also to capture an image of
each TSI before it is stained. We planned for this but
couldn't afford the design and construction of the necessary
low-distortion Macroscope.   That image would be visually
more akin to the corresponding RCI and therefore it is
likely to be especially useful in identifying homologous
landmarks.

An appropriate de-deformation algorithm to make the TSI
match the corresponding RCI would be applied to such image
pairs, (or triplets, if simultaneous comparison with the
unstained section is desired).   TSI images in deformable
format must be preserved long enough to be helpful in the
conduct of 3-D re-de-deformation.   Ultimate three-
dimensional re-de-deformation (to accommodate displacements
visible on 3-D which may not be detected on 2-D) await algo-
rithm developments intended by Fred Bookstein.

At the BMP Innsbrook meeting it was decided that for a
minimum scale rat brain "atlas" 512 x 512 pixels would be
sufficient information for 3-D reconstruction purposes.
Functional data obtained from other sources at higher mag-
nifications e.g., from specially stained sections in another

23

laboratory--intended to be added to the correct three-space of the "atlas," could be readily compressed to conform to the dimensions of the remainder of the "atlas."

(g) Cameras on Microscopes

2048 x 2048 video CCD MOS solid state well-tested cameras appear to be a reasonable future choice for TSI Microscopy. The TSI requirement is to be able to define boundaries, locate cell clusters, fiber tracts, boundaries between fiber tracts, etc., to outline and envelope anatomical objects, and to assemble these objects in 3-D reconstructions at microscopic levels of detail.

Bob Nathan advocated Perk and Elmer systems which have microscopes with a built-in halogen light source and 3-color filters. They can do 10"x10" scans to within 5 microns, thus providing considerable geometric fidelity plus pixel depths with multiple spectra. Unfortunately, these systems are extremely slow for whole human brain reconstructions. They would require about 6 hours to render an image of one human brain section, i.e., 36,000 hours to scan the 6,000 sections needed to represent a whole human brain by its least thick axis--in horizontal sections. Moreover, they cost $0.25 million. Their speed is to be compared with 1/8 seconds for Iconics, pixel by pixel analysis, i.e., needing a few minutes to scan a whole human brain section. Optimally, TSIs need microscopic magnification to permit resolution into the few micron range. For such resolution, human TSIs will probably require laser scanners operating at 1000 lines/inch.

1.2. Develop Methods for the Computer-Aided Acquisition of Tissue Images

(a) The Tissue Section Image Microscope

High quality digital Tissue Section Images (TSIs) are required in order to be able to de-deform tissue two-dimensionally to conform to the undistorted reference images taken from the cut surface of the block, the RCIs. Charles Wurtz worked out the design and had constructed a Tissue Section Image (TSI) Microscope. It arrived only a few days before the end of the Contract. Nevertheless, it has now been put to work, largely through the efforts and skill of Mark Shin (See Figure 1b).

The development of whole tissue section imaging microscopy is proving to be one of the most innovative and exciting contributions of the Brain Mapping Project to date. The TSI Microscope is stabilized on a large granite block. It is highly adaptable for camera mounting, drawing tube access, nose piece and turret for objectives. It supports a

computer-controlled stage that is large enough to hold whole human brain sections (and sections of the even larger brains of whales). It has an especially wide field illumination light source and condenser, although still not sufficiently uniform over the whole field. The stage has position control registers in both x and y axes, with digital display in microns, all under control of the MicroVAX and coupled to the MegaVision system.

This microscope constitutes a simple but useful exploratory tool for rapid, accurate, computer-operated digital image reconstruction of whole tissue sections. We put up a modest Circon CCD camera which we can modify to serve as a line camera for continuous section sweeping in a horizontal or vertical direction, to make a "strip map," or we can use it with a square pixel array to make a composite mosaic.

The center of the camera image through the microscope is displayed on a black and white monitor that is useful to the operator for purposes of scanning whole sections, using a variable speed toggle switch, and for focussing the image. This is in addition to the field of view which is accessible to the operator directly through the normal operator viewing port of the microscope.

The MegaVision system is used to acquire, store in sequence, create and display composite mosaic images of whole or partial tissue sections. The main shortcoming of the present TSI Microscope design is that the light source cannot provide a sufficiently uniform field of illuminaion for low power magnification tissue section reconstruction. This leads to a "patchwork quilt" appearance of the composite synthetic image. This is especially objectionable with low magnification images (See Figure 9).

This difficulty of illumination was anticipated from the beginning and the best system that was considered to be possible was engineered into the microscope. The roughly circular unevennesses in uniformity of illumination do not interfere with good quality imagery patch-by-patch. They are hardly noticeable to the viewer because the eye quickly adapts. They become noticeable when multiple patches are arranged into a large mosaic composition. Then the variations in illumination stand out; they are made perceptually more obvious because of their alignment along the x and y axes. In this way a "postage stamp" appearance becomes obvious. Of course these effects are reduced to virtual disappearance when higher magnifications are used. Then the field of view is reduced to the "sweet" part of the optical column and the center of the field of illumination (See Figure 10).

With the MegaVision it is possible to subtract for

25

uneven elimination and we are presently working on a proto-col to gain this advantage for TSI Microscope imaging.

Mark Shin did an excellent job of eliminating seams between patches in the composite mosaic reconstructions. There is such close tolerance for the computer control of the stage that he is able to keep the seams between adjacent images down to about a single pixel level.

It was noted earlier that the Circon CCD camera has a 525 *x* 480 line chip. This presents a problem because the MegaVision T scanner digitizer tries to map this awkward dimension into 525 x 525 scan lines. The difference of 45 scan lines manifests in presenting that number of blank lines in the upper margin of the digitized image. Shin has the computer control the movement of the stage so that that blanked strip is occupied with the adjacent rank of the mosaic image. The stage control is sufficiently accurate that patches can be made to abut one another uniformly and precisely so that a square pattern of mosaic images is reconstructed.

(b) Improvements in Brain Specimen Preparation

For most laboratory purposes, when animal and human brains are prepared for histology, three dimensional spatial integrity of the entire brain is not required. For purposes of whole brain mapping at microscopic levels of detail, how-ever, spatial integrity must be preserved as far as possi-ble. This must be maintained through all procedures required for brain processing, from the living brain, in the case of animals, and from the fresh cadaver in the case of humans, to the condition of the same brain embedded in block form ready for sectioning. This is the only way, too, by which proper database standards can be created that will appropriately serve the research and applications require-ments of various neurosciences communities.

The brain is served by a blood supply that is about ten times greater in volume than that of other organs. It is suspended in cerebrospinal fluid, and is subject to rela-tively abrupt shrinking and swelling. When removed from the brain's fluid bath, its relative weight is increased three hundred-fold. Its own weight then imposes plastic deformity and even dehiscence. Maintaining spatial integrity through every procedure from the living brain to completed graphic reconstruction is no simple problem.

The BMP requires creation of accurate whole brain reconstructions, and accurate comparisons between brains, gross and microscopic, so it was essential to develop and test entirely new and stricter brain and tissue preparatory methods.

26

These new methods constitute one of the major contributions of the BMP. They ensure that reliable Registration Control Images (RCIs) can be obtained prior to sectioning and that Tissue section Images (TSIs) represent tissue well preserved for microscopic study.

Spatial integrity is particularly difficult to maintain throughout the agonal period of perfusion. The brain must again be especially carefully protected against deformity during the process of removal from the skull and subsequent handling. We were uncertain of being able to accomplish this and began with the assumption that we would have to slice whole brains within the meninges and skull. [That the LKB giant cryomicrotome could do this was one of the attributes in its favor for our selection.] There could be no better mold to hold the brain than its natural cradle. Even there, there is still considerable room for distortion. A better technique had to be worked out. An unexpectedly reliable method was discovered by Charles Wurtz with the technical assistance of Cynthia Lemere. Their novel techniques for rat brain preparation, differ in three important respects from state-of-the-art methods with which we began.

First, they established that when a rat is allowed to cease respiration for a few seconds prior to perfusion-fixation, the brief period of asphyxia dilates the cerebral vasculature and enhances both perfusion and staining.

Second, they found that while lithiumcarmine staining in vivo was better for digital image acquisition than any other of some twenty carmine formulae, it still yielded sub-optimal white matter/gray matter differentiation. Carmine dyes produce a red/yellow spectral contrast. Each of these colors is poorly resolved by digital imaging cameras.

Wurtz and Lemere tried to solve the spectral sensitivity problem by perfusing with low concentrations of osmium tetroxide. When delivered by vascular perfusion, cacodylate buffered 0.5% osmium tetroxide preferentially stains gray matter a light brown, while leaving white matter relatively unaffected. This osmium-brown has a broad spectral reflectivity, and it was felt that good anatomical differentiation could be achieved by this method. While the preparation yielded the expected coloration, the contrast proved insufficient for adequate digital image analysis.

To circumvent this problem they turned to methylene blue. This dye stains gray matter dark blue-green, and white matter yellow-green. These colors are satisfactorily separated by the MegaVision camera. Methylene blue penetrated tissues best when perfusion of the dye preceeded fixation (See Figure 6).

Third, they learned how to remove the brain especially

27

carefully from the skull and meninges, after fixation and without deformation. The guarantee of dimensionally stable removal of the brain depended on development of non-distorting perfusion techniques that stabilize the brain as a whole preparatory to its removal and final embedding.

Wurtz and Lemere also prevented brain edema and shrinking by carefully adjusting osmolarity of the perfusion solutions. Their chain-linked histological protocols combined thorough fixation using paraformaldehyde and glutaraldehyde. Brain removal from skull and meninges improved brain outline contrast in the RCIs. It facilitated software application during digital image processing, and reduced difficulties in removing and handling the delicate tissue sections. It also saved microtome blade damage which can scar the block face and spoil the quality of RCIs. Blade sharpening and replacement is expensive and takes a long time for blade turnaround. Bone cutting means that a large stock of expensive blades must be kept on hand.

To increase the cutting speed of the microtome and to increase the quality of tissue sections, they introduced embedding with egg-albumin polymerized with glutaraldehyde, as suggested by Dean Hillman. This medium, when blackened with a mixture of India ink and carbon (lamp-black), allowed sectioning of exceptional quality at 50 to 100 μm, and provided an excellent optical contrast with a minimum of back reflectance. This combination greatly improved the quality of the RCIs.

Furthermore, this improved method of preparation allowed sectioning at +5 $^{\circ}$C rather than at sub-freezing temperatures. This provided a further increase in the permissible speed of the cutting stroke of the cryomicrotome (See Figures 11 and 12).

1.3. Improve Accuracy of x-y Coordinates of Histological Sections--I

A major contribution to computer-assisted analysis of tissue sections was the development of techniques for composite, whole-section synthetic image acquisition and reconstruction of tissue sections done by TSI Microscope and computer. This is another first in the history of computers and microscopy. More importantly, it is applicable to morphological studies throughout all the life sciences. This software can be built upon for neuroanatomical feature detection and texture analysis.

(a) Development of Stage Control to Match Digital Image Dimensions

28

The computer driven stage is powered by two precision indexers which control the x and y axes. A library of routines was written in C language by Mark Shin to control the indexers. Communication linkage is established by a high level program by calling an initialization routine in the stage library. Thereafter, the program has direct access to the indexers and can precisely control movement of the stage platform.

The TSI Microscope with its computer driven stage and computer controlled imaging technology was developed de novo for the BMP, to create whole tissue section computer graphic mosaic image reconstructions. With this instrument, it is possible to digitize individual frames from the microscope-mounted solid state camera. The program controls the microscope stage so as to move step-wise across a stained, microscopically thin tissue section in an orderly fashion so that a mosaic of squares is sequenced and imaged with single-pixel accuracy in camera placement in both x and y dimensions.

The image on the microscope is scanned in mosaic fashion, digitizing each frame on station between moves of the computer controlled stage. The requirement here is to create a square "patch" for mosaic reconstructions of whole tissue sections.

Mark Shin established stage motion that corresponds to the dimensions of one frame of 512 x 512 pixels for each specified microscope objective. Thus, as magnification increases the number of patches increases, but each patch contains the same number of pixels.

Shin created a database containing the scale factors for each of the microscope objectives allowing the computer-controlled stage movements to match the camera magnifications precisely. Application programs consult this database. Depending on the magnification, the stage is moved an appropriate amount to capture the next tissue image without overlapping the previous frame or leaving a gap between frames.

We have devoted this new technological development to imaging monkey and human tissue sections (See Figures 9 and 10). Success with these monkey brain mosaics indicates that applications to tissue section imaging in the rat brain will be entirely straightfoward [2.1.2].

Whole rat brain wireframe fiducial "atlases" contain sufficient information to allow the 2-dimensional de-warping of both the macro-registration thin-section unstained images (macro-TSI) and the stained mosaic composite reconstruction of stained sections, the microscopic TSI (micro-TSI) images [SOW 2.1.5].

Inasmuch as the rat brain is less than 10% of the volume of the monkey brain, whole tissue section mosaic mapping can be achieved at correspondingly higher magnifications. The MegaVision image display system, however, is limited to 1 Mb per image. Therefore, storage can be complete but display requires compression of data to fit the 1 Mb format.

A whole monkey brain tissue section can marginally be accommodated in one mosaic image reconstruction at 2x magnification. It, too, has to be considerably compressed for purposes of display. Only about one-tenth of a whole human brain section can be accommodated at a similar level of magnification. We will need much more capacious image display systems to accommodate composite mosaic image reconstructions made up of an assembly of 1 Mb mosaic image reconstructions.

The accuracy of control of the TSI Microscope stage allows seamless junctions to be reconstructed in the course of assembling very large mosaic reconstructions. The storage of mosaic patches in proper order in our system can be accommodated for every mosaic image acquisition. With limited memory capacity our computer would have to dump the information to tapes repeatedly, and the sequencing would still be appropriate to make an immense composite mosaic reconstruction. Unfortunately, there is no place to manipulate or display such a composite image, not at UCSD or at the San Diego Supercomputer Center.

A practical financial hitch has influenced us to forego completion of the whole rat brain tissue section mosaic reconstruction [2.1.2] at this time. A simple, practical difficulty is this: A 20x objective needs to be closer to the tissue than our present coverslips permit. Coverslips of the requisite thinness are about ten times more expensive. Moreover, they have an average 80% rate of loss through breakage on slides that have enough space to hold four rat tissue sections. We consider, however, that the technical challenge has been successfully met.

A tissue section mosaic reconstruction of the rat brain at 2x magnification does not require full use of the power of the MegaVision 1024 x 1024 pixel imaging capability. The MegaVision however is not capable of accommodating magnifications higher than 2x when applied to whole tissue sections of whole monkey brains. And, the power of the MegaVision is trivial with respect to requirements for imaging whole human brain sections. The accumulation of synthetic images from whole human brain serial sections runs into many terabytes of data storage and manipulation.

1.3.1. Improve Accuracy of x-y Coordinates of Histological
Sections--II

The problem of tissue distortions with sectioning at
microscopically thin intervals has never been solved by his-
tologists. Integration and de-distortion is done by their
brains and hands. There. is often some sacrificing of sec-
tions, too.

When one is integrating small pieces of tissue this
does not much matter. Without having the task of accurate,
quantitative 3-D reconstructions an histologist can assume
that distortions between successive slides are inconsequen-
tial. Optimal choices of embedding material, careful, uni-
form motion of the microtome, exquisite care in removal of
the delicate section, etc., are carefully practiced by his-
tologists, and yet compression, dilation, differential
translation, breaking away, overlapping and gapping of tis-
sue, all occur.

The MegaVision system purports to have up to twelve
differentially moveable points for warping purposes. We
found, however, that if you use only two or three differen-
tial points the sections become more patently skewed than
before. If you put in more than about three points for dif-
ferential warping, MegaVision simply gives up and does not
solve the algorithm.

This is one of the hardest problems we must solve to
achieve accurate three dimensional brain mapping. Building
"de-deformation" algorithms of high differential complexity
is difficult. We would like to have implemented what we
call a "pushbroom" whereby a certain tear or fold or a piece
that remains intact but may have floated away from the rest
of the section can be rotated, translated and properly
replaced.

(a) Rationalizing Images for Two and Three Dimensional
Reconstructions

Requirements for brain mapping have two subordinate
problems that deserve consideration. The first, alluded to
already, is that RCIs include some data that lie at variable
depths beneath the relatively translucent surface of the
frozen block face. Thus RCIs contain some pixel data that do
not correspond to the plane of the TSI. Because of the
depth of focus, analysis of the RCI does not reveal such z-
axis complications. This does not usually constitute a com-
plication for the location of homologous landmarks in the
two images.

There is a further problem that was addressed exten-
sively in the Task Definition Workshop. What are to be

31

taken as the most appropriate fiduciary marks for the regis-
tration of images in the process of three dimensional recon-
struction. Introduction of fiduciary fine needles that
penetrate the brain tissue interfere with blood flow and
produce serum leakage from injured capillaries. Because of
the normally low oncotic pressure of extracellular and cere-
brospinal fluid, leaked serum proteins induce rapid local
and regional tissue edema. Similar damage is done by the
heat created by penetrating brain tissue with laser or par-
ticle beams. Tissue marking is actually accomplished by
tissue vaporization.

When thin sections are sliced by the microtome, the
fiducal marks so laboriously introduced are themselves dif-
ferentially displaced within the tissue as a consequence of
the slicing. Matching up the fiducial marks does not then
match corresponding parts of the tissue; one has a false
sense of correct alignment. Proper placement of fiduciary
marks does not ensure that the tissue sections are in proper
registration.

After examining a number of possibilities, we concluded
that biological fiducials are more plentiful, more useful,
and available at practically any scale in any part of the
tissue, to well below the level at which such marks can be
identified in RCIs.

We plan at present to take advantage of large and
moderate sized blood vessels when they are cut at close to
right angles by the microtome, for marking TSI alignments.
Eventually software can be developed for machine recognition
of such vessels, and a semiautomatic alignment procedure to
rationalize between RCI's and TSI's.

When the x, y, and rotational aspects of the overall
synthetic TSI image has been matched to the outlines of the
brain, ventricles, and other gross morphology of the RCI,
and finer details rationalized using blood vessels as mark-
ers, then the images can be differentiated by subtraction so
that what does not lie on the surface z plane of the RCI can
be eliminated from that image.

A more difficult problem lies in 3-D de-deformation.
Even when individual TSIs and RCIs have been matched as
closely as may be feasible, and even when the alignment pro-
vided by the successive RCI images has been ensured for
three dimensional reconstruction, there will remain
discrepancies in 3-D organization that are only discoverable
when the three dimensional object can be inspected through
the use of a volume rendering device such as is being built
by Charles Molnar and Fred Rosenberger at Washington Univer-
sity at Saint Louis. Then it will be recognized that some
nuclear groups, fiber tracts, and blood vessels are "stair-
stepping" in a way that does not obtain in reality. Then a

32

three dimensional de-deforming algorithm must be applied.
This has not yet been developed, and we look to Fred Book-
stein to build software to solve this problem. Adequate
three dimensional re-de-deformation of the TSI is by no
means a trivial problem. It's robust solution is essential
for purposes of the Brain Mapping Project.

(b) Clinical Scanning Already Benefits Brain Mapping and Will in Its Turn Benefit from Brain Mapping

We have used both computed tomography scans (CT-scans)
and magnetic resonance scans (MRI-scans) for purposes of
control of the premortem and postmortem three dimensional
condition of animal brains before sectioning, as detailed
elsewhere in this Report (See Figure 13). We have done both
CT and MRI scans for whole human for heads prepared for
atlas development, and have established protocols for
obtaining such scanned images for each of the three species.
The animals are imaged premortem under anesthesia as well as
postmortem, prior to perfusion and after perfusion. The
three dimensional reconstruction of scan images serve as
templates for comparison of scans from living specimens. As
data accumulate, this reflexive system of comparison and
analysis will become increasingly useful.

It is terribly time-consuming (measured in weeks) and
expensive (measured in thousands of dollars) to slice a sin-
gle human head. It is also very desirable to obtain a broad
database for assessment of what may be taken as "normal"
gross human neuroanatomy. We have begun to develop a data-
base and to acquire data from other sources involved in
scanning large numbers of living human brains. This data-
base will contribute to very much needed knowledge for
estimating the limits of normal variations in gross neu-
roanatomy. It will also help to define some of the morpho-
logical phenomena encountered among classic neurological
conditions. With the help of John Hesselink, Medical Direc-
tor, Magnetic Resonance Institute, at UCSD, and Terry Jerni-
gan at the Veterans Administration Hospital, we intend mak-
ing three dimensional reconstructions from clinical scans
already made for us in the course of human brain preparation
for the BMP. These scans have the advantage that they can
be verified neuroanatomically, in detail. Gradually, an
important clinical database can be established, with
appropriate controls. This is also not a trivial problem.
For example, every time an MRI magnet is put into action it
sets up a somewhat different field: there may be "pillow"
or "hourglass" distortions or other field deviations which
occur in all three planes of projection. To obtain an
undistorted MRI, it is necessary to put in a suitable model
of the head with gelatin-salt in glass tubes in three orien-
tations the image of which can be used to de-deform the
image of a human head put into the same field in the same
location on the same day.

33

Clinical scanning can be useful to the BMP and, in turn, the BMP will increasingly contribute to clinical scanning, both by providing quantitative brain models and by increasingly demonstrating what may be considered "normal limits." In making whole brain reconstructions from clinical scans we have received encouragement and help from William Oldendorf.

(c) Side Contributions to Brain Development and Brain Evolution

The Brain Mapping Project has sparingly allowed utilization of its hardware, software and conceptual developments to help advance fields of investigation closely related to quantitative morphology and three dimensional computer graphics reconstruction. This has been done by the PI in non-BMP time, on the basis of strict non-interference with BMP activities and progress, by way of becoming acquainted with a few important related research puzzles. We have learned some new applications and improvements for BMP software and have confronted an unusual assortment of tissues and stains as well as other challenges to digitization, in respect to the following problems: (1) attempts at quantitative resolution of the gap between macroscopic and microscopic domains of brain mapping; (2) reckoning the reciprocal relations between clinical scanning (computed tomography and magnetic resonance scanning) as controls for brain mapping purposes, and seeking better interpretations of clinical scans through utilization of primitive brain maps generated in this Project; (3) mapping three dimensional growth of the human embryo, using slides from the Carnegie Laboratory for Human Embryology, at the University of California Davis; (4) three dimensional morphometric analysis of experimental brain infarctions in monkeys; (5) reconstruction of serial sections of a human temporal bone; and (6) three dimensional reconstruction of an important fossil skull.

Given the powerful potential of brain mapping systems, it is desirable to utilize the evolving computer graphics capabilities to deal with display and analysis of morphometric change over time, i.e., adding the fourth dimension. We already have four human embryos (stages 13, 15, 17 and 19) digitized for cerebral ventricles, outline of brain and spinal cord, and outline of the body as a whole. The four embryos were obtained, thanks to Ronan O'Rahilly, Director of the Carnegie Institute of Embryology, at the University of California Davis. The specimens are accurately dated and superbly cut and stained. It will be possible to utilize (i) neuraxial levels; (ii) the midline; (iii) external contours, dorsal and ventral midline profiles and circumferential profiles at successive neuraxial levels; and (iv) localizing features such as the Vth cranial nerve to establish homologous landmarks as a framework by which to

manifest differential growth in dynamic computer graphics.
This will contribute to embryology in ways that have hereto-
fore not been practicable.

By the same token, there are a number of fossil skulls
that are clear of stony material from which close CT-scans
can be obtained to allow three dimensional reconstruction of
the "fossil brain". We have already done this on a fossil
skull of a werewolf recovered intact from the LaBrea Tar
Pits in Los Angeles, through the efforts of Harry Jerison,
with close scanning (1 mm) provided by William Glenn and
Michael Rhodes.

With hominid skulls obtained from museums, it should be
possible to estimate the dimensions of the brain stem, the
sizes and intervals of the cranial nerve foramina, the ten-
torium and dimensions of the hemispheres. In some specimens
it is possible to measure some gyral markings which provides
additional clues to evolving brain morphology. Whereas pre-
viously only a few measurements could be made in such speci-
mens and endocasts, it is now possible to obtain relatively
credible data on brain evolution. We are assured coopera-
tion of several key people for such endeavors, and progress
really awaits the development of improved algorithms for
three dimensional reconstructions and for demonstration of
dynamic measures of changes in three dimensional shape.

1.4. Improve Alignment of x-y Whole Section Images With z Axis

The technical requirement here is to obtain accurate
RCIs, with fixed camera in relation to the cut surface of
the block, that is, the camera-blockface spatial relation-
ships including both verticality (that is, the film plane to
be exactly parallel to the plane of section) and distance
must be rigid and constant. Through the entire length of
human brains cut coronally, for example, there is sufficient
distance to produce a skewed reconstruction if these condi-
tions are not satisfied precisely.

Charles Wurtz worked out how the movement of the LKB
sledge could be stopped precisely at a fixed station in
relation to the scaffolding that holds the camera.   The
scaffolding itself is borne by the pillars that rise and
fall with the microtome, hence the distance, and thereby the
magnification to the camera is kept constant throughout cut-
ting the whole thickness of a human brain block.   He also
used precise physical instruments to measure the uniformity
of distance of rise and fall and repositioning of the knife
blade during each stroke and between successive sectioning
strokes, as well as over a long continuing series of
strokes.   He built a housing to cover the block specimen to

prevent sublimation from the surface when the specimen had
to be left for more than several minutes between strokes.
By such means it is possible to ensure that each RCI main-
tains stable x - y relations to the specimen throughout all
sections.

From the RCIs, outlines of the hemispheres, brain stem
and cerebellum are derived. These are automatically in per-
fect registration. They are used to create wireframe three
dimensional whole brain reconstructions (See Figure 8).

For synthetic images derived from already cut sections,
such as the whole human brain material from the Yakovlev
Collection, we use the Evans and Sutherland Picture System 2
which we have been employing for this purpose for a dozen
years. Its virtue is that it can scale, rotate and
translate 50,000 points in three-space in real time. An
algorithm for alignment, implemented by Phil Cohen, allows
the operator to see a succession of sections simultaneously
in three orthogonal planes, en face, vertical and horizontal
and to select and move any given section to ensure its
alignment. Moreover, numbers relating to spatial alignment,
direction and amount of rotation or translation can be iden-
tified and used for control purpose. There are some prob-
lems in interpreting some motions of three dimensional
objects in free space, hence these data can be useful. This
system allows us to take any vector images and align them to
one another. Thus, wireframe images in vector form can be
aligned usefully on the E&S system. It is somewhat cumber-
some to transform raster images from the MegaVision and
MicroVAX systems to vectors and, after E&S alignment, recon-
vert them back to raster data. To simplify the problem, at
some sacrifice in precision, Kathy Drinkard, a medical stu-
dent volunteer, implemented software that allows operator to
control parameters of alignment of a raster to a vector sys-
tem and back again. We used the E&S to align all the sec-
tions for the human brain "Atlas" depicted in the skillful
neuroanatomical drawings of Larry Stensaas.

Cynthia Lemere made digital images of three whole mon-
key brain serial sections, cut along the three classical
orthogonal planes. Using MegaVision and making black and
white silhouettes via thresholding she was able to get the
MegaVision system to outline the whole hemisphere, brain
stem and cerebellum (See Figure 14). These provided three
wireframe "atlases" of the monkey. The mounted sections,
however, could not be controlled by RCIs and therefore were
only approximately aligned. There was not time to do all
three monkeys via the E&S which would have assured an even
closer approximation.

There is no hesitancy in our conviction to insist that
RCIs are an absolute necessity if we are going to be able to
create accurate, three dimensional reconstructions of whole

36

human brains. We can easily appreciate the difficulties that obtain otherwise.

Arthur Toga has done an exceptionally fine job in the alignment and reconstruction of his monkey brain and is to be commended for the adroit algorithms he has devised for this purpose. In short, what is needed is more automation in acquisition of undistorted brain blocks, RCI imaging during careful sectioning, and powerful computer systems for TSI matching to RCIs and three dimensional algorithms to ensure internal alignment throughout the entire reconstruction.

Fred Bookstein has been eager to apply himself to this attractive mathematical problem of three dimensional shape measurement and manipulation, but we have not yet found the funding for this purpose.

1.4.1. Superimposition of Block and Slice Images

We are still a long way from being in a position to superimpose TSIs with their corresponding RCIs. There is the necessity ahead, given the powerful 2-D and 3-D alignment algorithms we anticipate, with reducing operator time so that the machine can be given intelligence or acquire intelligence to recognize corresponding landmarks by itself.

a   *Program Warping of Images to Remove Distortion*

There is, as noted above, only very primitive capacity for program warping to remove complex distortions. At best, now, they can rotate and translate and perhaps manipulate a few simple geometric distortions. Our experience indicates that this is a profoundly difficult problem.

b   Program Warping With Operator Intervention

The MegaVision system is the only one with which we are familiar. Judging by the difference between their claims (of up to 12 differential warping loci) and their performance (2 or 3 at the most), we are inclined to be skeptical. Most engineers are not familiar with the complexity of differential distortions that are commonplace with microscopically thin tissue sections.

c   Investigate Three Dimensional Registration

We know absolutely nothing about this. Bookstein claims that it is not too difficult mathematically and

37

requires only a few tens of thousands of dollars for completion. How readily such an approach can be built to work with relatively primitive imaging systems and whether it can be built in hardware is an open question.

We visualize that as three dimensional reconstruction at microscopic levels of detail become more commonplace, operators will be able to distinguish boundaries more readily by eye when "moving through" a three dimensional display. It should look something like swimming through a kelp bed in the ocean.

Perhaps, according to Robert Barnhill, with interactive linkage between operators and large-scale computer graphics systems, we can look forward to three dimensional boundaries being computer drawn, corrected, and compared, under general operator surveillance.

1.4.2. Intra-Sectional Deformations

This problem has been thoroughly dealt with in the discussions throughout SOW Sections 1.3 and 1.4.

We consider that mapping the whole human brain at microscopic levels of detail deserves one of the highest priorities in contemporary goals of scientific endeavor. We believe that it deserves a priority equal or better than that for sequencing the whole human genome. In fact, these two now technically feasible opportunities will reinforce one another and provide a combined significance that is greater than the sum of their separate contributions.

2. ACQUIRE AND CREATE MORPHOMETRICALLY CORRECT LARGE SCALE BRAIN MAPS

This is perhaps the most innovative and exciting part of the Brain Mapping Project to date. It introduces a systematic method for acquiring magnified images in a sequence. From this sequence, the images can be reconstituted into a morphometrically correct large scale map. It involves computer-assisted operation of a custom made Tissue Section Imaging Microscope, the TSI Microscope (Figure 1b). The microscope employs the Circon CCD camera for image acquisition, and the MegaVision system for image editing, management, storage and retrieval. All microscope and image management functions are under control of the MicroVAX.

The operation of tissue image acquisition for creation of large scale brain maps involves capturing, filing and accessing sequential square "patch" images and assembling them into exact re-order for the creation of large-scale, multi-patch synthetic "mosaic" maps. With the TSI Microscope, synthetic maps can be created from any size brain section, up to 20 x 20cm, at 2x, 4x, 10x, and 20x magnifications. The data accumulated during this process are so enormous that they tax the memory capacities of a small computer system such as ours. And the amount of data contained in large scale tissue maps are too massive to display on a modest computer graphics system, such as the 1024 x 1024 MegaVision system.

Although designed and commissioned many months previously, by Charles Wurtz, various components of the TSI Microscope began arriving during the last month of the Contract. The microscope could not be fully assembled until beyond the end of the Contract. Nevertheless, during the period of Contract Extension, Mark Shin implemented software that controls the stage and acquires digital images stepwise in accordance with simple instructions presented to the operator.

The operator uses a variable speed toggle switch with which to position the stage in any desired location in relation to visualizing the tissue section through the microscope. The operator then selects the light and contrast values to use in acquiring magnified images from a particular specimen. The location of the image sequence is then roughly bounded, and the computer executes the sequence by placing the tissue section correctly in the microscope field, acquiring each image (in 1/30 second), and moving on to precisely station the section for the next and subsequent images to be acquired. The microscope scans a given number of mosaic elements of the magnified section along a horizontal row and proceeds with a second third and subsequent rows, etc., all aligned so that individual patches of the

39

final synthetic mosaic reconstruction are in perfect order
and juxtaposition. A full tissue section or an area of a
tissue section can be acquired in this way, according to the
operator's wishes. Any rectangular array of any size can be
acquired: the present limit is in image memory storage capa-
city. Even so, by filling MicroVAX memory and emptying it
on tape repeatedly, any desired large scale image file can
be acquired. The limitation is on how that large an image
can be outwardly expressed.

On request, then, the computer delivers a synthetic
image made up of mosaic patches captured by the CCD camera
and composed into a single panoramic representation of the
tissue section as reconstructed by the MegaVision system.

Each frame is reduced and stored on disk is 64 x 64
bytes plus 2048 bytes for header and color table, totalling
6,144 bytes. Each frame, as displayed on the MegaVision is
262,144 bytes. This means that even a given frame can't be
displayed without compression. Since the MegaVision can
display only 1 Mb, this means that even with compression, we
can only display a mosaic made up of 16 x 16 mosaic patches.
In principle, the TSI Microscope, in one operation, could
acquire images from a given tissue section, up to the max-
imum size of the microscope stage, but one would have to be
repeatedly unloading memory in excess of the capacity of the
MicroVAX onto tape in order to keep up with image acquisi-
tion by the microscope. It is a case of the Sorcerer's
Apprentice.

Then there is the problem of representation of the
reconstituted synthetic mosaic tissue section images.

The computerized stage operates with two precision
indexers which monitor the x and y axes. A library of rou-
tines was written in C language to control the indexers.
The communication link is established by a high level pro-
gram that calls for an initialization routine in the stage
library. Once initialization is achieved, the program has a
direct link to the indexers and can precisely control move-
ments of the stage over the whole area of the stage, 20 x 20
centimeters. The stage is large enough to accommodate not
only whole human brain sections but sections of the somewhat
larger-brained whales. A right-angle registration plate has
been affixed to the stage so that individual tissue section
slides can be inserted against the margins of that plate.
This ensures that each slide can be restored to exactly the
same stage position when it is inserted repeatedly onto the
TSI Microscope stage again for imaging purposes.

The digitizer of the MegaVision has a limited resolu-
tion of 525 by 525 lines. The image obtained from the TSI
Microscope must be scanned in a square-patch mosaic fashion
for the acquisition of single frames. The whole tissue

section is composed of square patches which are systematically reconstituted into a whole composite tissue section image.

Successive square patches must be acquired stepwise with computer control of motion of the indexers. The rectangular shape and limited size of the MegaVision digitizer is accommodated by establishing the exact stage movement that corresponds to the width of one frame of a given, specified microscope objective. An appropriately scaled database containing the scale factors for each of the microscope objectives was developed by Shin. Application programs consult this database and, depending on the magnification, move the stage an appropriate amount so that the frames seamlessly abut one another on four sides, without overlapping or leaving gaps with frames adjacent in the same rank or with frames adjacent in the ranks directly above and below.

2.1. Prepare Whole Rat Brain Atlases

We have not completed this objective, and the reasons are simple. As noted in the section above, the TSI Microscope has the capacity to conduct the whole operation without difficulty. We are satisfied that the technical capability for making such an "atlas" is at hand: this includes computer-controlled tissue section image acquisition and large scale synthetic tissue section mosaic image reconstruction. We have satisfied ourselves that these two achievements can be applied to "atlas" production for rat, monkey and human brains.

What is technically not yet satisfied includes: sufficiently uniform full field illumination in the TSI Microscope to eliminate the "patchiness" of the synthetic image. We do not yet know whether this problem can be solved for low level magnifications in this microscope, or perhaps any affordable microscope. More importantly, we do not have computer memory capacity adequate for producing a whole brain atlas. Producing segments of such an atlas and reconstructing the segments into a "quantitatively spatially equivalent atlas" can be done and reproduced with photography or paper printout, but it cannot be displayed as a whole in three dimensional graphics form in any equipment available to us, including that in the San Diego Supercomputer Center.

What is more fundamental is that we do not have the necessary algorithms or hardware capabilities to de-deform tissue section images to conform to the corresponding registration control images. Therefore, any "atlas" prepared at this time would carry with it all of the idiosyncratic individual tissue section distortions that were imposed by the

41

sectioning procedure. We not only need to de-deform an
appropriate number of landmarks on the TSIs to conform to
the truth-bearing landmarks of the corresponding, undis-
torted RCIs, but we do not have the monitor equipment neces-
sary to compare and warp the images to achieve and demon-
strate satisfactory correspondence of TSIs to RSIs.

We have so far dedicated the TSI Microscope to proving
the technical prowess of the computer TSI imaging system for
making "atlases," using monkey and human tissue section
material predominantly, rather than making the actual
"atlases" themselves.

We have established: (1) that putting together a com-
plete whole brain synthetic tissue section reconstruction
can be accomplished entirely under computer control, using
this microscope; (2) that sequential RCIs already taken from
the cut surface of whole rat brain blocks of several rats
serially sectioned in their entirety in different planes of
section are in ideal registration, perforce of the fixed
relations between RCI camera and blockface. We have thus
concentrated on solution of the methodological problems
rather than on executing a specific "atlas" that would, at
this time, be both two dimensionally and three dimensionally
deformed.

Within the duration of the Contract such an "atlas"
production, even with geometric shortcomings, would have
turned out to be impossible because of the late arrival of
the equipment for the TSI Microscope. We shall have to be
satisfied that certain methodological problems for image
aquisition and image synthesis have been satisfied, and that
the registration control images are have provided geometri-
cally correct wireframe "atlases."

2.1.1. Three Dimensionally Accurate Alignment

Only the external morphology, as interpreted by the
RCIs, is three dimensionally accurately aligned at this
time. We await two dimensional de-deformation and three
dimensional re-de-deformation algorithms and the requisite
monitors for display and warping performance purposes.

2.1.2. Tissue Section Image Maps

Here, we can rejoice in what we have to report and
demonstrate. This can be appreciated from what we have
already said, and particularly, from Figure 15.

42

2.1.3. Generally Agreed Upon Structure Maps (Wireframe Outlines)

We have succeeded in constructing wireframe and solid surface renderings of whole rat brains (See Figure 8 a, b, c), whole monkey brains (See Figures 16 a, b, and 17 a, b) and combinations of wireframe with accurate internal mapping of identifice structural organization in the whole rat brain (See Figures 18 a, b; 19 a, b).

2.1.4. Prepare One or More Rat Brains

Three whole rat brains were sliced through full dimensions of the specimens, RCIs were taken of each section, and contours were drawn using the MegaVision system, by Cynthia Lemere. These contours were reconstructed three dimensionally and presented graphically as wireframe and solid modeled figures (See Figures 8 a, b, c). Additional rats were similarly sectioned, digitized for wireframe "atlasing" and for internal structure/function manifestation, by Dean Hillman (See Figures 18 and 19). Due to improvements in specimen staining and embedding quite good computer interpretation of outside boundaries can now be achieved with the MegaVision system. Some difficulties remain to be overcome when thresholding the captured RCIs in order accurately to distinguish and contour by computer discrimination, white matter and ventricles.

A series of whole rat brains were prepared according to a protocol for systematic exploration of various dyes, mordants, embedding material, etc., including the following:

> Ammonium carmine (RCIs) 1; Boracarmine (stained, not sectioned) 1; Lithium carmine (trial sectioning on one) 3; Picrocarmine (trial sectioning on two) 21; Osmium (RCIs on one) 7; Methylene blue (sectioning on four; RCI and wireframe reconstructions on three) 9; Neutral red (trial sectioning on two) 2; Luxol fast blue (trial sectioning on one) 2; Unstained (trial sectioning) 2. Outcome of image analysis: Methylene blue has reasonable advantages. Trials with various embedding media: outcome: preferential advantages for Egg albumin with gelatin, blackened with India ink and carbon (See Figure 12).

2.1.5. Test Bed for Two and Three Dimensional Warping Algorithms

By the 5th quarter we had completed three satisfactory whole rat brain wireframe fiducial "atlases" in precise registration. Their contours are three dimensionally

accurately aligned. They constitute an appropriate test bed
for two- and three-dimensional de-deformation. The
appropriate algorithms await the mathematical genius of Fred
Bookstein for whom we have as yet not been able to obtain
the requisite funding.

2.2. Prepare Whole Monkey Brain Atlas

We prepared, according to a similar protocol followed
in humans, a single whole monkey brain, stained with
Methylene blue and embedded in black egg albumin and gelatin
(See Figure 20). This is properly vapor-locked in a frozen
state and held in storage until we can be confident enough
of both automatic cryomicrotome tissue section capture and
simultaneous automatic RCI acquisition with the MegaVision
system, techniques that are under continuing development,
using rat brains.

Arthur Toga was successful in developing methods by
which to create computer graphic three dimensional recon-
structions of a whole monkey brain (See Figures 16 and 17).
His data are derived from a single animal. The serial sec-
tions were scanned and digitized as detailed in the Toga
References. The sections were re-aligned using several
methods. They were either aligned manually by indicating
translational rotational correction factors, or they were
aligned automatically using a registration tool set. This
tool set is comprised of algorithms which are based upon the
notions of: centroid of the mass, principal axis, best fit,
and fiducial alignment. The algorithms are executed itera-
tively such that the results of one are fed into the other.
The process continues until the increment of change is
smaller than a pre-set level.

Although Toga is not entirely satisfied with the
results of the alignment procedure we have developed so far,
we believe that his work represents a major advance toward a
completely accurate solution of a very difficult problem.
It reasonably satisfies the requirement for three dimen-
sional accuracy in whole brain mapping and three dimensional
computer graphic reconstruction, display and analysis.

Until now, these algorithms have been applied only
within a single brain and have not yet been tested on dif-
ferent brain data sets. Moreover, the multiple brain data-
base on which it had been intended to test these algorithms
for interbrain registration and comparison purposes has not
yet been implemented. The time to complete the database and
interbrain registration algorithms is greater than the time
allowed.

44

2.2.1. Prepare a Minimum of One Complete Monkey Brain

Toga prepared one complete monkey brain, complete with an "atlas." The sequence of its preparation and reconstitution of its three dimensional volume are illustrated in Figures 16 and 17.

2.2.2. Three Dimensionally Accurate Alignment

The accuracy of section alignment is evidenced by the fact that the sulci and other cortical landmarks in the monkey brain appear realistic and correspond to the locations of gross morphological landmarks on the surface of the original specimen. If the alignment algorithms did not produce excellently registered sections, you would see obviously skewed and distorted sulci and gyri following the surface modeling.

2.2.3. Tissue Section Image Maps

The tissue section image maps are depicted in Figure 17 b.   Three dimensional volumes of the whole brain can be re-sectioned along any arbitrary plane to illustrate the tissue section used in the original data collection, or along any arbitrarily devised plane. In this case, these maps depict functional activity, specifically, cerebral glucose utilization.

2.2.4. Generally Agreed Upon Structure Maps (Wireframe Outlines)

The structure maps which are delineated by wireframe outlines have not yet been completed for an exhaustive list of structures. However, the algorithms which were used to generate the surface of the whole brain are appropriate and competent for depicting substructure modeling to be rendered deep to the cortical surface. If the work continues, the database application and substructure wireframe maps will be completed in parallel and in the same brain three-space as whole monkey brain three dimensional wireframe and solid contouring reconstructions.

2.3. Prepare Preliminary Atlas of Whole Human Brain

Creation of a cytoarchitectural and myeloarchitectural reference "atlas" of the human brain was carried out using material from a single, serially-sectioned, celloidin embedded brain from the Yakovlev Collection at the Armed Forces Institute of Pathology (AFIP) in Washington, D.C.

45

Subcortical structures were mapped on photographic enlargements having a magnification of 12.5x, of whole brain Nissl and myelin stained sections using a dual stage micro-scope that permits optical superposition of adjacent serial sections. Adjacent Nissl and myelin sections could thus be superimposed, and next-sequential myelin to myelin or Nissl to Nissl could be similarly compared.

Mapping of cells constituting the subcortical cytoar-chitectural units was carried out under the microscope at 40x, 100x and 200x, and photographic documentation of each of the anatomical features of interest was provided on 35mm color transparencies.

Serial tracings of the brain cytoarchitecture were created at 0.7mm intervals to demonstrate the location of subcortical nuclei which were all named in accordance with conventions found in recent literature. (See Appendix B for Neuroanatomical List of Human Brain Subcortical Structures depicted in this "atlas" by Stensaas). Serial maps of brain myeloarchitecture were created at a similar 0.7mm interval using 35μm sections adjacent to the Nissl sections used for cytoarchitectural analysis. The principal myeloarchitec-tural units were identified on tracings in the maps.

Photographic documentation of the cytoarchitecture and myeloarchitecture in the form of several hundred 35mm slides has been described earlier in this Report.

2.3.1. Prepare One Preliminary Human Brain

BMP, mainly Charles Wurtz and Cynthia Lemere, with demonstrations and consultative advice from Wolfgang Rauschning, and with the special facilities provided by John Sykes and Bill Collins of the UCSD Willed Body Program, prepared eight intact human heads according to a careful, experimentally designed new protocol (See Figure 20). Most of these heads were imaged with Computed Tomography, thanks to Clint Stiles of Picker Corporation, or Magnetic Resonance Imaging, thanks to John Hesselink of the Magnetic Resonance Institute at UCSD, (or with both of these scanning pro-cedures). These procedures were undertaken for purposes of three dimensional clinical image reconstructions. The reconstructions will be used for comparison with serially sectioned whole brain computer graphics reconstructions obtainable from studying the anatomical material. The BMP goal was to generate a small number of "normal" whole human head preparations and to delineate them with state-of-the-art clinical scanning techniques prior to sectioning them in the LKB giant cryomicrotome for production of complete RCI sequences and selected tissue section image analysis. Several "ideal normal" heads were selected and prepared in order to benefit from inter-specimen comparisons, and so

46

that we could section through whole normal heads in each of
the three classical orthogonal planes of reference. Methods
for selection and preparation of these specimens were
detailed in BMP Quarterly Reports and summarized in the
Annual Report.

2.3.2. Three Dimensionally Accurate Alignment

Using data from Cinemorphology sequences, captured ear-
lier, which were acquired using a Mitchell, 35mm pin-
registered motion picture camera, using camera-blockface
alignment procedures similar to those for MegaVision system
RCIs, we were confident of three dimensionally accurate
alignment to proceed with the following:

2.3.3. Generally Agreed Upon Structure Maps (Wireframe Out-lines)

BMP created a single whole human brain wireframe recon-
struction and rendered the same with solid surfaces. We
also created wireframe reconstructions and rendered solid
surfaces on twenty subcortical parts of that brain in
correct dimensionally accurate whole brain three-space. For
the solid rendering, we used the Reynolds solid surfacing
software to produce solid models comparable to the wireframe
outlines we had made of the same structures (See Figures 21
and 22).

3. ACQUIRE AND CREATE SELECTED SUB-STRUCTURE BRAIN MAPS

3.1. Prepare Neurochemical Structure/Function Maps of Whole Rat Brain

Recent production of high titer polyclonal antibodies against choline acetyltransferase, the acetylcholine biosynthetic enzyme, together with technical improvements in immunolabeling procedures in David Armstrong's laboratory, permitted localization of cholinergic neurons within regions of the brain where they had not previously been detected (hippocampus, cortex, and hypothalamus). In BMP studies, Armstrong and his colleagues employed light microscopic immunocytochemical techniques to the whole rat brain in serial sections and reexamined the anatomy of the entire rat brain cholinergic neurotransmitter system. BMP work was conducted with technical help by Susanne Almstrom.

The Armstrong group generated accurate two dimensional maps of the distribution of cholinergic perikarya throughout the whole rat brain. Two dimensional tissue section maps of ChAT were prepared for insertion into one of the BMP three dimensional whole rat brain wireframe "atlases" reconstructed from RCIs acquired with the MegaVision system. Armstrong provided enough landmarks in his "atlas" to be able to make a reasonable fit of his data into the wireframe "atlas."

ChAT localization in three dimensions was complemented by other studies in Armstrong's laboratory involving characterization of the quantitative morphology of cholinergic neurons in the aged rat the brain and in brains of specifically lesioned animals. BMP Progress in Armstrong's laboratory has been published, or is in process, in five papers (See References in Appendix) which include quantitative morphometrics of cholinergic neurons in normal, denervated, and aged rat brains.

3.1.1. Maps Will Be Based On Cells Labeled By Neurotransmitter Specific Markers:

a   Acetylcholine

In addition to the work, cited above, in Armstrong's laboratory on acetylcholine, Dean Hillman created additional three dimensional reconstructions of the rat brain. Using BRAINMATE, developed at UCSD for the BMP Contract by Donal Hurley, a former student of Hillman's, external contours of the brain were digitized and reconstructed three dimensionally. Using monoclonal antibodies for

acetylcholinetransferase, each of the cells that manifested receptors was located in correct x, y, coordinates on each section. Then, all the sections were assembled three dimensionally and aligned in the form of a three dimensionally accurate   wireframe   "atlas."   This   illustrates structure/function relations for acetylcholine systems of the rat brainstem and telencephalon (See Figures 18 a, b; 19 a, b), with cell aggregations in three-space alone and with external boundaries of the brain stem and telencephalon added in stereospecific spatial relations.

b   Substance P

    Antibodies for substance p have been obtained, characterized and tested in John Morrison's laboratory, using monkey cortex for three dimensional localization in whole monkey brain mapping protocols. There have been no conclusive experiments to date with substance p as the labeling target for three dimensional mapping of the whole rat brain.

c   Catecholamines

    Both dopamine and norepinephrine have been extensively mapped three dimensionally in monkey cortex by John Morrison and his colleagues, but these techniques have not yet been applied to the whole rat brain.

3.1.2. Maps Will Be Based on Wireframe Imaging

    The BMP has produced a few whole rat brain wireframe "atlases." Note the localization of specifically labeled neurons, e.g., Dean Hillman's work noted above (See also the relevant figures 18 and 19).

3.2. Prepare Neurochemical Structure/Function Maps of Monkey Neocortex

3.2.1. Produce Quantitative Regional Profiles for at Least 80% of Cortex

    Somatostatin has been identified and localized in all neurons which reacted with the receptor label, in the fullthickness three dimensional space of monkey cortex throughout most of occipital, parietal, frontal, and temporal brain regions.

    The total aggregate of completed somatostatin localization represents 80% plus of the entire monkey neocortex.

49

This large-scale undertaking demonstrated the practical utility of these pioneering computer assisted methods for three dimensional mapping of an important brain structure/function relationship. This important task was conceived and executed by John Morrison, Warren Young, and their colleagues. Throughout most of the Contract period, they were obliged to us a more primitive, less efficient hardware system. The BMP Zeiss Axiophot Widefield Research Microscope was delivered late, but nonetheless proved its capability and efficiency in the completion of the somatostatin mapping, although the Maerzhauser stage still lacks a shim that had to be remanufactured to conform to the original specifications.

For purposes of accurately and quantitatively localizing somatostatin throughout so much neocortex, Morrison and his colleagues depended on the EMMA software package designed by Warren Young and Mark Shin.

A three dimensional representation of somatostatin, together with a specifically identified beta amyloid polypeptide associated with familial Alzheimer's Disease, also found in monkey cortex, was created by Morrison and his colleagues, using these same methods for three dimensional reconstruction. An example of this clinically important structure/function analysis was published as a cover of Science, volume 235, 22 February 1987. It served as the herald for four accompanying articles on the beta amyloid polypeptide and its genetic linkage in familial Alzheimer's Disease. The Legend to the BMP-assisted cover illustration states: "A color graphic display of an optical density scan of prefrontal cortex from a cynomolgus monkey, hybridized with an RNA probe transcribed from complementary DNA clone lambda-Am4 coding for Alzheimer beta amyloid polypeptide. Each color represents an optical density range of grain clusters, with red as highest, green as intermediate, and blue as lowest density. See p. 873. Graphic provided by John H. Morrison, Gerald A. Higgins, David A. Lewis and Michael C. Wilson, Scripps Clinic and Research Foundation, La Jolla 92037; and Sina Bahmanyar, Dmitry Goldhaber, S.K. Shankar and D. Carleton Gajdusek, National Institutes of Health, Bethesda, Maryland 20205; Computer software (E.M.M.A.) by Warren Young and Mark Shin, Scripps Clinic and Research Foundation."

Copies of this Science cover were sent to the US Army Medical Corps Research and Development Command shortly after publication.

3.2.2. Structure/Function Maps Shall Be Prepared for Two Neurochemicals

Using same these techniques, Morrison and his

colleagues have recently carried out similar three dimensional localization of all cells bearing dopamine receptors, throughout most of parietal and temporal cortex (comprehensively surveying about 35% of total neocortex), and for all cells bearing norepinephrine receptors throughout occipital, parietal and temporal cortex (comprehensively surveying about 60% of total neocortex).

3.2.3. Maps Shall Be Based on Wireframe Imaging

Arthur Toga has produced both wireframe and solid rendering reconstructions of the whole monkey brain, and has inserted functional data such as metabolic rate, spread of seizure activity, etc., into both wireframe and solid rendered representations of the monkey brain (See below SOW 4), we have not yet inserted neurochemical structure/function data into three dimensional wireframe reconstructions.

All structure/function related data we have are available in in computer graphics displays as individually digitized sections bearing both neurochemical and neuroanatomical information, combining xyz parameters with each structural and functional entity so that they can be successfully mapped within three dimensional reconstructions.

In some BMP files, two specific neurochemical labels are exhibited along with neuroanatomical and spatial information.

3.3. Prepare Map of Structural Organization of Human Thalamus

The main contribution here derives from the work of Larry Stensaas, described in detail in SOW 4.1, in which the entire brain stem and diencephalon, including the human thalamus were outlined at 20x magnification, digitized, aligned and displayed. For comparison purposes, we newly digitized another whole human thalamus and also made three dimensional comparisons with three reconstituted whole monkey thalami, as follows in the remainder of this section.

Jason Doctor, Marney Blair and Jessica Chou, outlined on semitranslucent tracing paper the whole human thalamus from serial sections of the entire brain stem prepared by Paul Glees, Professor of Anatomy at the University of Goettingen, West Germany. Glees had made a present of these beautifully prepared slides to the Quantitative Morphology Laboratory some years previously.

Tracings, carefully rendered by volunteers under Livingston's supervision, included the major functional groups of nuclei in the thalamus: i.e., sensory relay,

51

sensory association, motor association, limbic association
and diffusely projecting groups, such as the intralaminar
nuclei and reticularis. Several sequences of these con-
scientiously rendered two dimensional tracings were digi-
tized on the Evans and Sutherland Picture System 2. The
digitized sequences were aligned to establish the anatomical
congruity of the reconstruction procedures. For want of
time, this particular human thalamus has not yet been fully
digitized and aligned. The images available on the E&S sys-
tem are in the form of wireframe reconstructions.

For comparison between monkey and human thalami, we
capitalized on and added to some previous work in this
laboratory. Using monkey serial sections, prepared in 1947
by Yakovlev and Livingston, adjacent sections of which are
in the Yakovlev Collection at the AFIP, Xu Lu-xi, Associate
Professor of Anatomy at Beijing University, painstakingly
outlined each of 29 identifiable thalamic nuclei at 12.5x
magnification. She did this in each of three matched monkey
brains sectioned at right angles to one another in the three
classic orthogonal planes. The three sequences through the
whole brains of these animals provided the thalamic material
digitized by Xu. Since the brains were similar in size and
cut in the three orthogonal planes, they each served as mor-
phometric controls for one another, e.g., the profile of
horizontal sections was used to verify the length and z-axis
of the sagittal sections; the coronal series was used to
verify the width and z-axis of the horizontal sections; the
sagittal series was used to verify the width and z-axis
dimension of the horizontal series, etc. The digitized sec-
tions were aligned on the Evans and Sutherland system using
the ALIGN program of Phil Cohen.

BMP volunteers and staff developed wireframe atlases of
these three thalamic renderings, including the thalamus as a
whole and each of the 29 sub-structures of the thalamus.
The thalami in these series were displayed both as wireframe
reconstructions and as solid surface renderings, using the
Reynolds CONTOUR VIEW software (See Figures 23 and 24).

3.3.1. Wireframe Maps Shall Be Based on Slides from Yakovlev Collection at USAFIP

This has been fully described in this Report in Scope
of Work section 4.1. Examples of some of the completed
wireframe reconstructions are given in Figures 21 and 22).

3.3.2. Relaxation of Registration Requirements

(a) Methods Employed to Align Registration of Unaligned
Human Brain Sections

As presented in this Report, Stensaas' careful tracings
from serial sections examined directly in the microscope at
12.5x magnification and projected onto photographic blowups
of the same sections, were digitized by Stensaas and Liv-
ingston on the Evans and Sutherland system. Alignment is by
the ALIGN program, written by Phil Cohen, which allows
sequences of digitized sections to be represented simultane-
ously in three orthogonal planes of section. Thus, four to
six sections, depending on the burden of total data, are
projected simultaneously in profile for two of the planes of
reference, and en face for the third plane of reference.
With the en face projection, two sections, with any choice
among the several sections exhibited in the other plane, are
projected in wireframe outline of whole and sub-structural
parts of whole sections. One of these Sections is taken to
be the "Reference section" to which all other sections in
the series will be aligned. The first group of sections is
selected somewhere close to the mid-region of the entire
sequence of sections so that "drift" will be minimal
throughout the whole sequence. The Reference Section is
held stable by the software. The secti₁ to-be-aligned can
then be rotated and translated to a ᴉ ᴉn its outline and
internal features as closely as possible to the Reference
Section. The projections in the two other planes of refer-
ence move also. Their simultaneous projection on the screen
allows the operator to see the profile of the sections in
those projections. This helps to avoid "drift" and other
misalignment tendencies when alignment is addressed only in
the en face projection. The operator has prior knowledge as
to what the profiles in the various planes and projections
"should" look like and can maneuver the sections undergoing
alignment procedures so as to obtain "best fit" alignment by
external and internal appearances from any desired point of
view.

Once an adjoining section has been satisfactorily
aligned, the operator indicates acceptance, and that section
becomes the Reference section for the next adjacent section.
Working both directions from the middle of a long sequence
allows the operator to create anatomically responsible deci-
sions throughout the entire stack. If, after completion of
a long run of sections, or the entire stack, the operator
can go into the series and undo and redo any desired sec-
tion. When the entire stack of sections has been satisfac-
torily aligned, the data relating to three-space control of
alignment are stabilized for each section in reference to
all other sections in the stack. Whenever that three dimen-
sional object is called up for imaging or dynamic display,
the whole block of reconstructed tissue is exhibited as an
intact structure. The align data constitute a separate
add-on of data assigned to each section and to the whole
stack of sections and these data go with the section or
stack henceforth. They can be modified at any time without
disturbing the internal vectors that were "immortalized"

when the section was first digitized. This means that
alignment data remain separate from the detailed neuroana-
tomical data representing the digitized contents of each
serial section.

The entire catalogue of two dimensionally accurate neu-
roanatomical structures drawn from serial sections of the
whole human brain (excepting neocortex) by Larry Stensaas
(See list of anatomical structures in Appendix B) was digi-
tized by Stensaas and Livingston. They used the TALOS
tablet and the Evans and Sutherland Picture System 2 for
this purpose. There were three fiducial channels, marked by
the insertion of fine needles. throughout the whole brain
stem. The fiducials and numerous other landmarks were used
for alignment purposes with the ALIGN program implemented by
Phil Cohen on this system. Although celloidin sections are
remarkably stable, we still had great difficulty achieving
satisfactory alignment. Once aligned, the structural out-
lines of numerous structures were displayed on the E&S moni-
tor, singly and in functional groups. (Examples of this
three dimensional wireframe production of human brain sub-
structures are given in Figures 21 and 22.)

3.4. Map Structure/Function Relationships in Retina

(a) General Approach to Comprehending and Accelerating Neurosciences Progress

One of the main purposes of the BMP is to facilitate
neurosciences comprehension of structure/function relations
of the nervous system as-a-whole. Much of this part of BMP
activity has been advanced by Floyd Bloom, Dean Hillman and
Harvey Karten. Their attention has become focussed on the
development of a powerful, computer-aided neuroscience data-
base. Karten's contribution to an evolving concept of a
neuroscience database as it applies to the BMP follows:

The purpose of a comprehensive neuroscience database is
to provide an inventory of neurons, connections,
transmitters, physiology, pharmacology, and behavioral
aspects of brain structure/function organization. There is
an imperative need to provide a standardized source of
information, easily accessible, that will permit correla-
tions within the rapidly growing mass of data of importance
to advancing research and clinical understanding of the
structure/function relations of the brain. There is at
present no existing database that provides an adequate model
for the development of a powerful neurosciences database.
Indeed, a powerful neurosciences database would provide
inspiration and contribute as a model for other life sci-
ences. Such a database will be of immense importance to
research progress in the neurosciences and to generally
clarifying the role of the nervous system in normal and

pathological conditions.

The goal of this part of the BMP involves developing a format for collecting and retrieving fundamental selected ("vetted") information concerning the brain. Such information must be keyed to both structural and functional systems, component cell patterns, connections, transmitters, receptors and trophic factors, features of ontogenetic development and organization, susceptibility to pharmacological agents, neurotoxins and other deleterious agents, role in physiological, behavioral and pathological processes, and the effects of direct and indirect injury to the nervous system.

Methodological advances within the past couple of decades have provided unexpected capabilities for the collection of valuable information in each of these areas. Expanding growth of methods and data has overwhelmed existing methods for data collection and retrieval. Accelerating progress unaccompanied by adequate methods and experience in retrieval represents an undesirable handicap imposed on existing opportunities for basic and clinical research, teaching and service.

Of significant immediate help to investigators and clinician will be a universally accessible database containing information on many diverse and some neglected aspects of brain organization and function.

Establishment of a suitable neuroscience database requires development of new methods for data collection, evaluation, organization, storage and retrieval, within the framework of an "expert system."

With Floyd Bloom's leadership, initial development of such a system is being designed and tried out with respect to several brain circuits and is engaging the database development skills of a diverse group of advanced neurosciences research laboratories. For example, in the BMP, Karten is developing a database system for the retina which may become a useful prototype for database development for the nervous system as a whole.

(b) Studies on the Retina:

The retina is desirable for detailed structure/function analysis for several reasons, all pertinent to solving generic brain mapping problems. The retina is an embryologic extension of brain tissue, structurally and functionally brain. It comprises a thin, layered neuronal network with a limited number of cell types. No other brain circuit is equivalently circumscribed between input and output. There is a large body of information available regarding the anatomy, physiology, pharmacology, and psychophysical

properties of the retina.   The retina is thus relatively
well understood as an integrative subsystem of the brain.

    Retinal features make possible quantitative spatial
analysis of defined neuronal populations. Recent histochem-
ical studies of the retina reveal an unexpected diversity of
biochemically specific neuron types within the population of
horizontal, amacrine and ganglion cells. Identification of
neurotransmitters, important in its own right, is not
enough. There are several oligopeptides that can serve
modulatory as well as communicative functions in neuronal
circuits. Receptors of all sorts need to be characterized
functionally because different receptors can have entirely
different consequences with respect to the same transmitter.
What is not understood is what specific information-
determining processes take place, where, and by what chan-
nels? It is known, for example, that there can be two-way
communications between neuronal processes without dispatch
of signals via axons. Amacrine cells lack axons; yet they
play a critical role in integrative processes and informa-
tion relay in the retina. It is desirable from the point of
view of understanding and analyzing biochemical diversity
throughout the brain that we investigate retinal cell types,
make quantitatively accurate reconstructions of their circu-
itry, and analyze their structure/function relations with
respect to their role in physiological and psychophysical
functions of the eye.

    Karten and his colleagues generated software for col-
lecting information on cell density and average cell spac-
ing. This software can be applied to any appropriately
stained neural tissue throughout the brain. Procedures are
employed to combine functional specificity with structural
maps.

(<u>c</u>) <u>Adrenergic Transmitters in Horizontal Cells</u>

    Karten is investigating both avian and mammalian hor-
izontal cells. They mediate lateral interactions among pho-
toreceptors. With the exception of the still disputed pos-
sibility of GABA neurotransmitters, the identify of
transmitters in horizontal cells was unknown at the begin-
ning of the BMP. On the basis of previous Golgi studies,
two types of horizontal cells had been identified in the
mammalian retina, Type A and Type B. A very important find-
ing by Karton's group was the demonstration of PNMT in Type
A horizontal cells. PNMT is the enzyme responsible for the
final stage of synthesis of epinephrine in neural tissue.
This enzyme was first found by Karten and colleagues in the
ferret retina. The evidence was published in J. <u>Neurosci-
ence</u>. Subsequent studies demonstrated a similar population
of horizontal cells in the rat; studies have been initiated
to determine whether adrenergic horizontal cells occur in
the human retina.

Using morphometric methods provided by BMP technology, the number, density and regional distribution of adrenergic horizontal cells have been investigated. The feasibility and success of this discovery is due to the provision of equipment, computer facilities and software by this Contract. Details of this research were provided in the Sixth Quarterly Report, giving examples of quantitative morphology using immunohistochemical methods in a well defined brain circuit.

(d) Nicotinic Acetylcholine Receptors in Retinal Amacrine Cells

Research of the last decade has demonstrated that acetylcholine is restricted in its distribution within the retina to a limited population of amacrine and ganglion cells. The cholinergic amacrine cells consist of two distinct populations, an orthotopic group with cell bodies lying within the inner plexiform layers (IPL), arborizing in layer 1c-2, and a group of displaced amacrine cells with cell bodies in the ganglion cell layer, with dendritic arborization within layer 4 of the IPL. Cholinergic amacrine cells constitute approximately 15% of all amacrine cells (average of approximately 3,000 orthotopic and 3,000 displaced amacrine cells per square millimeter in the central retina).

(e) Gamma-Amino Butyric Acid (GABA) and GABA-A Receptors in the Retina

GABA is one of the major inhibitory transmitters of the retina, and is estimated to occur in about 40% of all amacrine cells. (Glycine, a second inhibitory transmitter, is estimated to be present in an additional 40% of retinal amacrine cells.) Identification of precise populations of these distinctive amacrine cells has proven difficult due to the generally high density of staining of dendritic arbors within the IPL and a faint and inconsistent pattern of staining of GABAergic somata. There are at least two major types of GABA receptors in the central nervous system, GABA-A and GABA-B. GABA-A receptors are better characterized and monoclonal antibodies specific to the GABA-A receptor have been generated. Current work on the monkey retina in Karten's laboratory is directed towards identifying this population of GABA-receptive neurons and obtaining quantitative data on their number and specific distribution.

(f) Ganglion Cell Transmitters and Modulators

With support of the BMP, Karten and colleagues have demonstrated substantial heterogeneity in the biochemical characteristics of ganglion cells: Approximately 1% contain a catecholamine synthesizing enzyme (tyrosine hydroxylase), 3% contain substance p, and a third population contains

cholecystokinine-octapeptide (CCK-8). The results of two studies were recently published and the analysis of CCK-8 is nearing completion.

Studies on the human retina have been initiated in collaboration with Donald Minckler of the SCRF. Despite delays in some necessary equipment and software to count cells automatically, a fullscale analysis of the distribution of various neurotransmitters, neuropeptides and receptor molecules is now making substantial progress based on methods developed for avian and mammalian studies.

Importantly, the retina provides an excellent testbed for the development and utilization of a database that could be considered prototypical for development of a more comprehensive database for the brain.

3.4.1.   Specify Structure-Function Relationships Between Amacrine and Ganglion Cells

As noted above, (3.4. (d)), cholinergic amacrine cells have been identified and localized in the retina. Identification of cells receiving cholinergic input would provide important information regarding the consequences of activation of cholinergic systems in the retina. It would also tell us something about the effects of exogenous agents likely to alter the levels of acetylcholine within the retina (e.g., agents that affect the levels of acetylcholinesterase, cholinergic receptor sites, etc.).

Using monoclonal antibodies directed against specific subunits of the nicotinic acetylcholine receptors, developed by Jon Lindstrom of the Salk Institute, Karten has identified well-defined populations of retinal ganglion cells containing the nAChR, and analyzed their three-space distribution within the IPL in relationship to the location of the cholinergic amacrine cells. The nAChR positive ganglion cells constitute approximately 18% of all ganglion cells. The laminar distribution of nAChR within the IPL is sharply restricted to the same laminae that contain the acetylcholinergic dendrites of amacrine cells. Thus, unlike apparent discrepancies, referred to as "receptor mismatch," reported in other parts of the central nervous system, there appears to be a precise relationship of transmitter and receptor distribution within the retina. The results of this study are in press (Keyser, et al, in Visual Neuroscience).

Double labeling for both ChAT and nAChR demonstrated that there is no apparent co-localization of these two substances in any amacrine cell. This implies that the cholinergic amacrine cell does not receive a direct input from other cholinergic neurons. Estimates of the number of nAChR

positive ganglion cells indicates that not less than 15% and not more than 30% of ganglion cells are cholinoceptive. There is no evidence for acetylcholine in any other retinal cell types (photoreceptors, bipolar, horizontal and ganglion cells).

Collection of the quantitative data and computer plots of regional distributions were made possible through the availability of hardware and software provided by the Contract (See Figures 25 and 26).

3.4.2. Basemaps on Differential Peptidergic Identifications of Amacrine Cells These were reported in detail in previous Quarterly Reports.

4. CREATE CYTOARCHITECTURAL AND MYELOARCHITECTURAL REFERENCE BRAIN "ATLASES"

4.1. For the Human Brain:

4.1.1. Location of Major Units at 0.7mm Intervals

Stained serial myelin and Nissl sections of one representative "reference" human brain were selected by Larry Stensaas from the Yakovlev Collection at the Armed Forces Institute of Pathology. These sections were analyzed and the cytoarchitectural units (CU) of the brain stem and telecephalon were mapped, exclusive of neocortex. Serial maps were created at an interval of 0.7mm using photographic enlargements at 10x magnification. The original slide served as the negative.

Each CU was then outlined on the photographic enlargement by examining the original slide under the microscope and carefully tracing the outlines, using individual cells as landmarks. Stensaas labored through a total of six increasingly refined editions of this "Reference Atlas" in order to establish, to the best of his ability, boundaries and nomenclature that would be widely accepted by the world community of neuroanatomists.

[See Appendix B: List of Neuroanatomical Structures outlined by Larry Stensaas and digitized and aligned by Stensaas and Livingston. The location of these named structures in the three-space of the "Reference Atlas" brain was assured by the careful tracing and preservation of neuroanatomical boundaries throughout each section, at 0.7mm intervals.]

4.1.2. Alternate Celloidin Sections Stained for Myelin and Nissl

Stensaas prepared myelin stained images at 10x and 40x using 35mm photomicrographs taken at 2mm intervals. Myelin stained sections at an interval of 0.7mm were also prepared as photographic enlargements at a magnification of 10x and the principal CUs and myeloarchitectural units (Mus) were mapped with reference to each individual section, viewed by means of a light microscope. 35mm color slides of the MUs were prepared at 2mm intervals using a light microscope equipped with 10x and 40x objectives. A total of approximately 1500 35mm slides were prepared in this way.

4.1.3. Preparation of Nissl Images of Nuclei at 40x, 100x and 200x, Using 35mm Photomicrographs at 2mm Intervals

Photographic documentation of each of the CUs of the Nissl stained sections was provided using 35mm color slides which were taken with a light microscope equipped for photography using progressively higher 40x, 100x, and 200x images of the same field of view. A total of 3500 slides were prepared of this material at 2mm intervals throughout the entire brain stem.

4.1.4. Store on Optical Disk

In collaboration with David Chabolla and Luann Teschmacher, medical students at UCSD, Stensaas then documented 2600 of the total of approximately 5000 color slide images of the CUs and MUs throughout 23 representative levels of the human brain. These were organized in carousels, projected, digitized and recorded on one-inch magnetic tape with appropriate time codes. This was done in the Department of Educational Media television studio at the University of Utah.

The CU slides showing neuroanatomical details at low, medium and high magnifications were labeled both with their Latin scientific names and their common names, and the section level was indicated for each group of brain images. This provides a direct correlation between the optical disk images and each level of the "Reference Atlas."

An optical video disk was then created from the one-inch master tape by the 3M Company as part of a University of Utah teaching project. The disk was entitled A Slice of Life. Images pertaining to the mapped Yakovlev brain were put into a new order to provide a sequential progression through the brain stem and these were recorded on 3/4-inch video tape for distribution for teaching and research purposes.

4.1.5. Employ Contemporary Nomenclature and Produce Table of Equivalents

Appendix B contains the nomenclature assigned to the human brain subcortical structures by Larry Stensaas.

4.2. For Rat and Monkey Atlases, Align Photomicrographs With:

4.2.1. Digital Renderings of Whole Brain Surface

We now have complete serial sets of sections from two whole rat brains. Tissue sections from the two animals were carefully removed from the cryomicrotome blade and stored in phosphate buffer. They have not yet been mounted, stained and photographed. There are approximately 250 sections stored for each brain. The RCI's which correspond to each of these sections are available in computer tape storage.

Completion of this task is awaiting tissue staining and photomicrography for alignment with existing digital renderings of whole rat brain surfaces.

4.2.2.

4.2.3.

4.2.4. Digital Renderings of Ventricular Surface, Myeloarchitectural Units of the White Matter and Cytoarchitectural Units of Gray Matter

These digital renderings are not entirely satisfactory with respect to complete computer controlled differentiation of ventricles, myeloarchitectural and cytoarchitectural units of white and gray matter. While we have been successful in detecting the outersurface of the brain with thresholding, we have not been as successful in contouring the ventricles and white matter. *Several problems have been* encountered. The outersurface is more easily defined because of it's light color set against the black embedding media whereas, the video image gray level differences inside the brain are not as sharp and therefore are not as easily detected. Changes in lighting, such as the amount of backround light (i.e., daylight levels), lamp movement and camera drift in light level gain over many hours of camera use, make accurate and consistent thresholding difficult to perform automatically.

Figure 1. a: Photograph of Registration Control Image (RCI) acquisition system. The long white bench-height cabinet is part of the refrigeration housing of the LKB giant cryomicrotome which is used to slice whole brain tissue sections. The microtome operates automatically, with adjustable angle of blade attack, and variable speed of sectioning, thickness of section, pause on station at selected intervals among cutting cycles, etc. The block, frozen or solidly embedded specimen, is moved by a powerful motor along a steady base track in the floor of the refrigerator. Following each cut, the knife is raised during the return course of the block and the returned to a precise setting, lowered by the incremented value of thickness of the section. Operator continuous control of cutting speed is enabled by the knee-lever with a white plastic upright blade is seen lower right. Control of microtome is set up on the black instrument control box sitting on the left top. Next to the right is the MicroVAX system terminal and keyboard by which the operator calls up the SLICE program which controls the cryomicrotome and the RCI acquisition. Immediatly over the location where the block is stationed between slices, erected on a scaffold, is the MegaVision camera and Zoom lens. Illumination is provided by lamps mounted to the same scaffold, inside the microtome chamber. The black shroud which covers lens, lamps and base of the scaffold to the sides of the microtome block traveller, has been removed. The MegaVision monitor is seen to the right, with an inverted, transilluminated whole monkey brain tissue section presented in place of the usual registration control image.

Figure 1 b: The Tissue Section Imaging Microscope (TSI Microscope) is based on a heavy granite slab that is mounted on a sturdy table. The computer controlled giant stage holds a slide with twelve whole monkey brain slices, alternately stained for fiber (a modified Weil stain) and cells (Nissl). The glass slide is slid against a right angle jig that ensures accurate replacement of the same slide on subsequent occasions. The MicroVAX computer, not shown, controls two Compumotor driven stage indexers, front and left, which accurately control the x and y positioning of the slide. Stage position verification is by quartz light scaling monitors which display these values in microns in two boxes which are not seen, sitting below the TSI Microscope table. The light column comes from a light source and condenser beneath the table, through a hole in the granite slab. The microscope has an objective turret with 2x, 4x, 10x, and 20x PlanAPO Nikon lenses and space for another objective. Focussing is by the two black handles seen at the sides of the top of the microscope support column, L and R. The light beam is split to allow operator to examine the image via traditional eyepieces in front and for controllable

light   access   to the Circon CCD camera, seen with its cable
coming out from the top of its housing. A Panasonic video
monitor, to the right, shows the center of the camera view,
in this case, part of the temporal horn of the lateral ven-
tricle and part of the hippocampus in a Nissl stained whole
monkey brain section. The MegaVision monitor, not seen, is
used to setup light values in the acquired image and to
display the composite mosaic reconstitution of a large re-
gion or the whole of a brain tissue section, depending on
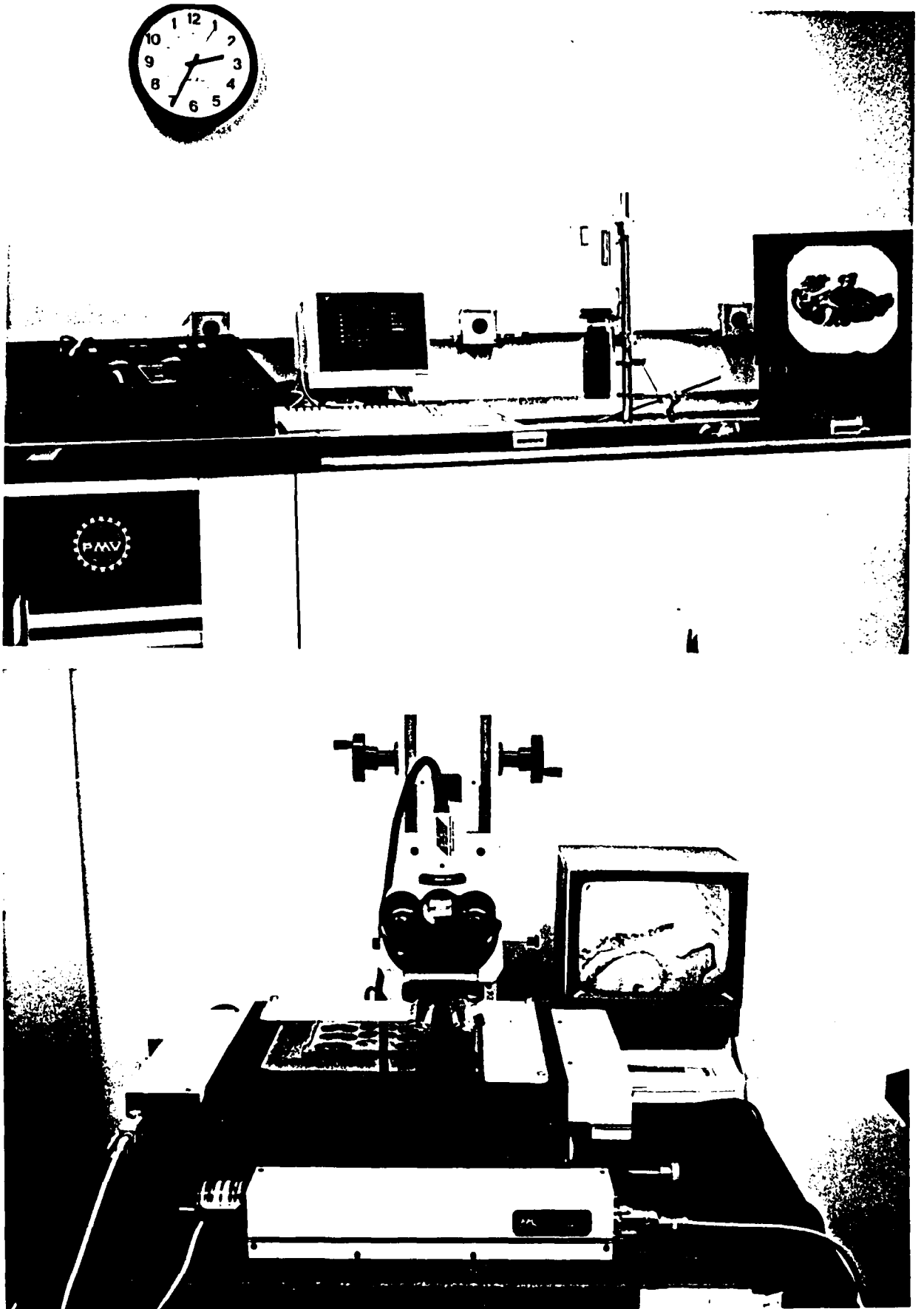size of the specimen and degree of magnification.

Figure 1

Figure 2. Sketch by Michele Frost of scaffold support for lights and camera mounted on the columns that support the LKB giant cryomicrotome knife. The specimen block is mounted on a travelling belt that moves back and forth (arrows) beneath the simplified representation of the knife mount. The scaffold maintains a precise distance and exact angle, normal to the blockface, so that blockface and camera are always in registration. The lamps, L&R, only one of which is illustrated, are Examatron, the macro-zoom lens on the camera is Tamron 70-210mm and the camera is the standard 1Mb MegaVision camera.
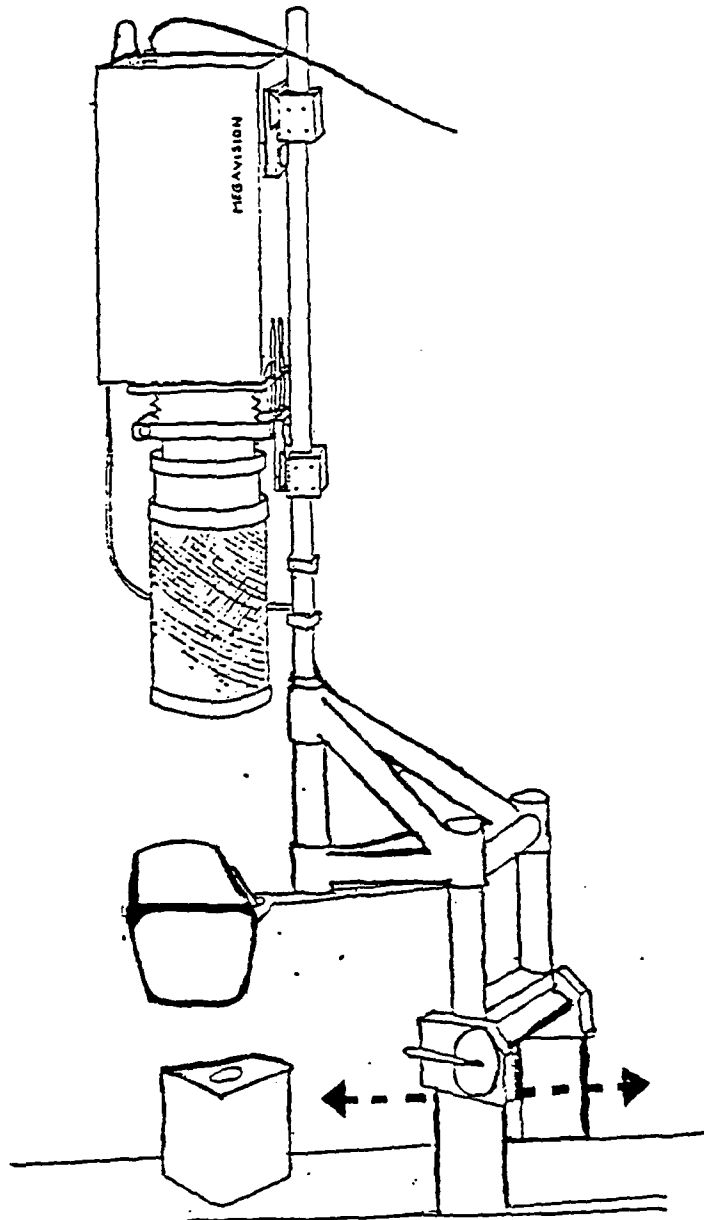
66

Figure 2

67

FIGURE   3

TYPICAL SPECTRAL SENSITIVITY CHARACTERISTIC
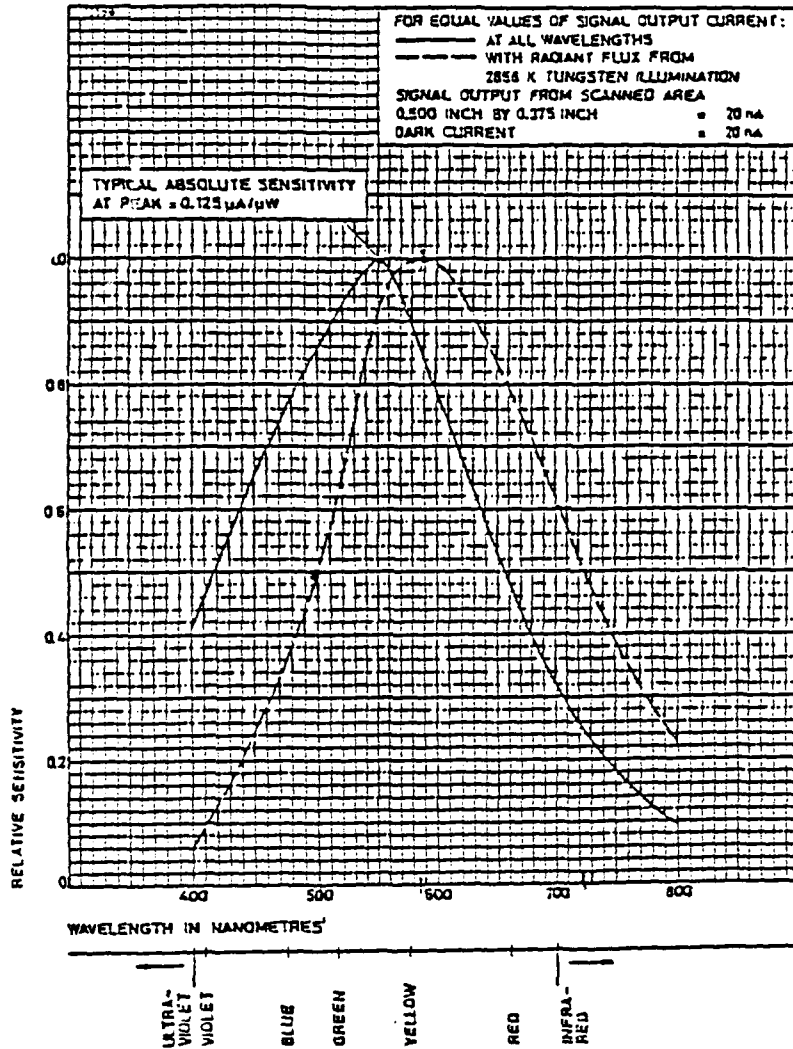
FIGURE 3

(Top) Spectral response curve of the Circon CCD camera. Note the substantial fall-off of sensitivity in those wavelengths associated with picrocarmine dyes (680nm). (Bottom) Characteristic spectral response of MegaVision camera. Note that with tungsten illumination (dashed line) the red component of the carmine stain (the gray matter) generates nearly 80% max output, while the yellow component (white matter) generates almost exactly 100%. This is a much greater degree of differentiation than available from the Circon CCD camera, and partly explains the improved contrast we see with the MegaVision-lithiumcarmine combination.

Figure 4

```
           ABM SLICER V1.1
            (c) 1987 UCSD

   0  - Exit slicer

   1  - Initialize scanner

   2  - Change/reset environment

   3  - Capture shading mask

   4  - Continuous scanning

   5  - Capture image
```

SELECT ?

```
test   dir /monkey/monkey2   images 18    time 12:00pm
```

The ABM Slicer program is designed for automatic acquisition of blockface images. In the first step, the camera is initialized by adjusting the analog circuits to provide optimum use of the analog-to-digital converter range. The working directory, root filename, current sectioning depth and increment may be changed with Option 2. Option 3 provides a continuous live image. A black surface image is captured for correcting non-uniform lighting using Option 4. In Option 5, images are then captured by accumulating and dividing to reduce noise. Automatic filenaming is used in storing the images.

Figure 5

ABM MAPPER V1.1
(c) 1987 UCSD

0 - Exit mapper

1 - Start/Stop megavision

2 - Re-initialize megavision

3 - Change/reset environment

4 - Initialize mapper

5 - Convert to gpx format

6 - Apply shading mask

7 - Produce contour

Select ?

```
srcdir /monkey/monkey3 (70) dstdir /monkey/monkey4  (3)
image  hrat12400              megavision  on        time 12:00pm
```

The ABM Mapper us designed to produce contours from the captured grey-level images. The MegaVision unit is turned off and on with Option 1. Option 2 resets the Megavision working environment to the original predetermined parameters. Option 3 allows the operator to change the working directory, root filename, depth of image in brain, sectioning increment and directory destination of the· contoured image. Copies of the original grey-level images from one directory are placed into a temporary working directory in Option 4. Images in the working directory are converted to GPX format with Option 5. Option 6 corrects the images for non-uniform lighting using the pre-captured shading mask. In Option 7, contours are produced in vector format after user-interactive image editing and anatomical structure selection.

Figure 6 a1. A whole rat brain blockface in the coronal
plane of sectioning has been imaged by the MegaVision sys-
tem. The specimen was embedded in egg albumin with gelatin,
blackened with India ink particles and carbon black to
reduce spurious reflections from the cut surface of the
block. The image includes the outline of the two hemi-
spheres, the third ventricle, above and below, the lateral
ventricles surrounding the dorsal hippocampus, the thalamus,
internal capsule, putamen and part of the globus pallidus,
optic tract, and part of the hypothalamus. These features,
when examined in closer detail, exhibit a number of land-
marks which can serve as control loci by which the displaced
(translated, rotated, compressed, dilated, torn, folded)
homologous landmarks on the corresponding tissue section im-
age, the TSI, can be de-deformed to conform to this particu-
lar RCI. The normal microscopic view, through eyepieces and
the monitor, can be used for focussing.

Figure 6   a2. Computer drawn outline of the exterior of
the rat brain RCI shown in a1. This outline is obtained by
use of MegaVision capabilities and BMP SLICE software.   The
raw RCI image is converted to a black and white silhouette
around which the computer draws a tracing. Note that it did
not follow in the midline into the interhemispheric cleft.
BRAINMATE software enables an operator to amend such defi-
cits in the computer drawn outlines. The corrected outlines
become the basis for wireframe whole brain reconstructions.
Since the RCIs are taken from the same camera position viz-
a-viz the blockface, the outlines are in perfect registra-
tion.

Figure 6 b1. Similar RCI capture at a more anterior coron-
al section level.

Figure 64

a

Figure 6b

b₁

b.
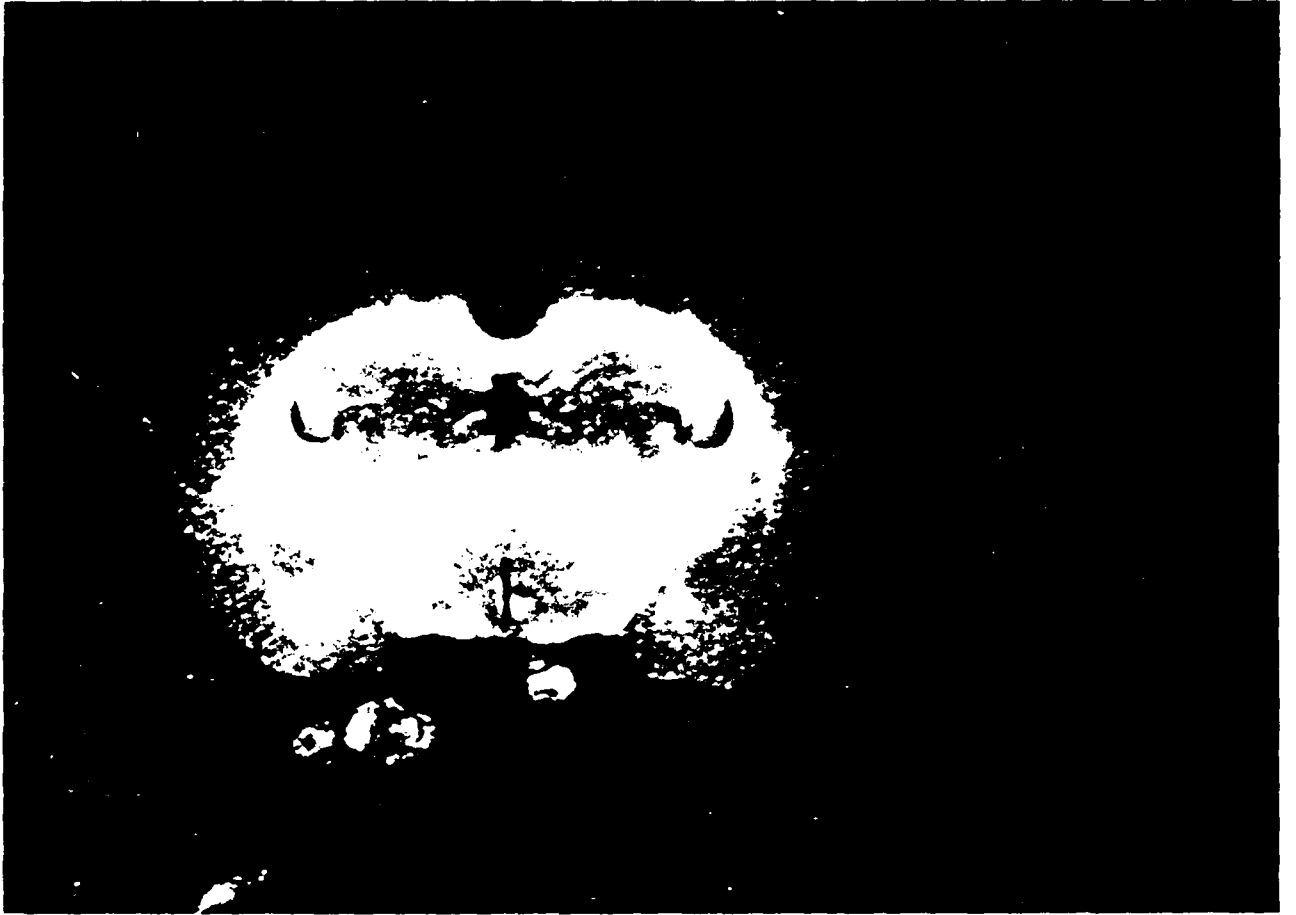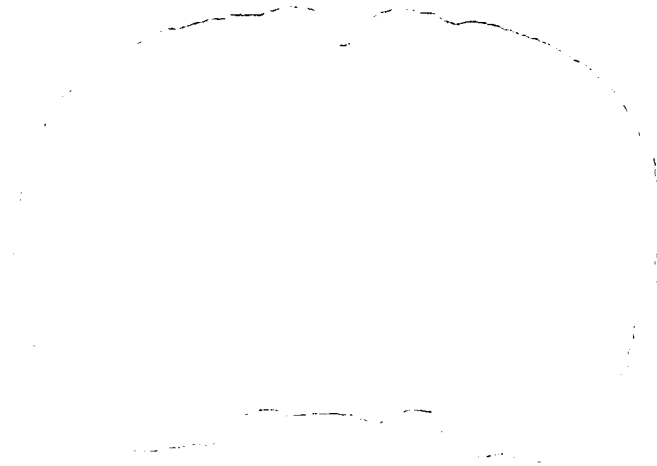
Figure 7 a. On the left is an image acquired by the MegaV-
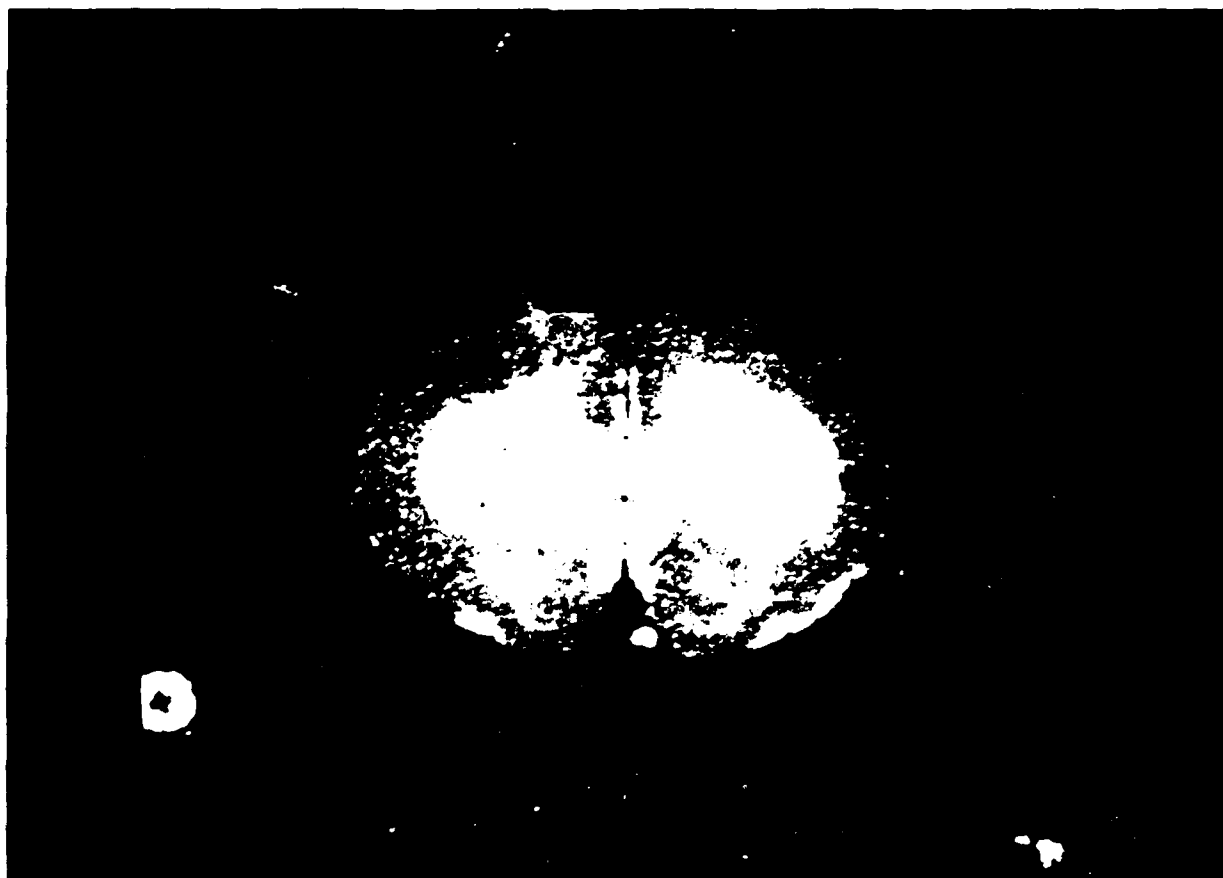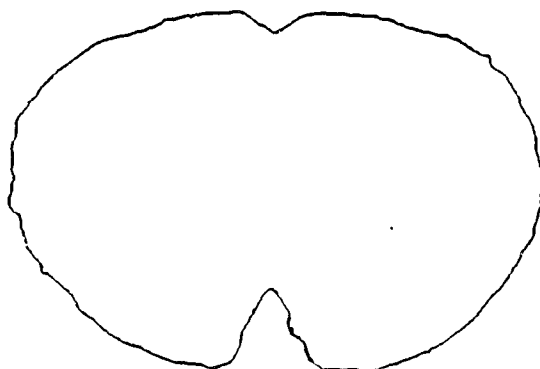ision of a whole human brain horizontal section above the
level of the corpus callosum, stained by the Bielschowsky
method to show myeloarchitecture. On the right is the
result of applying the ROTATING BAR algorithm in a system
library and database package devised by Tarek El Rashidy and
Glen Harding. About four-fifths of the operator's task is
accomplished automatically by the computer. BRAINMATE
software is used, after the stage here illustrated, to
correct errors in surface following by the automatic system.

Figure 7 b. This illustrates how the operator can retrieve
sections previously captured and inspect boundaries that
have been traced by computer to examine them at any desired
scale, with the corresponding original images presented in
the same view. The two images can be simultaneously
scrolled for inspection and for the application of correct-
ing procedures, e.g. by using BRAINMATE. The automatic
boundary detection in this case is preliminary, before use
of CONTOUR FOLLOWER, so the boundaries exhibited are more
primitive than in Figure 7 a. Ordinarily, CONTOUR FOLLOWER
is applied before final operator corrections are undertaken.

Figure 7
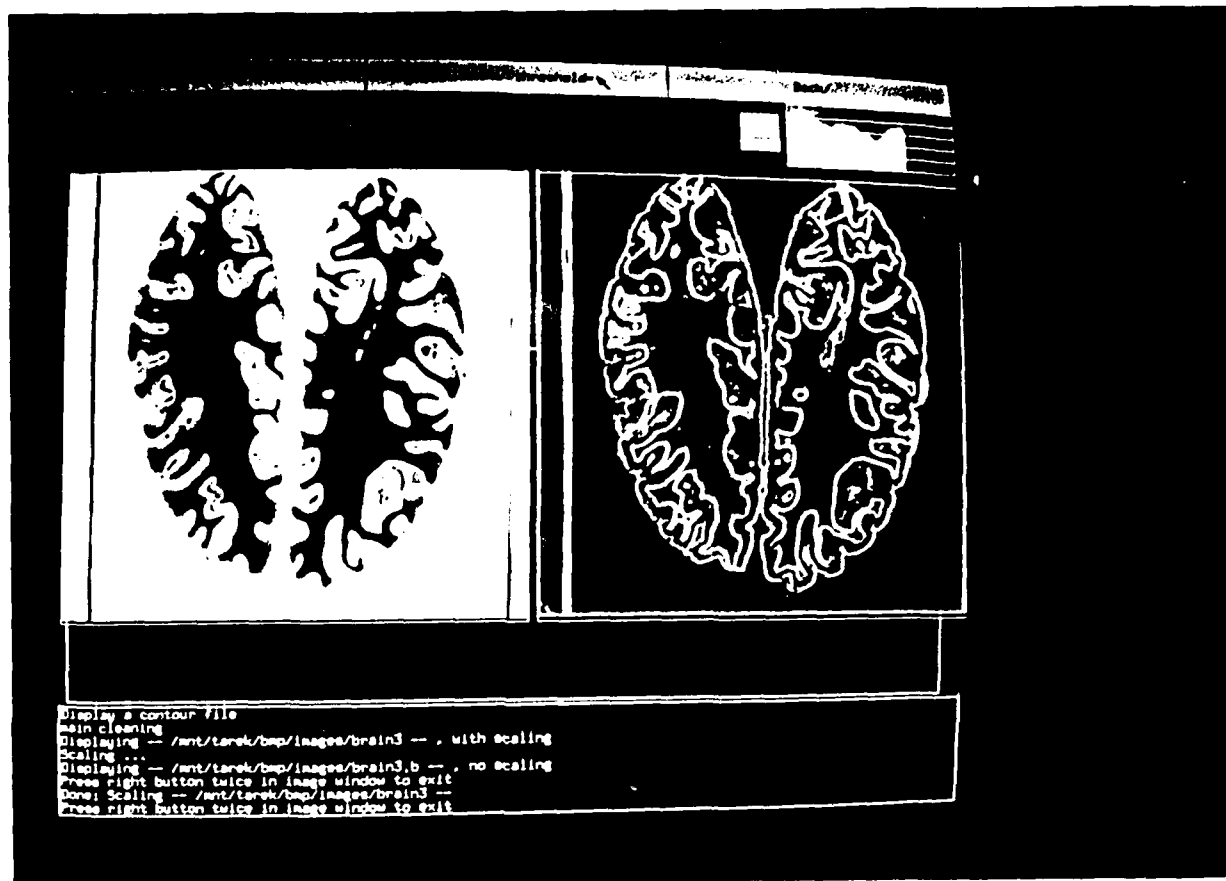
a
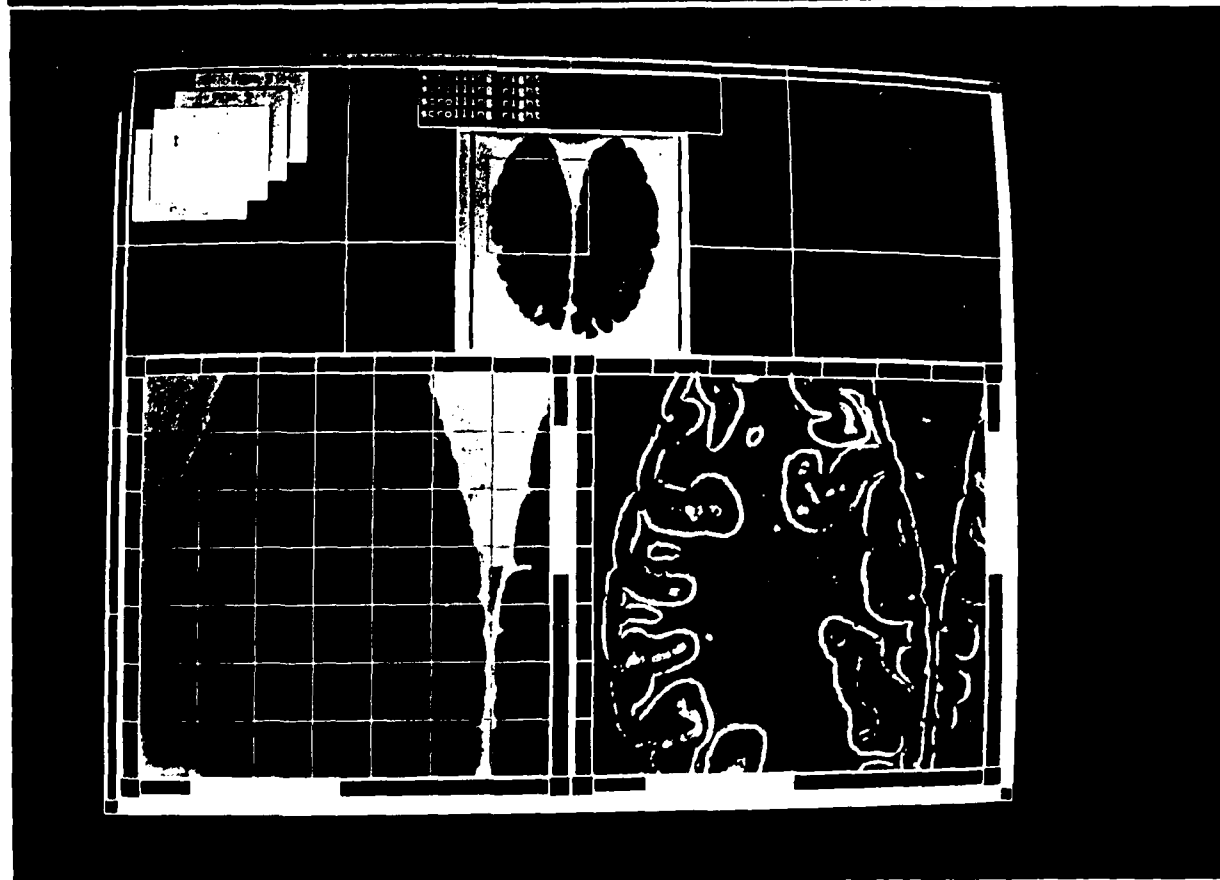
b

Figure 8 a1. Solid surface rendering of whole rat brain sectioned coronally and reconstructed first as a wireframe image which is then subjected to the Reynolds CONTOUR VIEW software to provide a solid surfaced, shaded, reconstruction. This is a direct posterior to anterior view, x = 0, y = 0.

Figure 8 a2. Wireframe view of the same whole rat brain sections in the same perspective, printed with a less than top quality laser printer.
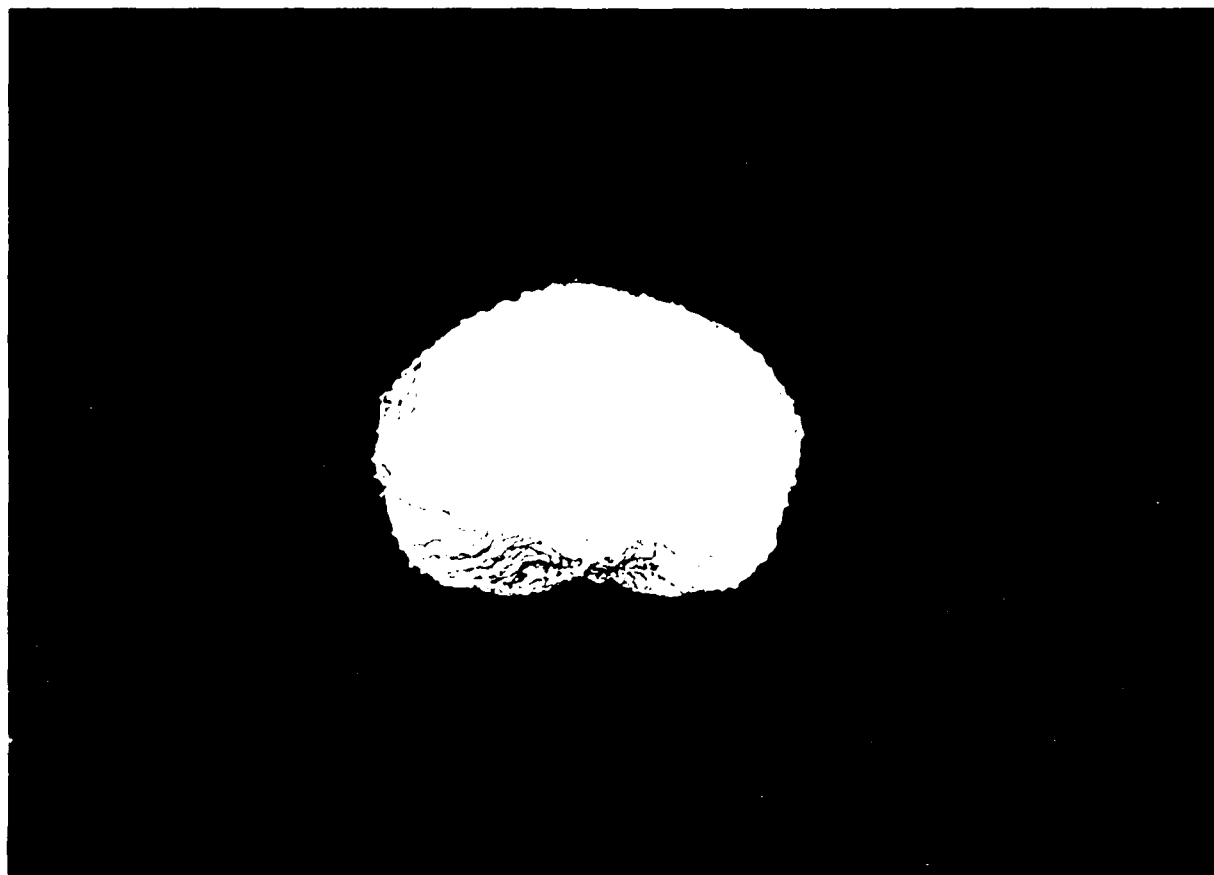
a₁
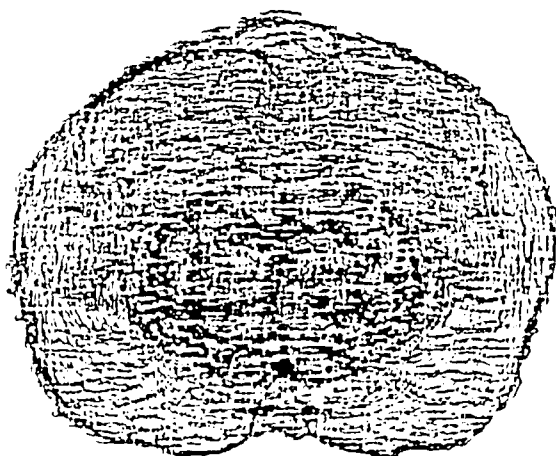
a₂

Figure 8 b1.   Coronal whole rat brain reconstruction as in
Figure 8a, with rotation of both x and y axes to present any
desired angle of view.   The mid-medullary brain stem can be
seen, the cerebellum, the two hemispheres, and in the remote
distance anteriorly, the olfactory bulbs.   x = 35, y = 35.

Figure 8 b2. Wireframe view of the same whole rat brain but
at a slightly different perspective, x = 20, y = 135.   The
same structures can be made out, and the perceptual advan-
tage of solid surface modeling is obvious.

Figure 8b
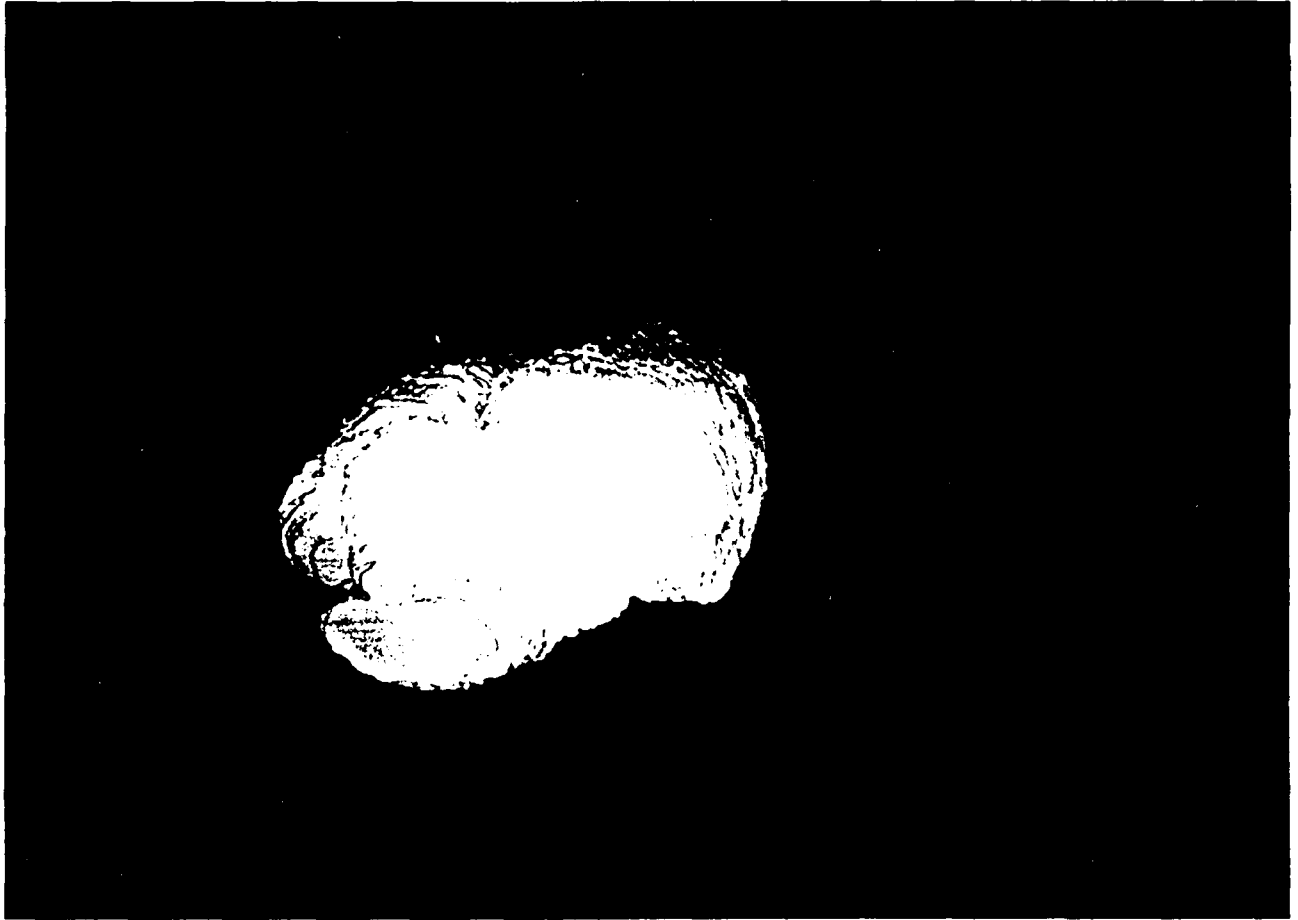
b₁
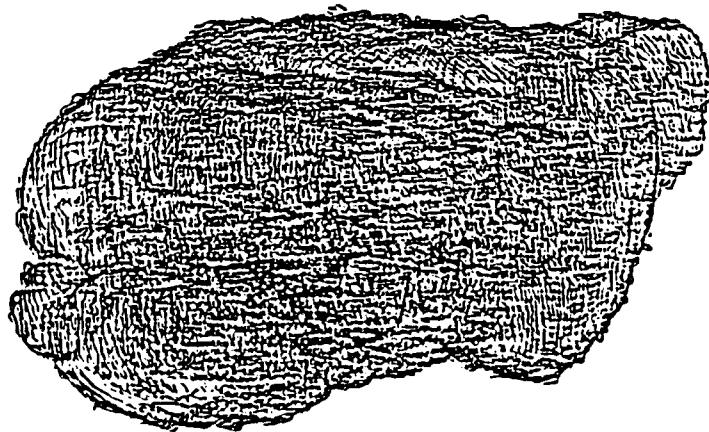
b₂

Figure 8 c1. CONTOUR VIEW representation of the same brain as in 8b, now with x = 40, y = 75. The brain stem, cerebellum, hemispheres and olfactory bulb and tract can be seen to advantage.

Figure 8 c2. Wireframe three dimensional reconstruction of the same brain, but represented in a radically different perspective. The olfactory bulbs are to the left, the brain stem toward the viewer to the lower right. Again, the advantages of CONTOUR VIEW is clear.

Figure 8c
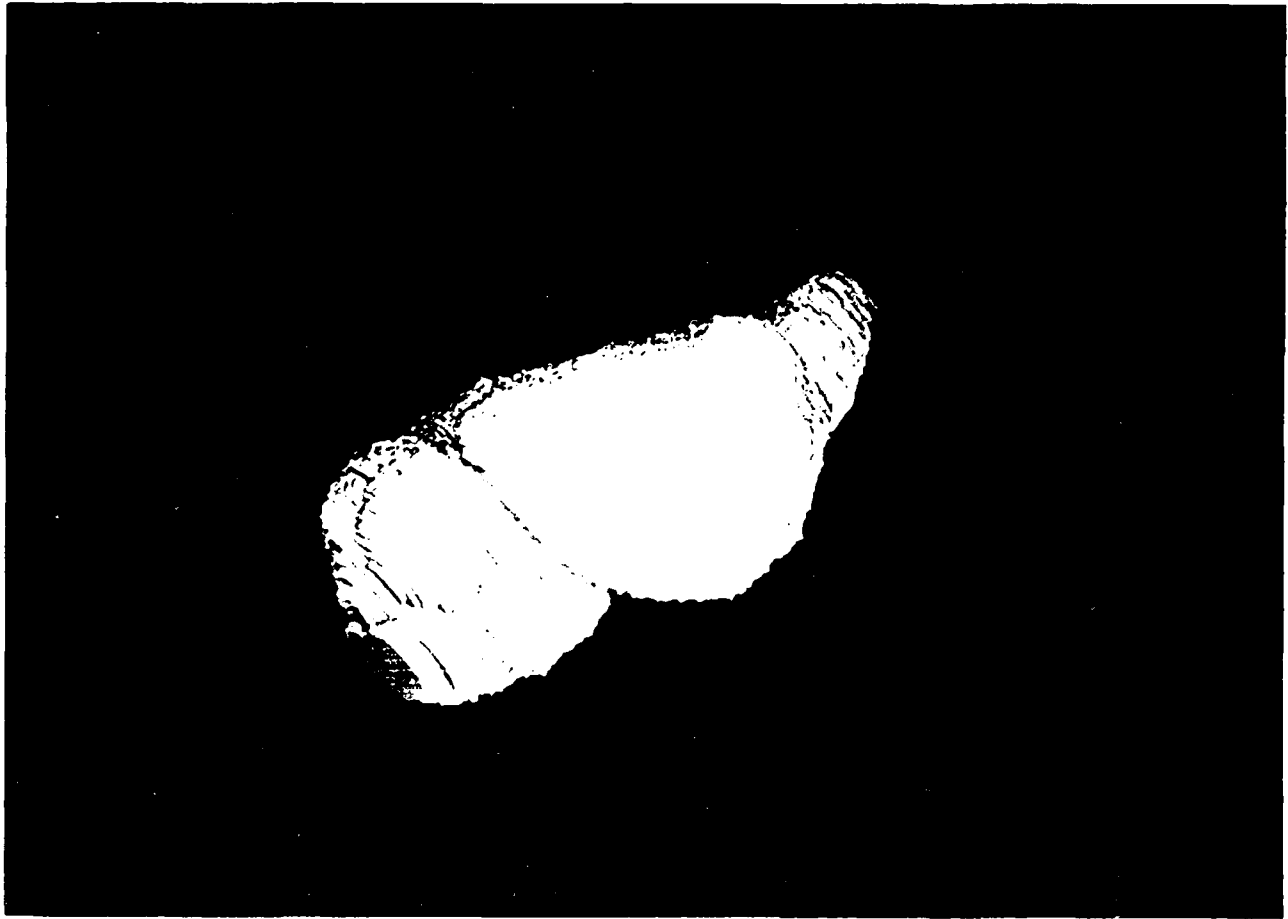
c_1
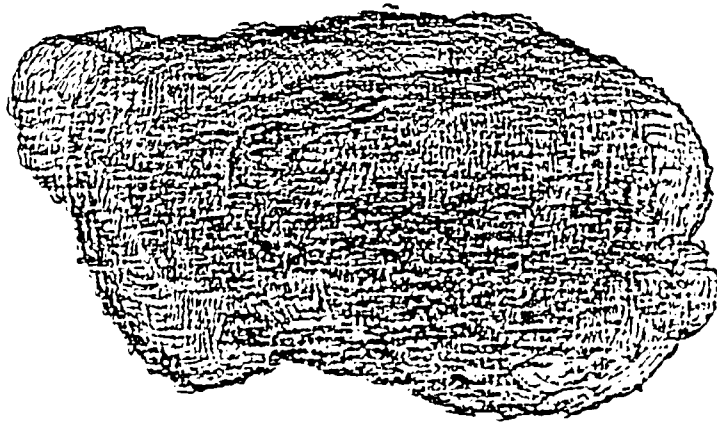
c_2

Figure 9 a. Large-scale reconstruction from whole monkey brain horizontal section, stained for cells. Anterior is toward the top. The cerebral cortex can be plainly seen, including some differentiation e.g., between the more laminar cortex posteriorly and the more granular cortex anteriorly. Moreover, this section illustrates, in the frontal lobe regions of the section, how increasingly tangential planes of cortical transection present increasingly thick appearing cortex, with layers spread out, an illusion because the cortex is simply cut tangentially. Computer reconstruction and tissue texture analysis to differentiate cytoarchitectural regions are presented some difficulty in making comparisons between such differently appearing projections. In principle, it should be possibe for future software to present serial section data at any angle desired, e.g. normal to the cortical surface, for purposes of tralditional cytoarchitectural comparisons. [The computer might do as well three dimensionally without reconstitution in a plane normal to the cortical surface, but, in that case, it should be done for the sake of the operator!] This reconstructed image consists of an array of 11 x 13 individual MegaVision images captured at 2x magnification the CCD camera mounted in the TSI Microscope. The images are acquired at full 525 x 525 pixel value but the composite reconstruction is compressed so that the overall image falls within the 1Mb projection capability of the MegaVision system.

Figure 9b. A lower level whole brain section from the same brain as in Figure 9a. This horizontal section cuts through the corpus callosum, septum, fornix, thalamus, and cerebellum near the midline, and the caudate, putamen, internal capsule, and hippocampus more laterally. This large-scale reconstruction consists of 14 x 17 mosaic elements, reconstituted and presented in drastically compressed format.

82
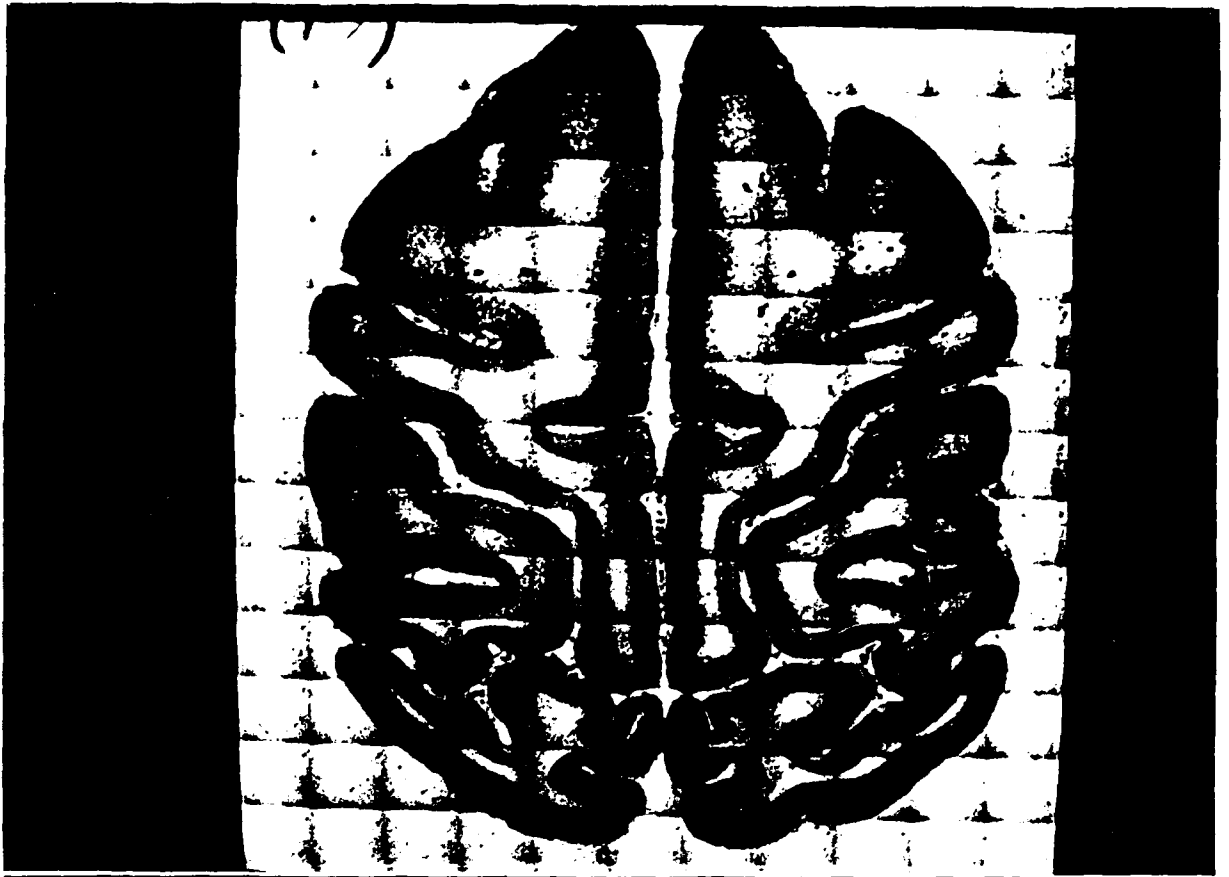
a
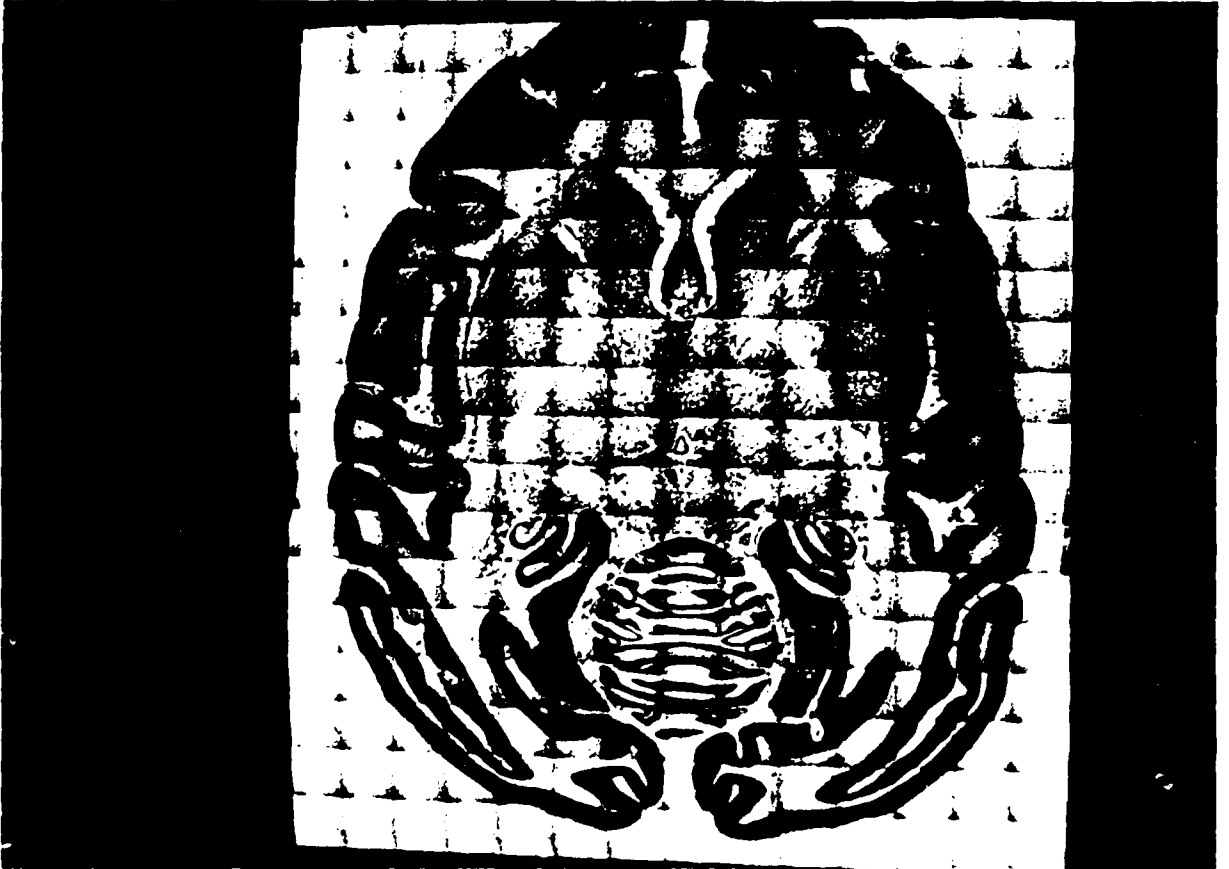
b

Figure 10a. Ten times magnification of a small portion of a whole monkey brain section, stained for fibers. This array consists of 16 x 16 mosaic parts reconstituted into a single, compressed-data image, which is presented in the MegaVision monitor. The section shows beneath a region of the hippocampus the medial part of the temporal pole. Magnification 4x. Coronal section, level 2260.

Figure 10b. Similar magnification of a monkey whole brain section, stained for cells. The 16 x 16 array shows part of hippocampus and temporal lobe further anterior than in Figure 10a. with delineation of cell layers in hippocampus, temporal lobe cortex and part of the amygdala. White matter is obviously pale and has only sparse cell definitions. Magnification 4x. Horizontal section, level 751.

Figure 10c. TSI Microscope mosaic reconstruction from a coronal section stained for fibers, showing the striations caused by fibers streaming across the internal capsule. Coronal section 2260 at 10x magnification. Note that the "postage stamp effect" due to non-uniform illumination of the field in each TSI captured is markedly reduced as magnification increases; the microscope is looking increasingly at the "sweet center" of the optical column.

Figure 10

a
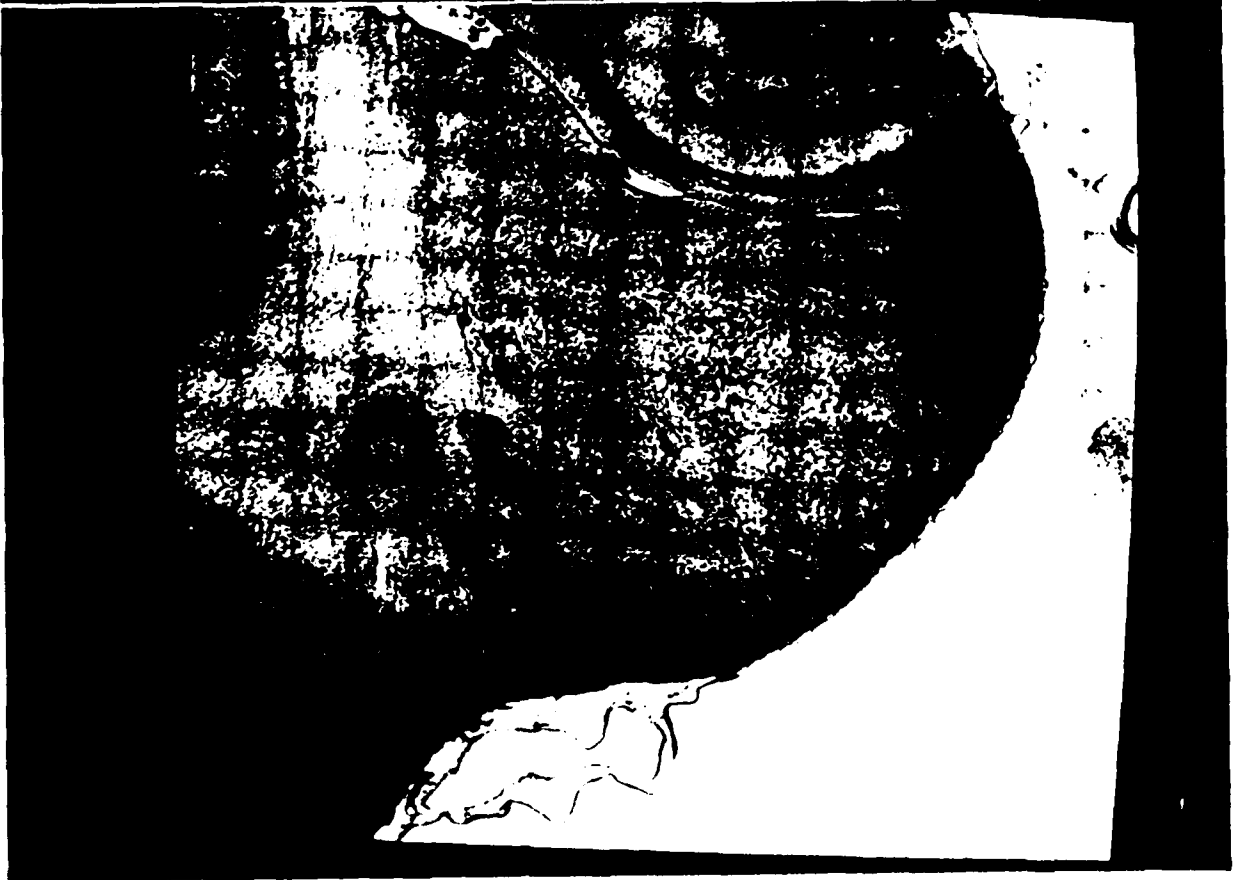
b

Figure 10c
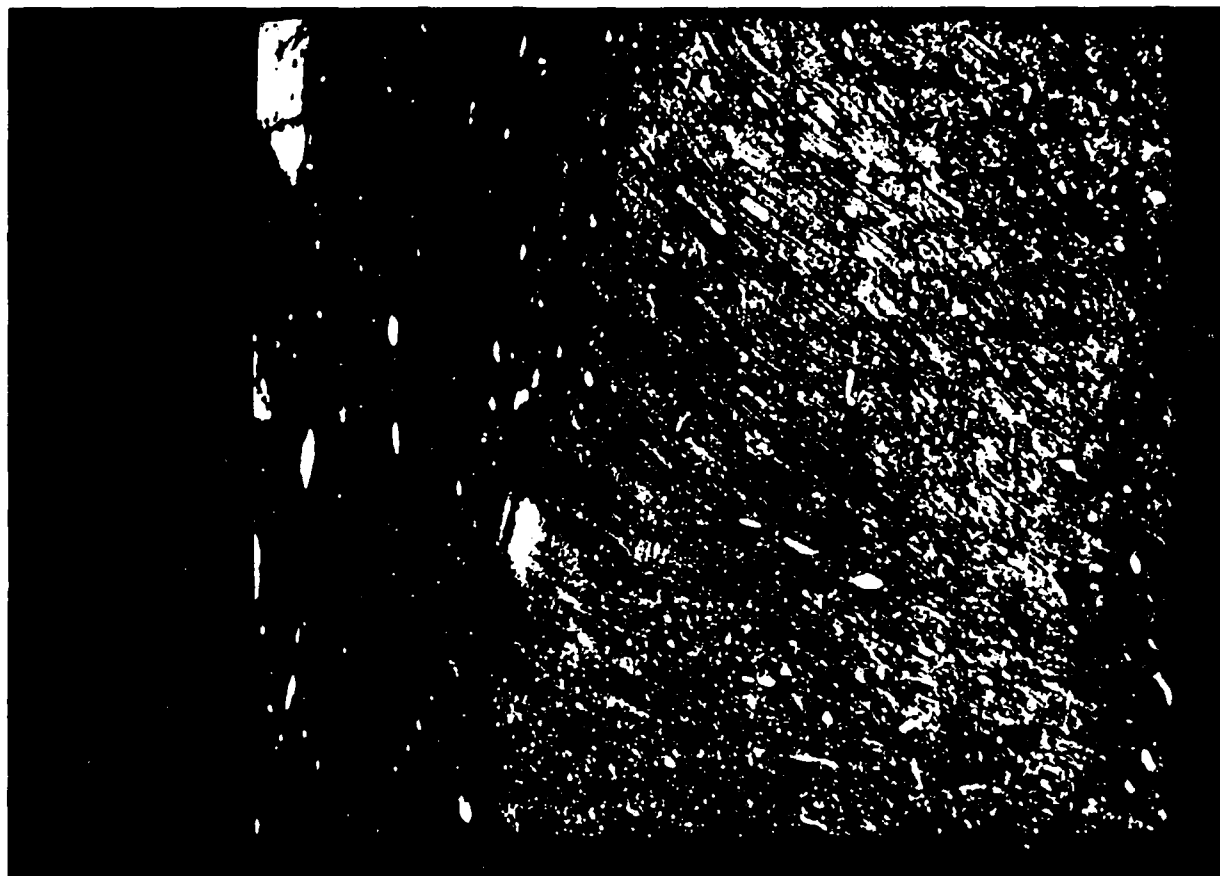
FIGURE 11

Specimen Preparation
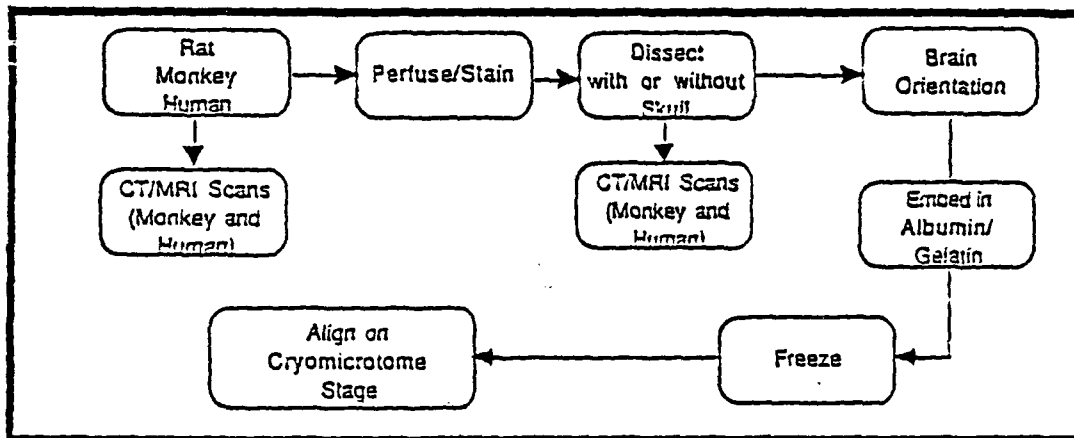
Figure 12

Development of Perfusion Protocols

Rat Perfusion Protocol

Standard Rat Perfusion Followed by Trials of:

Experimental Stain Protocol
Evaluation by Trial Sectioning

Successful Stain Protocol Evaluation
by Microtomy and Image Acquisition

Insufficient
Differentiation
Between Gray
and White Matter

Images w/o Skull
Yielded Best Results—
Used for Software
Interface
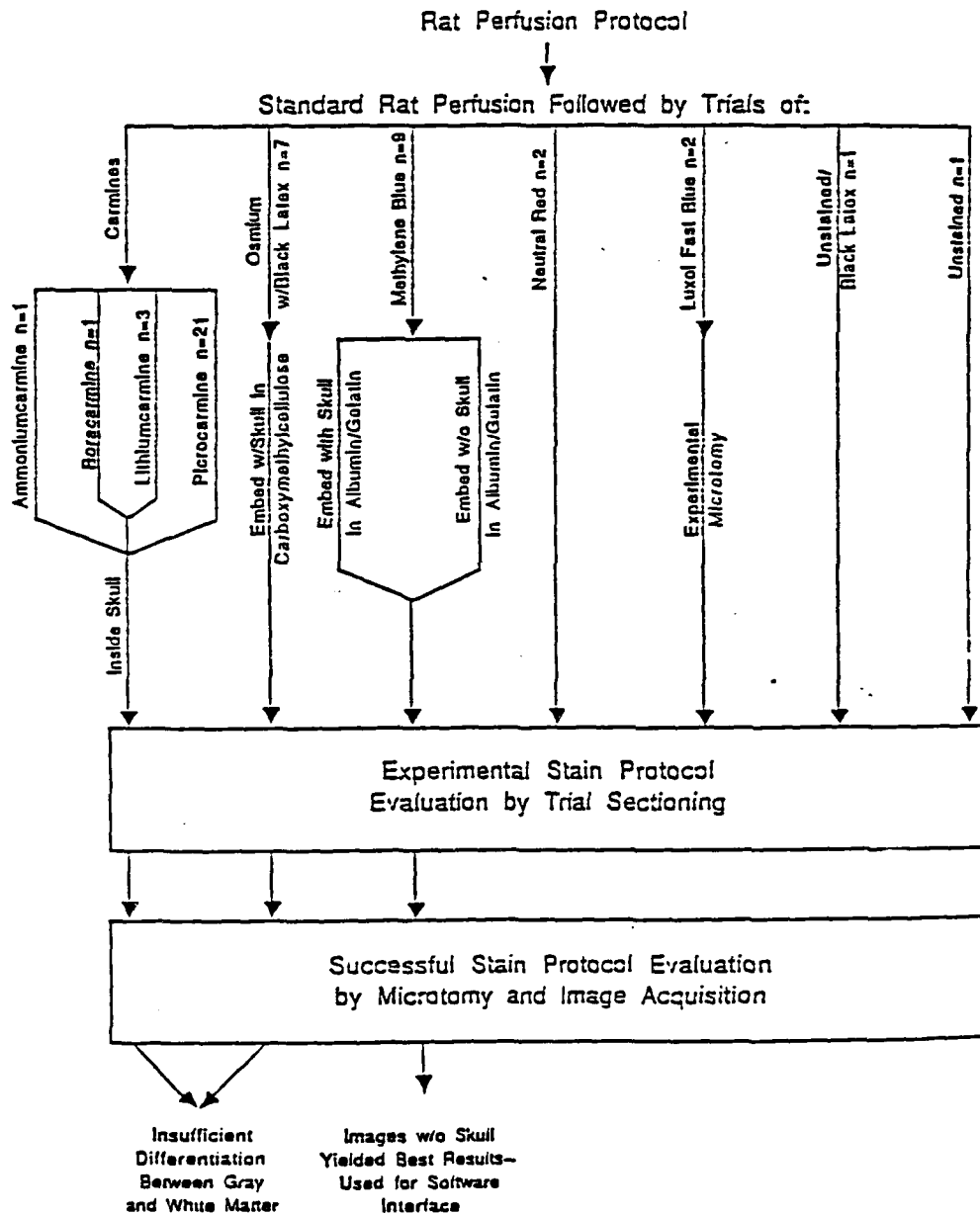
Figure 13. Digital images were captured by the MegaVision 1024 x 1024 camera of part of a series of whole human head MRI scans, used as controls for BMP brain registration from cadaver specimen, roughly coronal sections. The Megavision monitor displays nine images simultaneously in vastly compressed image format for operator scanning purposes. A good deal of detail can be seen even in these reduced images.

Figure 13
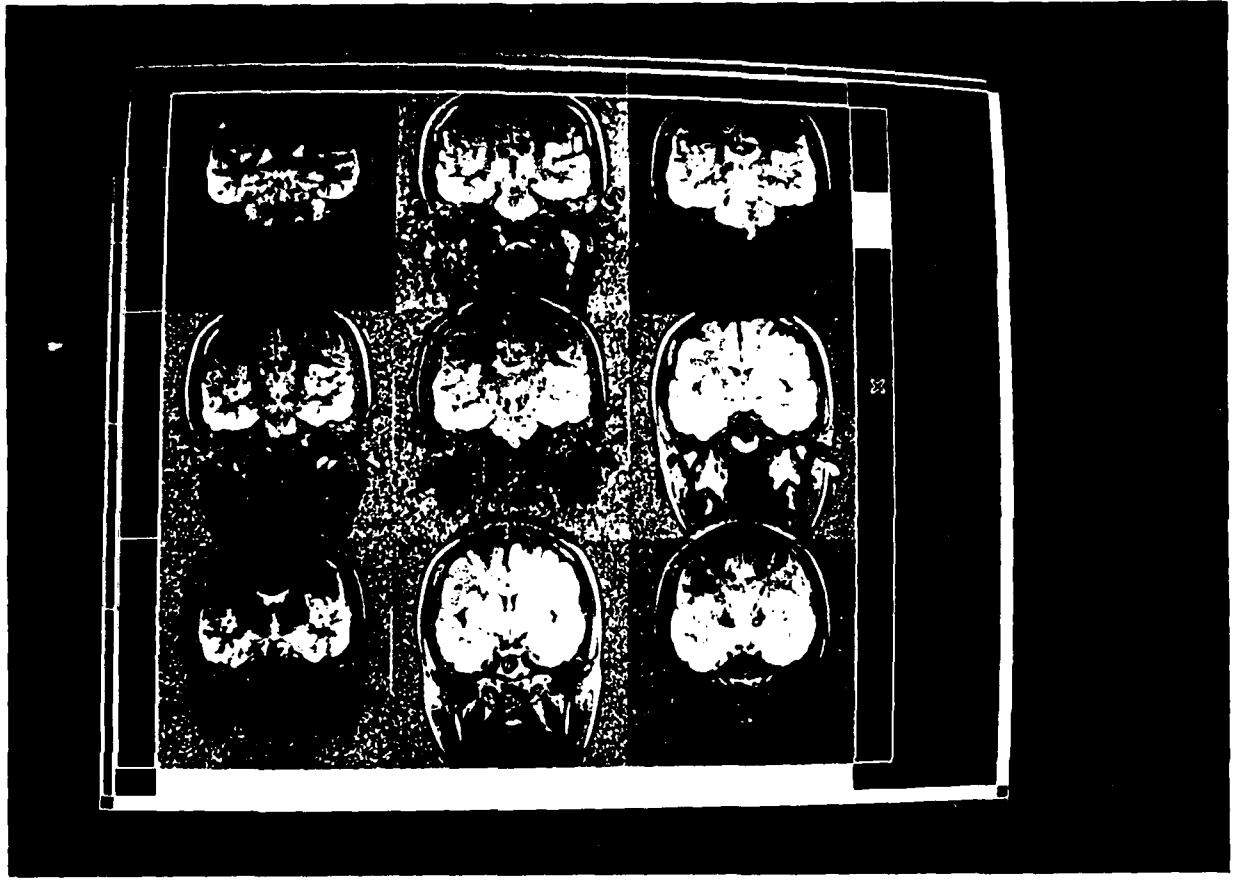
Figure 14 a. Whole monkey brain sagittal section, fiber stained, acquired by the MegaVision camera with transillumation from a lightbox. The objective of this imaging program is to obtain silhouettes of each of three entire whole brain series, cut at right angles along the classic orthogonal planes, stained for fibers and cells in alternate sections, for purposes of approximation of wireframe reconstructions. Since the monkey brains were matched for size and cut in planes at right angles to each other, each outline serves as an accurate dimensional control for outlines in the other planes of section.

Figure 14

a

b

Figure 15   a.   TSI Microscope   reconstruction   of   composite
image   using 15 x 10 individually acquired images.   Parts of
Frontal, Temporal, Parietal and Occipital lobes can be   seen
in this section.   The putamen is prominent, as is the hippo-
campus lying in the floor of the temporal horn   of   the   la-
teral   ventricle.   Part of the hemisphere of the cerebellum
is also seen.   The MegaVision monitor   projection   has   some
distortion   and   the   photograph   of the monitor contributes
further distortion to the image which distortion, along with
the   enormous   data   reduction,   reduces   the quality of the
reproduction.   The individual original mosaic images, howev-
er,   are much less distorted and their composite reconstruc-
tion is quite accurate for purposes of quantitative morphol-
ogy.   The problem comes with our limited means for reproduc-
tion.

Figure 15   b.   TSI Microscope image of   whole   monkey   brain
coronal section image, occipital region.   This shows part of
the midline and lateral cerebellum on both sides   below   the
hemispheres.   The lines of Genari can be easily seen in the
occipital cortex, even in this greatly compressed   reconsti-
tution.

Figure 15

a

b
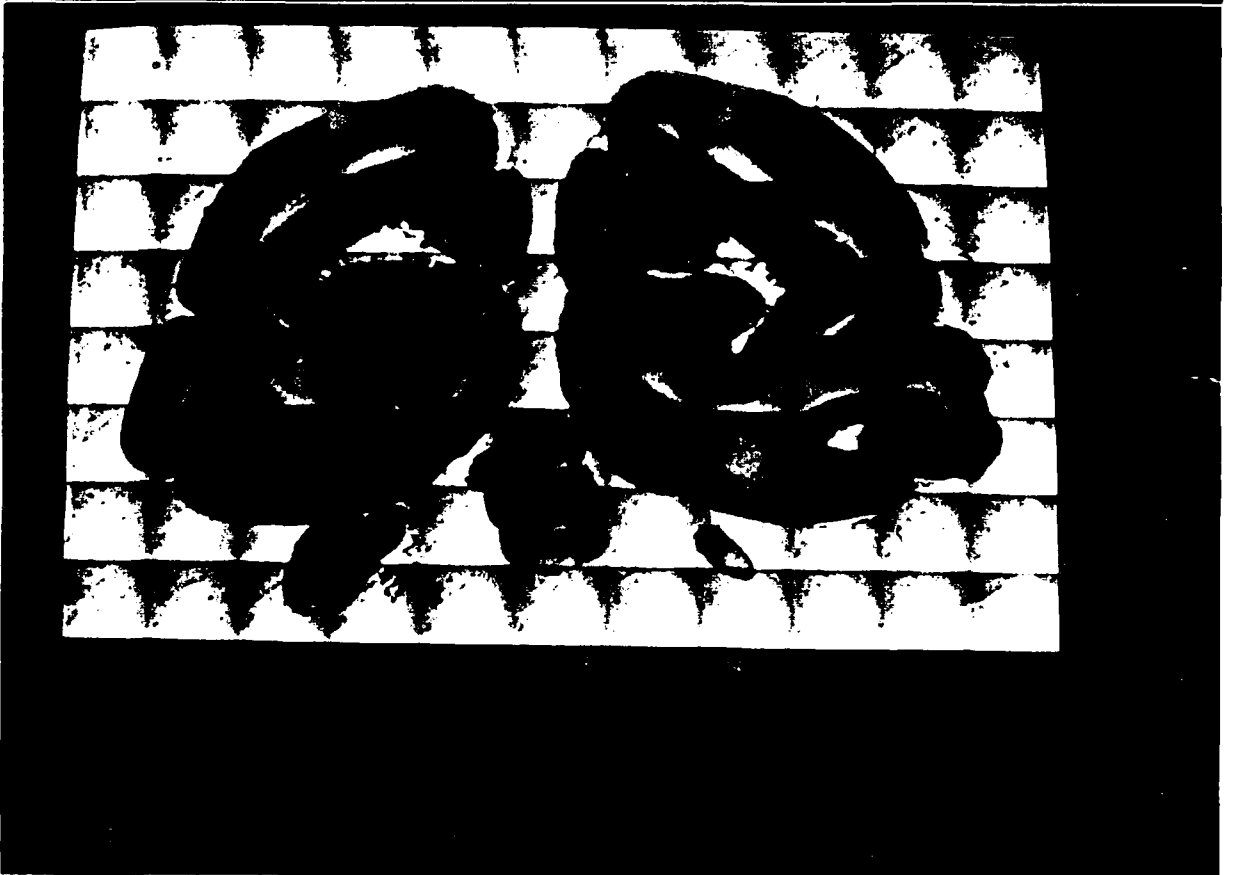
THREE-DIMENSIONAL COMPUTER GRAPHICS BRAIN-MAPPING
PROJECT(U) CALIFORNIA UNIV SAN DIEGO LA JOLLA
R B LIVINGSTON 24 MAR 88 DAMD17-86-C-6093

1/2

F/G 6/4   NL
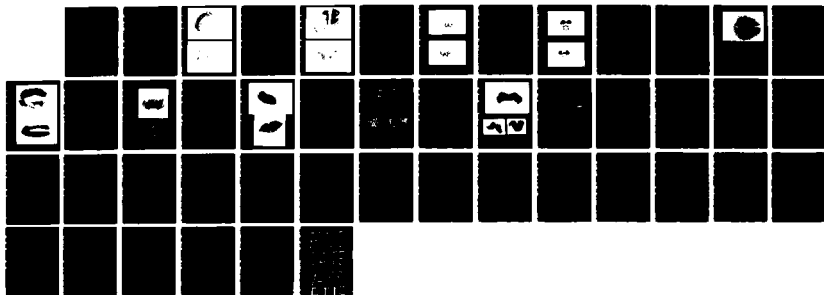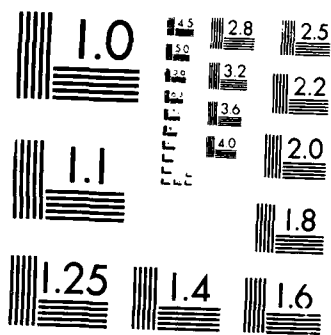
MICROCOPY RESOLUTION TEST CHART

NATIONAL BUREAU OF STANDARDS-1963-A

Figure 16 a. This and Figure 17 illustrate some of the BMP contributions made by Arthur Toga Consultant principally responsible for the reconstruction of whole monkey brains using computer graphics techniques. This image shows the stacking of outlines of successive serial coronal sections, with some of the anterior sections removed to allow a better sense of perspective. This method of stacking contours was used by Toga to provide a framework for the synthesis of the whole brain surface.

Figure 16 b. This illustrates the triangulation algorithm applied to stacked outline sections, in a different projection from 16 a. The triangulation is used to establish the basis for surface rendering. The surface rendering vastly improves the verisimilitude of whole brain reconstructions.

Figure 16
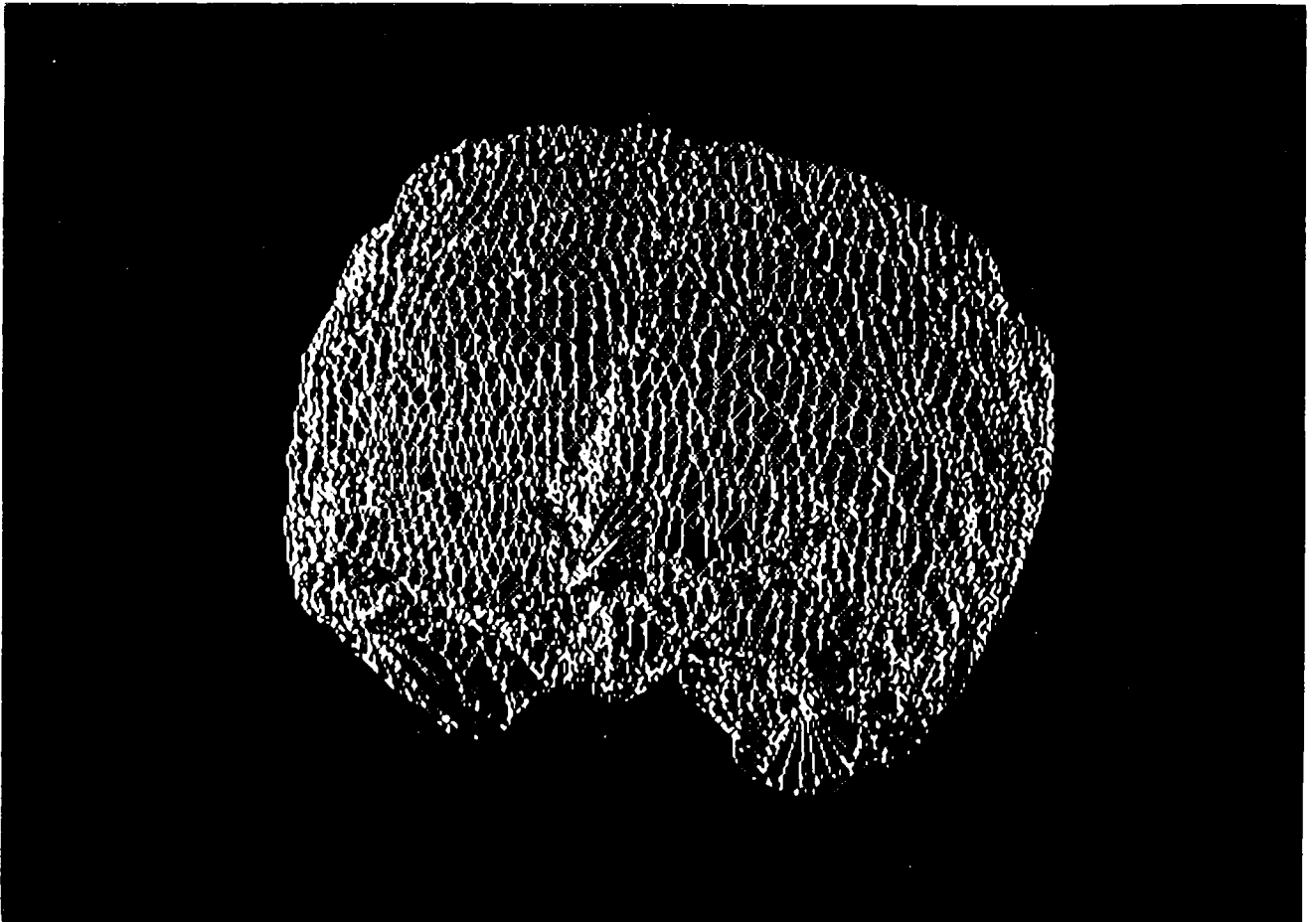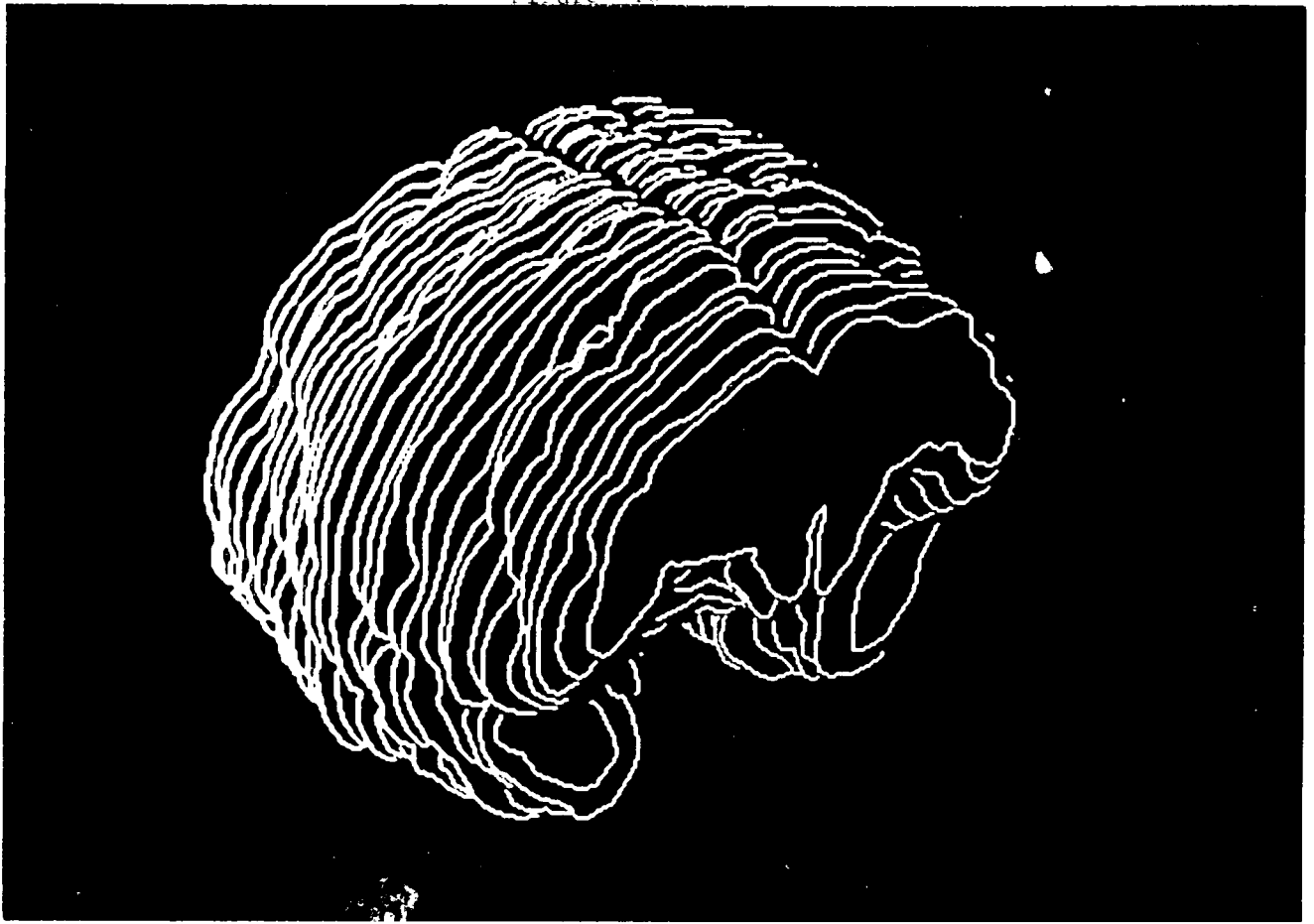
Figure 17 a. This illustrates a completely surfaced, shaded representation of the three dimensional reconstruction of the whole monkey brain. The shading algorithm used includes factors for specular surfacing. Note highlights of the surface, which improve the realistic appearance of the reconstruction. This Figure also shows a round object that is represented on the superior surface of the left hemisphere. This object represent a functional measure of cerebral metabolism.

Figure 17 b. The three dimensionally reconstructed whole monkey brain has been rotated and two arbitrary faces have been reprojected onto the three dimensional reconstructed block. The left hemisphere has a whole section view on which the frontal operculum, Sylvian fissue and part of the temporal lobe appear. This projection allows examination of structures underlying the frontal motor speech area, Broca's area. The coronal plane of section, because it is from the original plane of section, is somewhat more exact. It represents typical frontal white matter and cortex. This is approximately the plane of section for white matter sectioning in the now-discontinued practice of psychosurgery, frontal lobotomy. The middle of the posterior orbital surface of the frontal lobe is the only cortical area of representation of the vagus nerve.

Figure 17

a
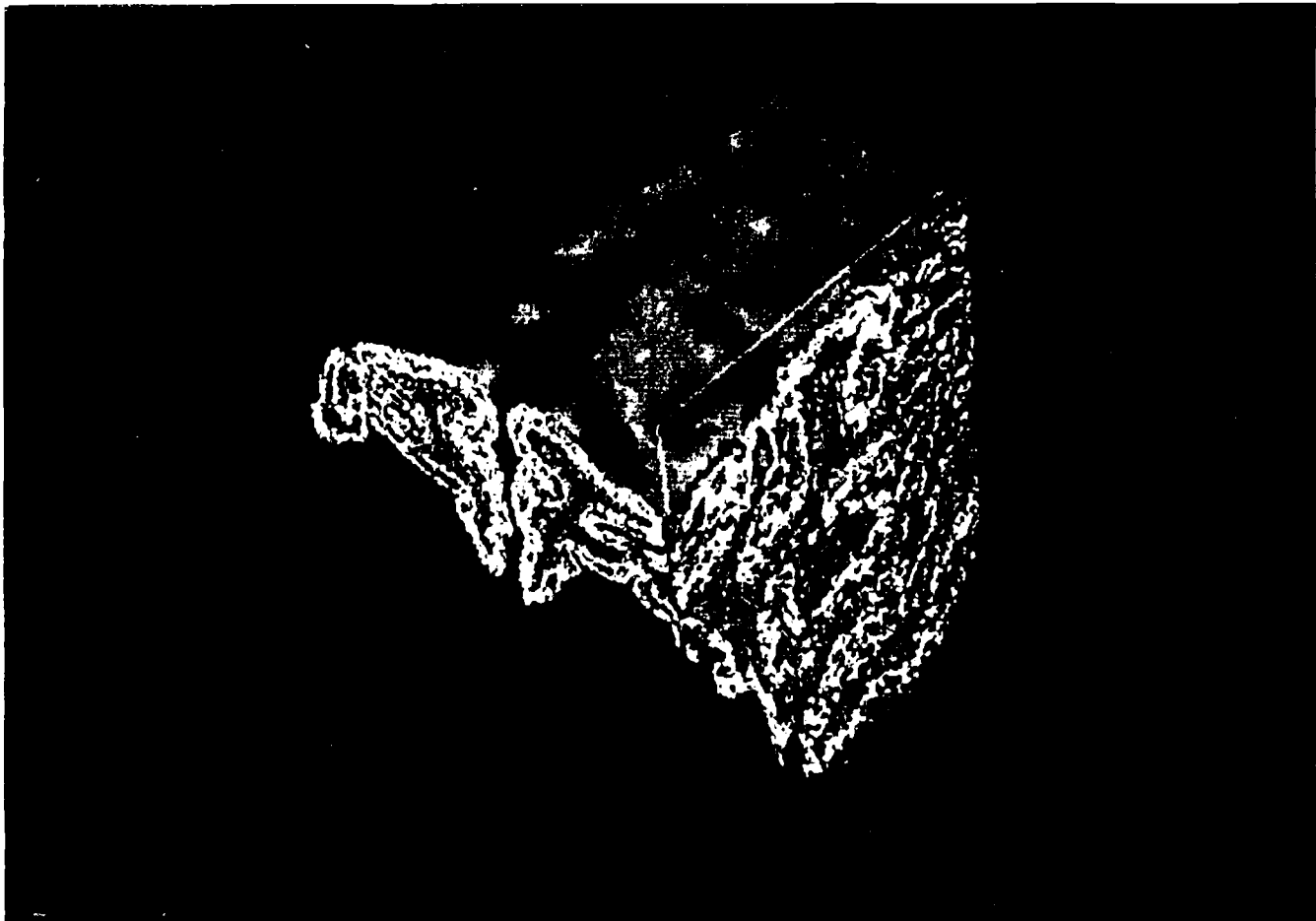
b

Figure 18 a. The images in Figures 18 and 19 come from the
laboratory of Dean Hillman, Consultant principally responsi-
ble for the reconstruction of the whole rat brain.   This
Figure illustrates a wireframe three dimensional reconstruc-
tion of the hemispheres and brain stem of the rat (frontal
projection viewed from slightly above the horizontal axis of
the hemispheres). About 24 sections of the whole brain are
represented in blue outline.   In the same three-space,
orange spheres are projected as a means of identifying all
of the cells marked by monoclonal antibodies for cholineace-
tyltransferase.

Figure 18 b. All cells in the rat whole brain three dimen-
sional projection of the hemispheres and brain stem which
reacted to monoclonal antibodies to chonineacetyltansferase,
are demonstrated by orange spheres. The projection is an
anterior ventral view.

Figure 18
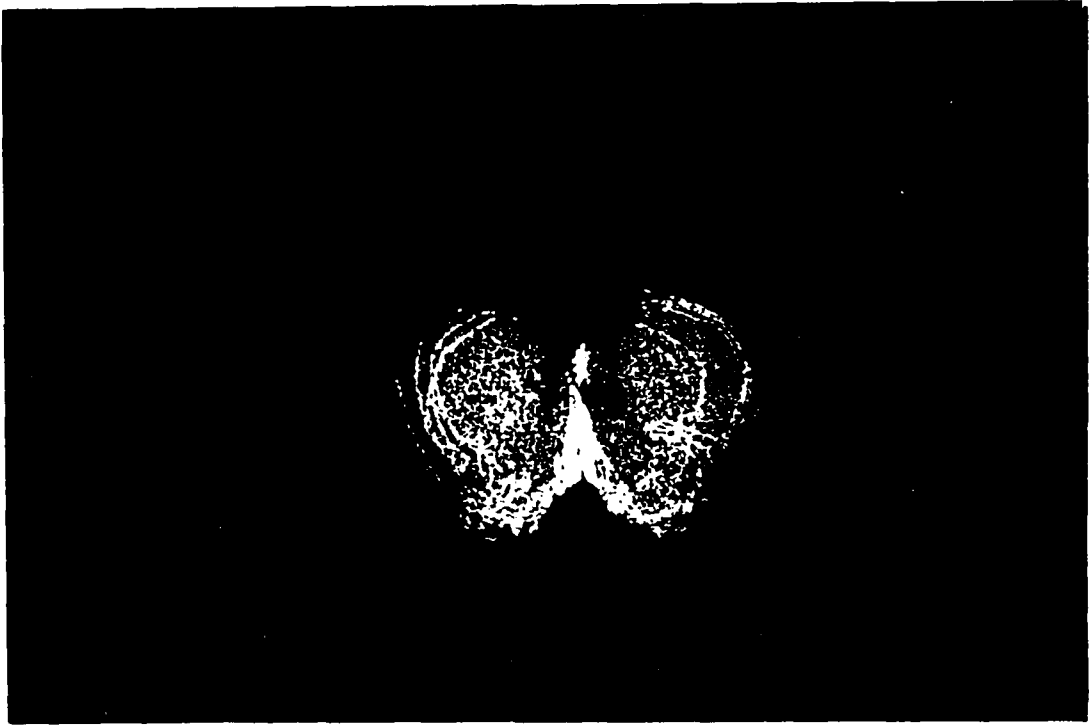
a
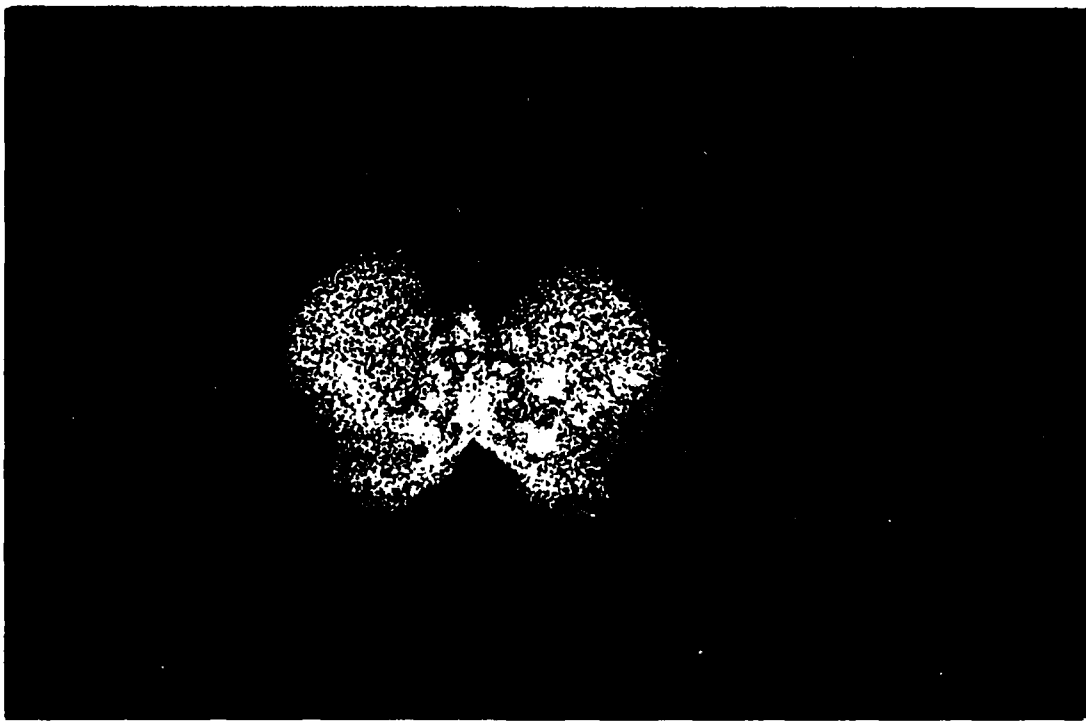
b

Figure 19 a. Wireframe three dimensional reconstruction of rat forebrain, hemispheres and brain stem in a dorsal, some-what posterior view. The hemisphere and brain stem surfaces are represented by blue contours. Within the same three-space, orange spheres (whitened by superposition with blue lines) represent all cells marked by monoclonal antibodies to cholinacetyltransferase.

Figure 19 b. Three dimensional reconstruction of accurate three-space location of all cells in the rat forebrain which reacted to monoclonal antibodies for cholineacetyl-transferase. The view is anterior, tilted slightly "nose up" compared to the posterior "nose down" view seen in Figure 19 a.

Figure 19

a

b

106
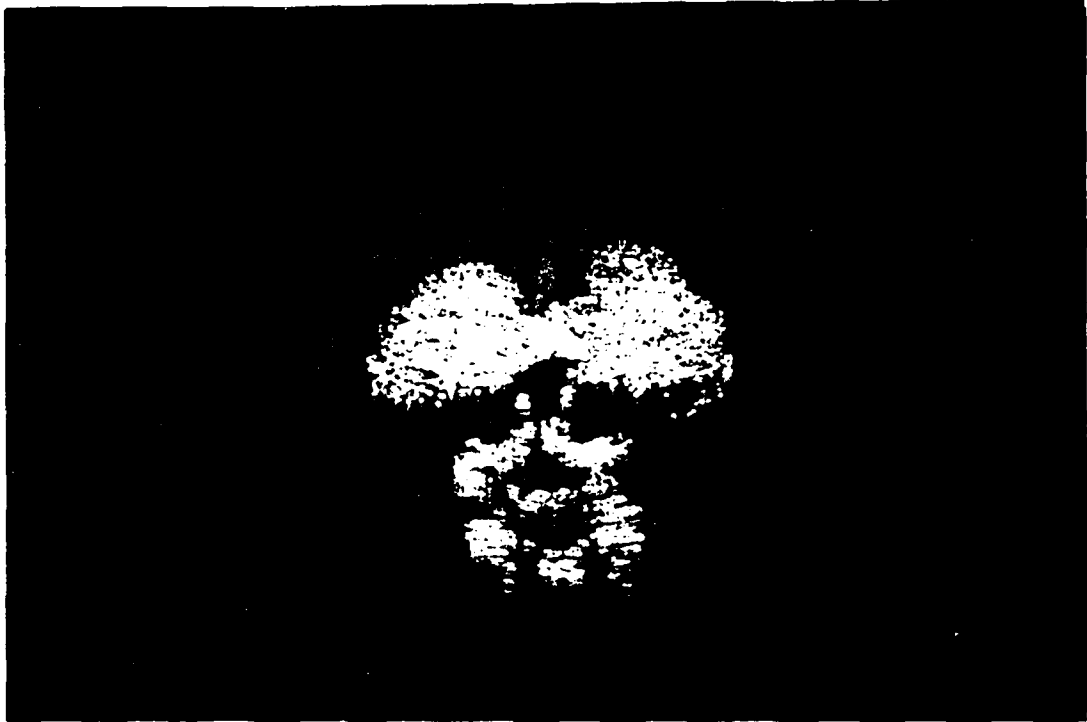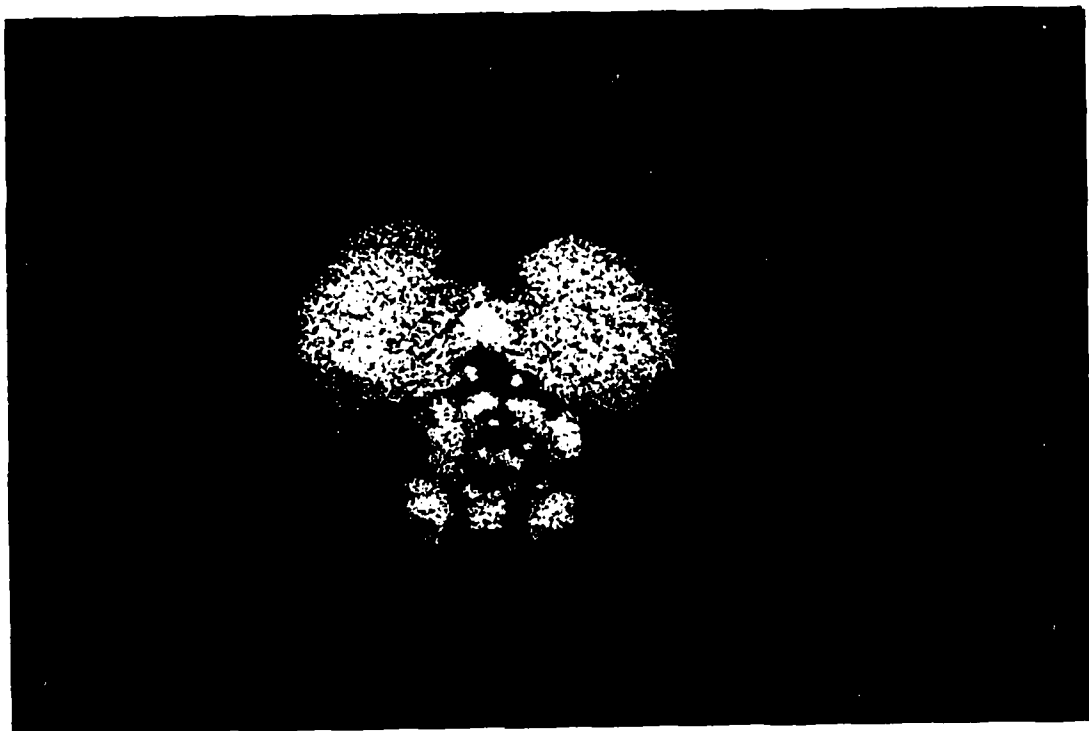
Figure 20

Primate Perfusion Protocol

Monkey

```
┌──────────────┐
│ Anesthetize  │
└──────────────┘
        ↓
┌──────────────┐
│ Insert Canula│
│ into Heart   │
└──────────────┘
        ↓
┌──────────────┐
│ Wash with    │
│ Phosphate    │
│ Buffer       │
└──────────────┘
        ↓
┌──────────────┐
│     Fix      │
└──────────────┘
        ↓
┌──────────────┐
│    Stain     │
│ (1 carmine,  │
│1 methylene blue)│
└──────────────┘
        ↓
┌──────────────┐
│   Remove     │
│    Brain     │
└──────────────┘
        ↓
┌──────────────┐
│  Embed in    │
│Albumin/Gelatin│
└──────────────┘
```

Human

```
                 ┌──────────────┐
                 │ Insert Canula│
                 │ into Arterial│
                 │  System      │
                 └──────────────┘
                         ↓
  6 ♂             ┌──────────────┐
                 │ Wash with    │
  2 ♀             │ Phosphate    │
                 │ Buffer       │
                 └──────────────┘
                         ↓
┌──────────────┐   ┌──────────────┐
│ Stain with   │   │     Fix      │
│ Picrocarmine │   │              │
└──────────────┘   └──────────────┘
        ↓                  ↓
┌──────────────┐   ┌──────────────┐
│     Fix      │   │  Stain with  │
│              │   │ Methylene Blue│
└──────────────┘   └──────────────┘
        ↓                  ↓
┌──────────────┐   ┌──────────────┐
│  Inject with │   │  Inject with │
│  Red Latex   │   │  Red Latex   │
└──────────────┘   └──────────────┘
        ↓                  ↓
┌──────────────┐   ┌──────────────┐
│ Embed within │   │Embed without │
│ Skull in Carboxy-│ │  Skull in    │
│methylcellulose│   │Albumin/Gelatin│
└──────────────┘   └──────────────┘
```

Figure 21 a. CONTOUR VIEW of top sequence of sections, taken at 1.1mm of a whole human brain, top view, anterior to the left. Reconstructions of this kind, detailed by hand digitization, are too labor-intensive to enable much science to be performed. When robust methods are worked out to enable fast, accurate machine reconstructions, it will be possible to make quantitative comparisons between brain and beteen the two hemispheres in the same brain. Asymmetries of this kind appear to be far more common than presently appreciated, where examination has been largely limited to measurements in areas of cerebral representation of language function. $x = 0$, $y = 0$.

Figure 21 b. This is a standard laser printer output for the same contours that were used for solid surface, shaded representation in Figure 21 a. $x = 0$, $y = 0$.

Figure 21
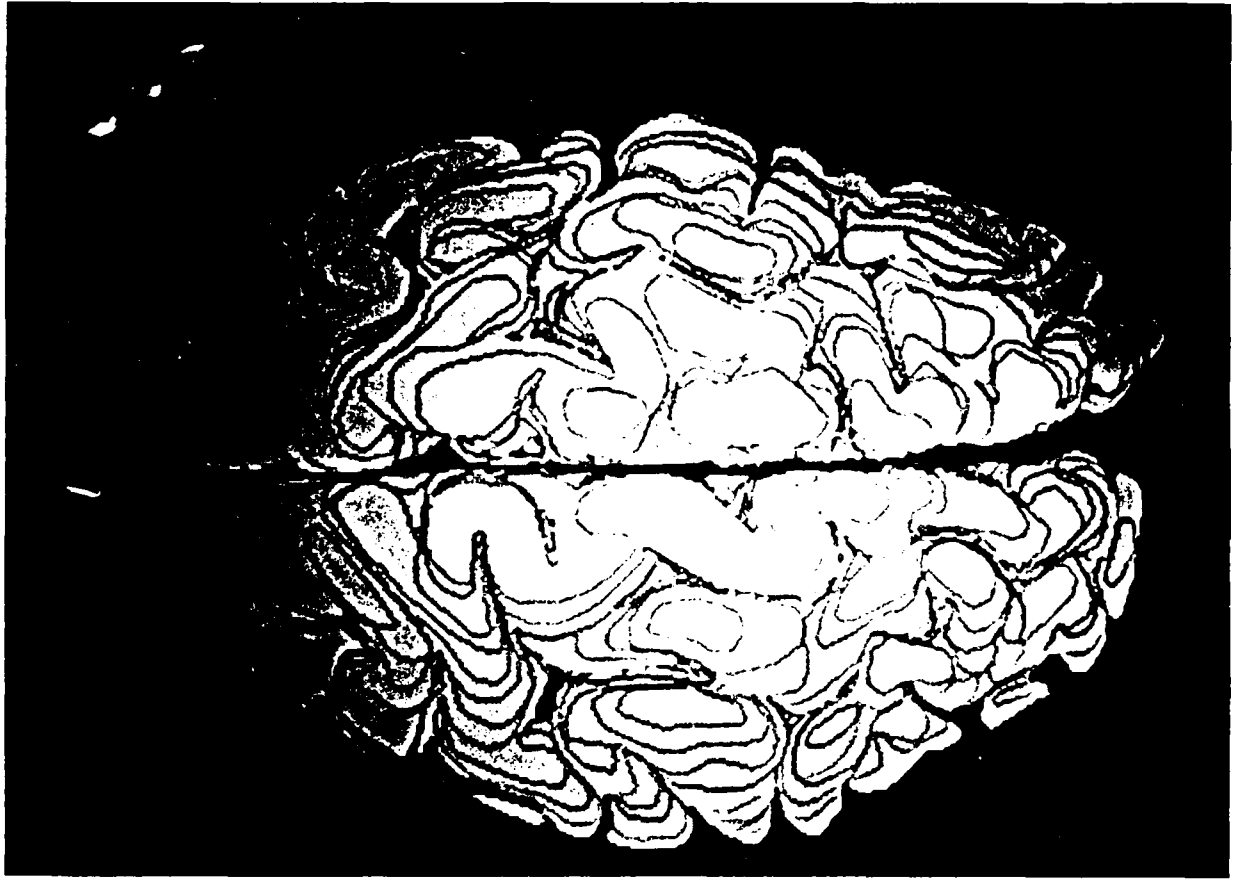
a
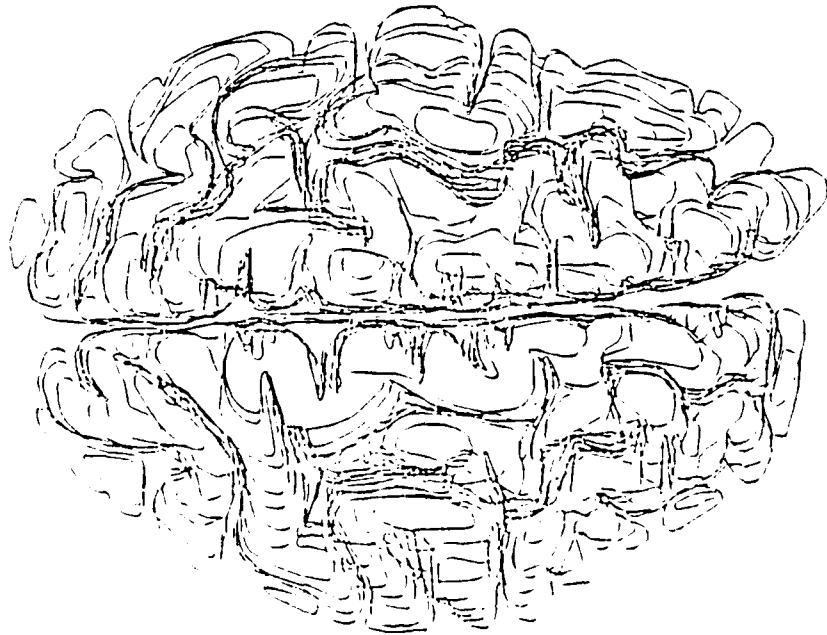
b

Figure 21 c. CONTOUR VIEW of a sequence of the lowermost representations of the cerebral hemispheres, seen from slightly to the left of midline, from below. Note that CONTOUR VIEW has some difficulties in tracing vector contours, made obvious by the straight lines. This difficulty is being corrected by Anthony Reynolds of Phildelphia, from whom we obtained the software. $z = 210$, $y = 0$.

Figure 21 d. Another view of the same data presented in Figure 21 c. The rotated view shows how some contours are effectively represented and how, when the straightline trouble begins, it can be appreciated in a variety of views. $x = 120$, $y = 0$.

Figure 21 (cont.)

c

d

Figure 22 a. CONTOUR VIEW of three dimensionally recon-
structed whole human cerebellum, perspective from x = 0, y =
0.

Figure 22 b. Wireframe three dimensional reconstruction of
the same whole human cerebellum, same perspective.

Figure 22
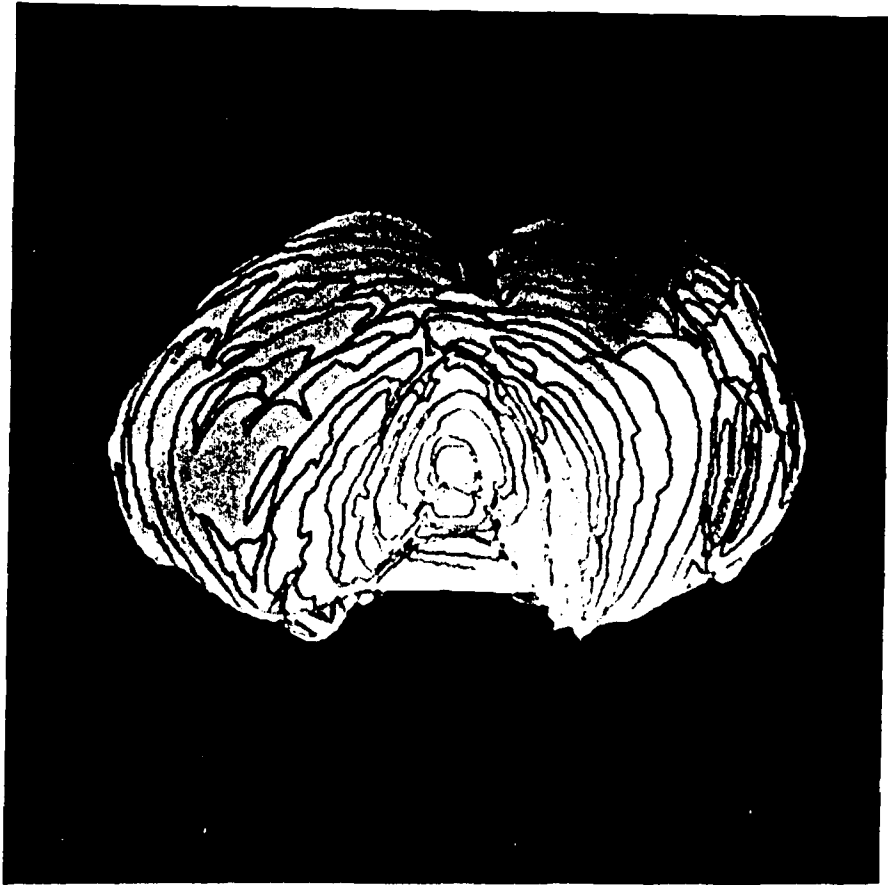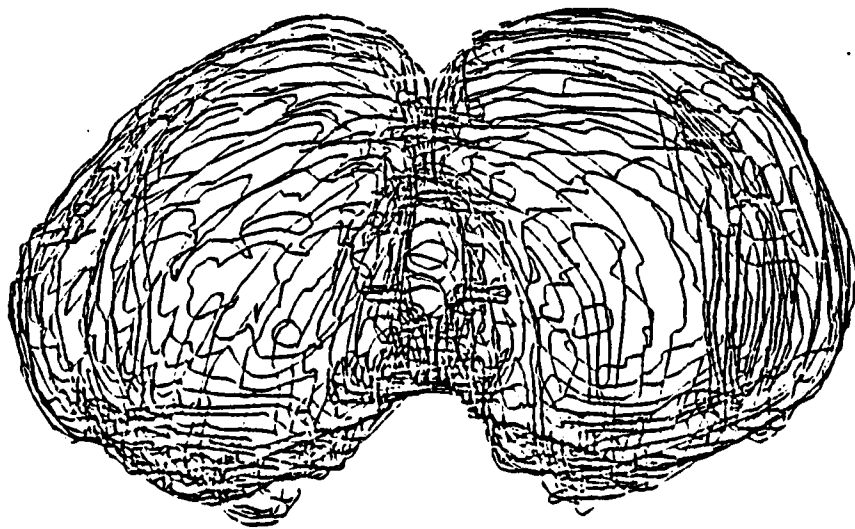
Figure 22 c. CONTOUR VIEW of whole human cerebellum, perspective x = 60, y = 120.

Figure 22 d. CONTOUR VIEW of uppermost sequence of layers of cerebral cortex, perspective x = 180, y = 60.

Figure 22 (cont.)

c

d

Figure 23 a. Wireframe three dimensional reconstruction of whole monkey thalamus, digitized from coronal sections by Xu, Luxi, Associate Professor of Anatomy, Beijing UNiversity School of Medicine, in the BMP laboratory. The midline surfaces of the reproduction do not mismatch, the ambiguity arises from the fact that the third ventricle was slightly curved. The domed surface at the top represents the bulge produced by the anterior nuclear group, limbic relay association nuclei. The inferior "horns" are produced by the lateral geniculate nuclei. Some other features can be made out on closer inspection, even from the wireframe reconstructions.

Figure 23 b. Similar wireframe view of whole monkey brain reconstruction based on horizontal sections, digitized by Xu. The thalamus is almost entirely inverted. The lateral geniculate bodies are seen at the upper right. Left is anterior. Perspective x = 130, y = 135.

Figure 23 c. Wireframe reconstruction from a third monkey, horizontal sections seen from below. A perspective of x = 0, y = 0. Although the thalamus represents only a small percentage of the whole brain, it has systemmatic two-way connections with all parts of the hemispheres and with subcortical structures and with hypothalamus and brain stem, so that it represents a miniature brain. Quantitative morphology of the whole thalamus will provide an excellent test bed for investigation of the whole brain.

Figure 23
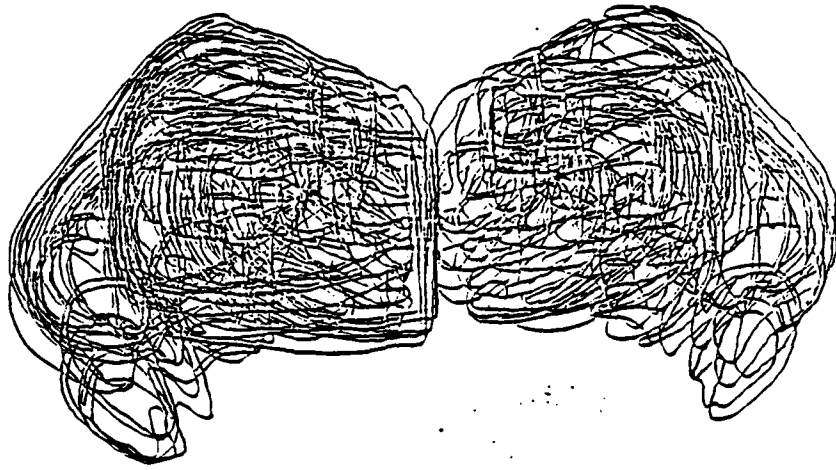
a
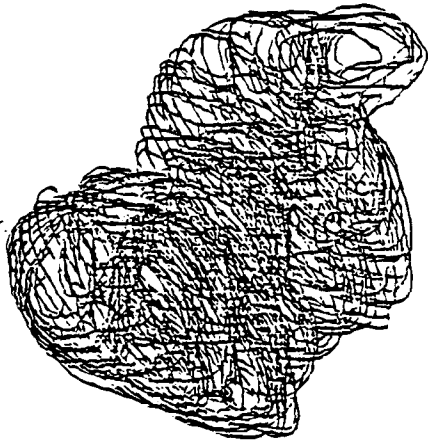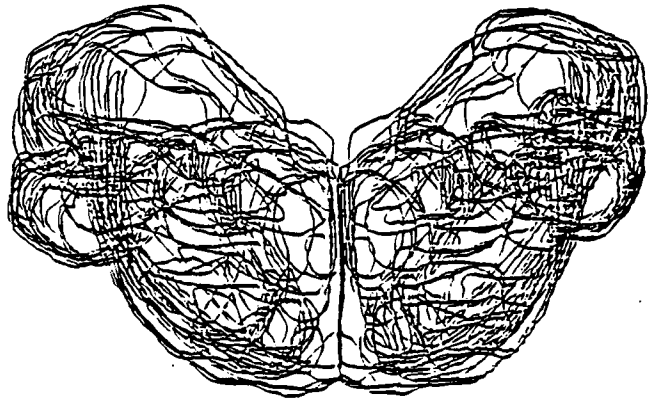
b   c

Figure 24 a. CONTOUR VIEW three dimensional reconstruction of whole monkey thalamus, digitized by Xu, coronal sections, posterior view, x = 0, y = 180.

Figure 24 b. Superior, angulated view of CONTOUR VIEW reconstruction of whole monkey thalamus, digitized by Xu. Perspective x = 200, y = 250.

Figure 24 c. CONTOUR VIEW of whole monkey thalamus seen from below. The lateral geniculate bodies are projected in the direction of the viewer, the right side, nearest, looks correspondingly paler because of the depth shading. Xu digitized 29 clearly identified sub-structures of the monkey thalamus in each of these animals. Programs allow rapid calculations of volume, surface area, centroid, spine, and other features of any given vector displayed structure. Perspective, x = 25, y = 165.

Figure 24

a
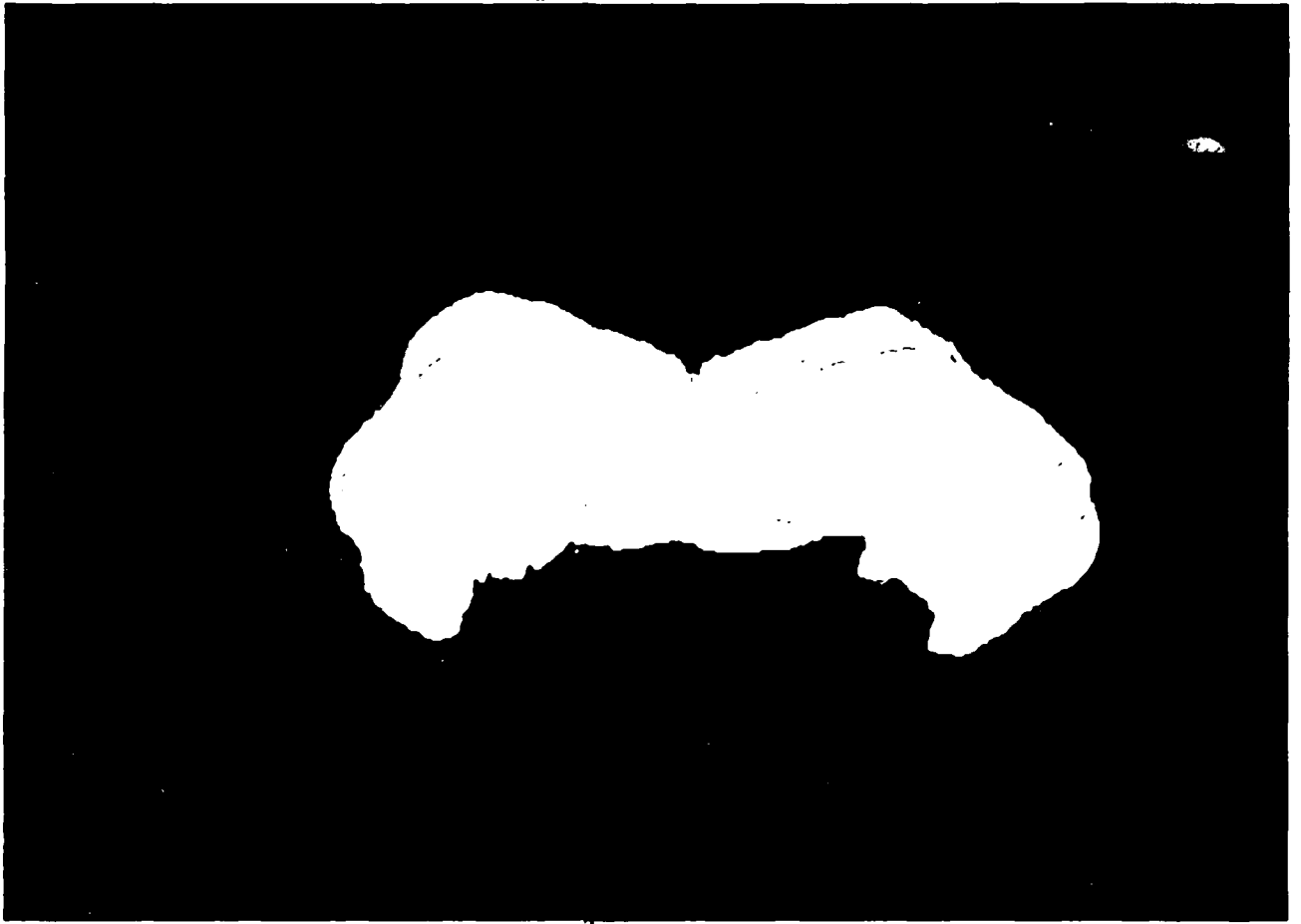
b
c

Figure 25:
Density of nAChR-positive ganglion cells in the chick retina. All numbers should be multiplied by 10 for density at each point. Circle indicates fovea. Scale bar = 1mm
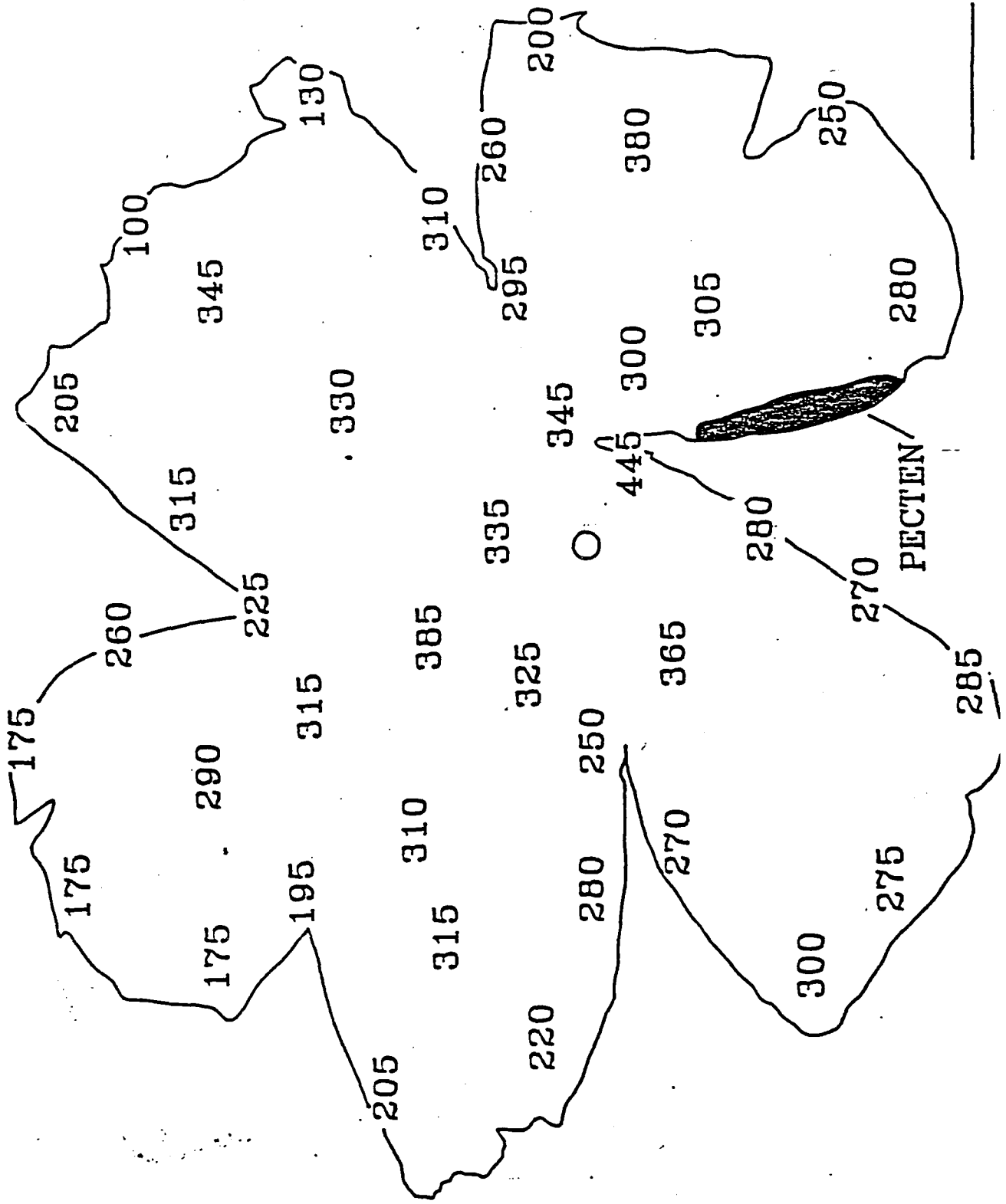
Figure 26:
The distribution of nAChR-positive displaced ganglion cells in the chick retina. Each dot corresponds
to 1 cell. Scale bar = 1mm
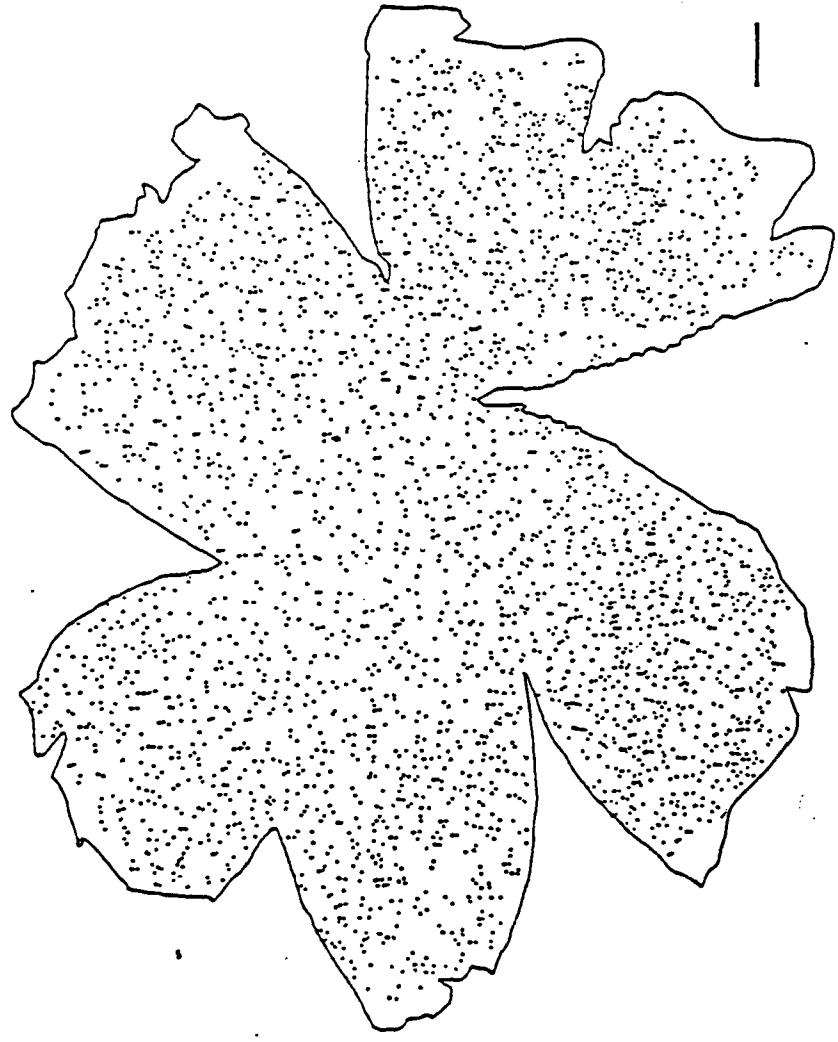
APPENDIX A

Participants in
Task Definition Workshop

David Armstrong	David Koons
Robert Barnhill	Robert Livingston
Floyd Bloom	Bruce McCormick
Charles Bridgeman	Don McEachron
Harry Carter	Ted Melnechuck
Shankar Chatterjee	Charles Molnar
Enrique Chung	John Morrison
Diana Clark	Hossan Mostefair
Wes Clark	Robert Nathan
Richard Colvin	Arthur Olson
Robert De Teresa	Thomas Porter
Jay Fillmore	R. Anthony Reynolds
John Folin	Donald Roberts
Michele Frost	Daniel Schlusselberg
Yuan-Cheng Fung	Wade Smith
Sheldon Furst	Larry Stensaas
Craig Goff	David Talton
Sam Goldwasser	Arthur Toga
Glen Harding	Bud Tribble III
Richard Hegge	John Williams
John Hesselink	Donald J. Woodward
Dean Hillman	Michael Yen
Harvey Karten	Warren Young

Project Volunteers

Gary Berkowitz	James Kapin
Marney Blair	Erika Karagouri
David Chabolla	Donald Knepper
Jessica Chou	John Konstanzer
James Conner	Adar Pelah
Jason Doctor	Smadar Pelah
Deborah Forster	Arthur Shapiro
Carolyn Gennrich	Richard Sharp
Brian Hays	Luann Teschmacher
Margo Hoover	Lawrence Weber

A list has been compiled of the brain objects that were completed from Dr. Stensaas' work in the winter quarter of 1987. The objects were hand contoured from the drawings of brain number 118, the Yakolev collection. Then raw data files were aligned and made into objects.

When naming the structures we found that the program would only accept names of 14 characters or less. This list will help in identifing the structure to its actual name from the raw drawing list.

Brain SP-118 Objects

Actual Object Name	New E&S Version
N. anterioris thalami = Anterior Thalamic Nucleus	antthaln.ob 001
N.anterodorsalis thalami = Anterodorsal Thalamic Nucleus	antdorthl.ob 002
N.dorsalis superficialis thalami = Dorsal Superficial Thalamic Nucleus	dorsupthl.ob 003
N.centralis thalami = Centre Median of Luys	cenmedluy.ob 004
N.commisuralis = Reuniens Nucleus	reuniens.ob 005
N.ventralis oralis = Ventral Oral Thalamic Nucleus	venorthl.ob 006
Ventralis intermedius thalami = Ventral Intermediate Nucleus	venintmed.ob 007
N. paralemniscalis = Paralemniscal Thalamic Nucleus	paralemthl.ob 008
N. parafascicularis = Parafascicular Thalamic Nucleus	parafasthl.ob 009
N.geniculatus lateralis pars magnocellularis = Lateral Geniculate Large Cell Component	latgenlrg.ob 010
N. geniculatus medialis pars magnocellularis = Magnocellular Medial Geniculate Nucleus	magmedgen.ob 011

N. geniculatus medialis =   medgen.ob 012
Medial Geniculate Nucleus

N. dorsalis posterioris thalami =   dorposthl.ob 013
Dorsal Posterior Thalamic Nucleus

Ventralis intermedius thalami =   venintmed2.ob 014
Ventral Intermediate Nucleus

N. dorsalis anterior thalami =   dorantthl.ob 015
Dorsal Anterior Thalamic Nucleus

N. ventralis anterior thalami =   venantthl.ob 016
Ventral Anterior Nucleus

N.medialis thalamic =   medthl.ob 017
Medial Thalamic Nucleus

N. peripeduncularis =   praegenic.ob 018
Praegeniculate Nucleus

N. pulvinaris =   pulvinar.ob 019
Pulvinar Nucleus

N. reticularis principalis =   retthl.ob 020
Reticular Thalamic Nucleus

N. faciculosus =   faciculosus.ob 021
Faciculous Nucleus

N. ventralis posterior internus =   venposint.ob 022
VPI

N. ventralis posterior pars   venposmed.ob 023
medialis =
VPM

N. endymalis =   endymalis.ob 024
Endymalis Nucleus

N. periventricularis(paramedian) =   midlinethl.ob 025
Midline Thalamic Nucleus

N.ventralis posterior thalami pars   venposlat.ob 026
lateralis =
VPL

N. zona incerta =   zonincprn.ob 027
Zona Incerta Principal Nucleus

N. limitans =   supragenic.ob 028
Suprageniculate Nucleus

N. parataenialis =   striamedul.ob 029
Nucleus of Stria Medullaris
(check #039)

N. subhabenularis =   subhabenul.ob 030
Subhabenular Nucleus

N. ventralis oralis thalami pars   venorint.ob 031
internis =
VOI

. N. cucullaris =   censupthl.ob 032
Central Superior Thalamic Nuclei

N. intralamellaris =   intmedlam.ob 033
Internal Medullary Lamina

N. intralamelaris pars compacta =   celgrpiml.ob 034
Large Cell Groups of the Internal
Medullary Lamina

N. habenularis lateralis =   lathabenul.ob 035
Lateral Habenular Nucleus

N. habenularis mixtocellularis =   inthabenul.ob 036
Intermediate Habenular Nucleus

N. habenularis medialis =   medhabenul.ob 037
Medial Habenular Nucleus

N. geniculatus lateralis pars   /#38 not found in archive/
mediocelluaris =
Lateral Geniculate Medium Cell
Layers

N. zona incerta caudalis   caudalzone.ob 040
(submedialis) =
Zona Incerta Caudal Nucleus

041 is used as   fuducial.ob 041
a registration mark

The objects in the table include the amygdala structures.

Brain SP-118 Objects

Actual Object Name	New E&S Version
N.basalis amygdali pars amgnoculularis = Basal Large Cell Amygdaloid Nucleus	baslrgamy.ob 101
N. basalis amygdali = Basal Amygdaloid Nucleus	basamy.ob 102
N. lateralis amygdalii = Lateral Amygdalois Nucleus	latamy.ob 103
N. endopyriformis amygdali = Endopyriform Nucleus	endopyri.ob 104
Cortex periamygdaloidius = Periamygdaloid Cortex	periamycor.ob 112
N. corticalis amygdali (presubiculum) = Cortical Amygdaloid Nucleus	cortamy.ob 113
N. centralis amygdali = Central Amygdaloid Nucleus	cenamygd.ob 133
N. intercalatus amygdali = Intercalate Amygdaloid nucleus	interamygd.ob 134
N.medialis amygdali(prosubiculum) Medial Amygdaloid Nucleus	medamy.ob 117
Periamygolaloid (enter transition area)	tranperamy.ob 179

Cortex prepiriformis posteriorus =   posolfcor.ob 125
Posterior Olfactory Cortex

N. accumbens septi   accumbens.ob 126
Accumbens Nucleus

N. stria terminalis =   strtrmprn.ob 127
Stria Terminalis Principal Nucleus

N. stria terminalis pars pericapsularis =   perstrtr.ob 128
Pericapsular Nucleus of Stria Terminalis

N.stria terminalis pars commisuralis =   commisstri.ob 129
Commisural Nucleus of Stria Terminalis

N. septi medialis pars ventralis =   medseptal.ob 130
Medial Septal Nucleus

N. taenia tecta =   taentecta.ob 131
Taenia Tecta

N. olfactorius anteriorus =   olftrigone.ob 132
Olfactory Trigone

Cortex insularis =   insularcor.ob 135
Insular Cortex
(no match in archive)

N. septic lateralis = Lateral Septal   lateralsep.ob 136
Nucleus

N. commisuralis anterior =   antcommis.ob 137
Anterior Commissure Nucleus

N. septi triangularis =   triseptal.ob 138
Triangualar Septal Nucleus

N. septi dorsalis interna =   dorsalsep.ob 139
Dorsal Septal Nucleus

Basalis pars compacta   basparcom.ob 140
Nucleus of Meynert

terminal vein   terantvn.ob 141
(anterior)

terminal vein   terposvn.ob 142
(posterior)

septal vein   septalvein.ob 143

great emmissary vein   gremmisvn.ob 144

stria terminals	striaterm.ob 145
taenia tecta (anterior)	taentecta.ob 146 131 149
fornix	fornix.ob 147
dorsal medial septal nucleus	dormsepta.ob 147
taenia tecta (posterior)	taentecta.ob 146 131 149
posterior horn of lateral ventricle 150 151 152 lateral surface ventricle III	latvenhorn.ob
subarachnoid space temporal lobe	tempsubara.ob 153
ventricular choriod plexus of posterior horn	vechplexu.ob 154
pineal body (exterior surface) 155 156	pinealbody.ob
subventricular zone of caudate nucleus	subvcaudat.ob 157
ventricular Neuroepithelium	venneuroep.ob 158
no archive extra-ventricular Neuroepithelium	159
no archives Neuroepithelial Peduncle (NeP.VentIV)	160
Globus Pallidus (outer)	glopallid.ob 161 166

The objects in the table are a continuation of the Telecephalic (forebrain) cu's.

Brain SP-118 Objects

Actual Object Name	New E&S Version
N. anterior Comm (posterior)	antecomm.ob 162
Posterior cerebral Artery (posterior temporal)	poscerebar.ob 163
Anterior cerebral Artery (Anterior temporal)	antcerebar.ob 164
Aqueduct of Slyvus(IV Ventricle)	ventrice??.ob 165
Globus Pallidus (inner)	see 161
Nucleus Basalis (medial)	nucbasal.ob 167
Nucleus Basalis (anterior)	nucbasal.ob 168
subarachnoid space (anterior)	antsubarac.ob 169
olfactory tuberole (posterior)	olfatubero.ob 170
claustrum (medial)	see 108 171
subarachnoid space (velum interpostion thalamic?)	velumsubar.ob 172
claustrum (anterior)	see 108 173
N. commisuralis anterior (most anterior)	see 137 174
N. centralis amygdali no match	175
N. intercalatus (anterior-medial)	cenamygd.ob 176/182/134

Anterior Comm   antecomm.ob 177
see 162

Basalis pars compacta   basparcom.ob 178/140
Nucleus of Meynert

cornu ammonic Hippocampus   corammonhi.ob 180

transitional subiculum   transsubic.ob 181

N. intercalatus   cenamygd.ob 182/134/176

subarachnoids   see 190 183
pons & cerebral

middle cerebral artery   midcerebar.ob 184

posterior cerebral   postcereba.ob 185
(anterior)

pituitary posterior   pituitarpo.ob 186

subiculum horn   subiculum.ob 187
(anterior)
114/119

internal carotid artery   intcarotid.ob 188

Basilar Artery   basilarart.ob 189

cerebellum   cerebpons.ob 190/183

posterior pituitary   pituitarpo.ob 191

hippocampal basal   hippobasal.ob 192/153

posterior inferior   picaart.ob 193
cerebellar artery

vertebral artery   vertebrala.ob 194

This list compiles all the hypothalamic cu's from brain 118.

Brain SP-118 Objects

Actual Object Name	New E&S Version
N. infundibularis = Infundibular Nucleus	infundibul.ob 201/216
N. paraventricularis = Paraventricular Nucleus	paraventnu.ob 203
N. prothalamicus principalis = Preoptic Nucleus	preoptic.ob 204/216
N. latrealis hypothalamicus = Lateral Hypothalamic Nucleus	lathypotha.ob 205
N. mammilaris medialis = Medial Mammilary Nucleus	medmammil.ob 206
N. mammilaris lateralis = Lateral Mammilary Nucleus	latmammil.ob 207
N. posterioris hypothalami = Ventral Tegmental Area of Tsai	ventegtsa.ob 208
N. dorsomedialis hypothalami = Dorsomedial Hypothalamic Nucleus	dorhypothl.ob 209
N. supraopticus = Supraoptic Nucleus	supraoptic.ob 210/218
N. tuberis lateralis = Lateral Tuberal Hypothalamic Nucleus	lattubhyp.ob 211
N. tuberomamillaris = Tuberomamillary Nucleus	tuberomam.ob 212
N. ventromedialis hypothalami = Ventromedial Hypothalamic Nucleus	venmedhyp.ob 213
N. parafornicalis = Perifornical Nucleus	periforn.ob 214 (nomatch)
N. ovoideus prothalamicus = Ovoid Preoptic Nucleus	ovoidpreop.ob 215
N. infundibularis = Infundibular Nucleus (nomatch, possibly is #201)	infundibul.ob 216/201

N. prothalamicus principalis -   preoptic.ob 217/124
anterior projection

N. supraopticus -   subraoptic.ob 218/210
Supraoptic Nucleus (lateral)

Mamilothalamic tract   mamiloth.ob 219
no archive

Suboptic neurohemal area   subopneur.ob 220
no archive

N. Suprachiasmaticus   supramatic.ob 221
no archive

This list compiles all the mesencephalic cu's from brain 118.

Brain SP-118 Objects

Actual Object Name	New E&S Version
N. interstitialis Cajal's = Cajal's Nucleus	cajalsnuc.ob 301
N. colliculi inferioris = Inferior Colliculus	infcollic.ob 302
N. colliculi superioris = Superior Colliculus	subcollic.ob 303
N. cuneiformis Cuneiform Nucleus	cuniform.ob 304
N. intracapsularis = Intracapsular Nucleus	intracapsul.ob 305
N. substantia nigra pars compacta = Substantia Nigra	subnigcom.ob 306
N. paranigralis = Paranigral Nucleus	paranigral.ob 307
N. parabrachialis pigmentosus = Parabrachial Pigmented Nucleus	parabrach.ob 308
N. trochlearis = IV Nucleus (no match see 401)	trochlearis.ob 309
N. Edinger-Westphal = Edinger Westphal Nucleus	edingerwes.ob 310
N. oculomotorius caudalis centralis = Caudal Oculomotor Nucleus	caudoclmot.ob 311
N. oculomotorius principalis Oculomotor Nucleus	oculomotor.ob 312
Grisium centrale mesencephali Periaqueductal Gray	peraqdctal.ob 313
no number 314 N. linearus posteralis = Linear Posterior Nucleus	linearpos.ob 315

N. ruber   rednuc.ob 316
Red Nucleus

Griseum centrale mesencephali   dorpraqdct.ob 317
subnucleus dorsalis =
Dorsal Periaquctal Gray

no number 318

N. trigemini mesencephalicus   mesenphal.ob 319
Mesencephalic V Nucleus

N. parabrachialis pigmentosos   parabracme.ob 320
Posterior Medial

N. Edinger-Westphal   edinwespha.ob 321
Anterior Medial

#####.ob 322
######

#####.ob 323
######

#####.ob 324
######

#####.ob 325
######

#####.ob 340
cerebellar hemisphere

This list compiles all the ponscytoarchitectural cu's from
brain 118.

Brain SP-118 Objects

Actual Object Name   New E&S Version

N. trochlearis =   trochlearis.ob 401
Nucleus IV
same object as 309

N. pontis centralis oralis =   ceoralpon.ob 402
Central Oral Pontine Nucleus

N. centralis superior =   censupnuc.ob 403
Central Superior Nucleus

N. dentatus =   dencerebel.ob 404
Dentate Nucleus of Cerbellum

N. globusus   globosenu.ob 405
Globuse Nucleus

N. emboliformis =   embolifnu.ob 406
Emboliformis Nucleus

N. fastigialis =   fastigial.ob 407
Fastigial Nucleus

N. cochlearis dorsalis   dorcochle.ob 408
Dorsal Cochlear Nucleus

N. cochlearis ventralis   vencochle.ob 409
Ventral Cochlear Nucleus
(see if this object is made)

N. locus coerulus   loccoerul.ob 410
Locus Coerulus

no number 411

N. subcoerulus   subcoerul.ob 412
Subcoerulus Nucleus

N.pedunculopontinus tegmenti subnucleus   pedunculpon.ob 413
dissapatus
Pedunculopontine Nucleus

N. facialis =   facial.ob 414
Facial Nucleus

N. interpeduncularis subnucleus dorsalis =   dorintped.ob 415
Dorsal Interpeduncular Nucleus

N. interpeduncularis subnucleus medialis =   medintped.ob 416
Medial Interpeduncular Nucleus

N. lemnisci lateralis   latlemnsc.ob 417
Nucleus of Lateral Lemniscus

N. ovalis   ovalretic.ob 418
Oval Reticular Nucleus

N. parabrachialis lateralis/sagulum =   latparbrch.ob 419
Lateral Parabrachial Nucleus

N. parabrachialis medialis =   medparbrch.ob 420
Medial Parabrachial Nucleus

N. Gudden =   gudden.ob 421
Nucleus of Gudden

N. griseum pontis =   pontinegry.ob 422
Pontine Gray

N. preipositus hypoglossi =   prepositus.ob 423
Prepositus Nucleus

N. interpeduncularis subnucleus lateralis   latintped.ob 424
=
Lateral Interpeduncular Nucleus
(no match)

N. raphe pontis =   raphepont.ob 425
Raphe Pontis

N. raphe dorsalis/supratrochlearis =   raphedors.ob 426
Raphe Dorsalis

N. papillioformis   raphemag.ob 427
Raphe Magnus

N. olivaris superior medialis =   medsupolv.ob 428
Medial Superior Olive

no number 429,430,431

N. tractus spinalis trigemini oralis =   spinalvor.ob 432
Spinal V Oralis

N. trigemini sensibilis principalis   prncsensv.ob 433
Principal Sensory V Nucleus

N. trigemini motorius   motornucv.ob 434
Motor Nucleus V

Griseum centrale pontis =   cenpongry.ob 436 (no 435)
Central Pontine Gray

N. vestibularis superior =   supvestib.ob 437
Superior Vestibular Nucleus

N. vestibularis medialis =   medvestib.ob 438
Medial Vestibular Nucleus

N. vestibularis lateralis =   latvestib.ob 409
Lateral Vestibular Nucleus

N. vestibularis spinalis =   spinvestib.ob 409
Spinal Vestibular Nucleus

N. olivaris superior lateralis   latsupolv.ob 409
Lateral Superior Olive

N. trapezoidalis =   trapezoid.ob 445
Trapezoid Nucleus

N. suprageniculatus =   supragenic.ob 446
Suprageniculate Nucleus

no number 447,448

N. vestibularis subnucleus "Z" =   vestib2.ob 449
Vestibular Nucleus Z

N. corporis pontobublaris   accpongry.ob 450
 Accessory Pontine Gray
the following structures are unclear names

                                          raphedors.ob 451 (see #42
6)   N. raphe dorsalis
        Anterior Dorsal

N. vestibularis interstitialis =   #####.ob 453
Interstitial vestibular nucleus(subnucleus
"rabbit")
no 447 or 542

N. abduscens =   #####.ob 454
Nucleus VI
the following names are all unclear

?????   ##.ob 455
?????

no 456   ##.ob 454
?????

Dentate Nucleus Cerebellum   ##.ob 457
?????

Anterior Ver   ##.ob 458
?????

Post Ver?????   ##.ob 459
?????

Dentate Nucleus Cerebellum   ##.ob 457

This list compiles all the rhombencephalon cu's from brain 118.

Brain SP-118 Objects

Actual Object Name	New E&S Version
N. ambiguus/retroambiguus = Nucleus Ambiguus	ambiguus.ob 501
N. centralis medullai oblongatae = Central Reticular Nucleus of Medulla	cenretmed.ob 502
N. gigantocellularis = Gigantocellular Nucleus	gigantocell.ob 503
N. cuneatus = Cuncate Nucleus	cuneatus.ob 504
N. gracilis = Gracile Nucleus	gracile.ob 504
N. hypoglossi = XII Nucleus	xiinuc.ob 504
N. olviaris inferior principalis = Inferior Olive	infolive.ob 504
N. olivaris inferior accessorius dorsalis = Dorsal Accessory Oli.e	doraccolv.ob 504
N. olivaris inferior accessorius medialis = Medial Accessory Olive	medaccolv.ob 504
N. lateralis medullae oblongatae,subnucleus ventralis = Lateral Ventral Reticular Nucleus of Medulla	lvretmed.ob 504
N. parvocellularis = Parvocellular Reticular Nucleus	parvoretnu.ob 512
N. raphe obscuris = Raphe Obscuris	rapheobscu.ob 514
N. Roller Nucleus of Roller	nuclroller.ob 515

N. supraspinalis =   supraspinal.ob 516
Supraspinal Nucleus

N. tractus spinalis trigemini   gelatinosa.ob 517
caudalis,subnucleus gelatinosus =
Spinal V Gelatinosa

N. tractus spinalis trigemini   magnocellv.ob 518
caudalis,subnucleus magnocellularis
=
Spinal V Magnocellular

N. tractus spinalis trigemini   zonalisv.ob 519
caudalis,subnucleus zonalis =
Spinal V Zonalis

N. tractus spinalis trigemini   interpolis.ob 520
interpolaris =
Spinal V, Interpolaris

no number 521

N. raphe pallidus =   nraphepal.ob 522
Raphe Pallidus

N. cunteatus lateralis =   extcuneate.ob 523
External Cuneate

N. tractus solitarii   solitarnuc.ob 524
Solitary Nucleus

N. dorslais motorus vagi   motdorsalx.ob 525
Dorsal Motor X

Area postrema   postrema.ob 526
Area Postrema

N. centralis medullae oblongatae   cenreimed.ob 527
subnucleus neuromelanosum =
Central Pigmented Reticular Nucleus
of Medulla

no numbers 528-535

Stratum gliosum subepedymale   vengramed.ob 536
medullae oblongatae =
Ventricular Gray of Medulla
not found on list

N. paragigantocellularis   pargigantce.ob 542
Paragigantocellular Nucleus

Ventricle IV   ventricle5.ob
see tele*object 165

N. cunceatus laterlis =   venmedlat.ob 544/545
Ventral Accessory
and ventre-medial accessory

Vertebral Artery   vertebral.ob 546
check #tele*194

APPENDIX C

REFERENCES BASED ON ADVANCEMENTS DEVELOPED
DURING THE PERIOD OF ARMY SUPPORT
OF THE BRAIN MAPPING PROJECT

Armstrong, D.M., Hersh, L.B. and Gage, F.H., Morphologic alterations of cholinergic processes in the neocortex of aged rats, Neurobiol. Aging, [In Press], 1988.

Armstrong, D.M., Terry, R.D., Deterera, R.M., Bruce, G., Hersh, L.B., and Gage, F.H. Response of septal cholinergic neurons to axotomy, J. Comp. Neurol., 264:421-436, 1987.

Britto, L.R.G., Keyser, K.T., Hamasswaki, D.E., and Karten, H.J., Catecholaminergic subpopulation of retinal displaced ganglion cells projects to the accessory optic nucleus in the pigeon (Columba livia). J. Comp Neurol., 269:109-117, 1988.

Buzsaki, G., Bickford, R., Armstrong, D.M., Ponomareff, G., Chen, K.S., Ruiz, R., Thal, L., and Gage, F.H., EEG activity in the neocortex of freely moving young and aged rats, J. Neurosci., [In Press], 1988.

Campbell, M.J., Lewis, D.A., Benoit, R., and Morrison, J.H., Regional heterogeneity in the distribution of somatostatin-28 and somatostatin-28(1-12)-immunoreactive profiles in monkey cortex, J. Neuroscience, 7:1133-1144, 1987.

de Lima, A.D., Bloom, F.E., and Morrison, J.H., Synaptic organization of serotonin-immunoreactive fibers in primary visual cortex of macaque monkey, J. Comp. Neurol., [In Press], 1988.

Ehrlich, D., Keyser, K., and Karten, H.J., Distribution of substance P-like immunoreactive retinal ganglion cells and their pattern of termination in the optic tectum of the chick (Gallus gallus). J. Comp Neurol., 266:220-233, 1987.

Ehrlich, D., Keyser, K., Manthorpe, M., Varon, S., and Karten, H.J., Differential effects of axotomy on substance P-containing and nicotinic acetylcholine receptor-containing retinal ganglion cells: Time course of degeneration and effects of nerve growth factor. Neuroscience. [Submitted] 1988.

Gage, F.H., Armstrong, D.M., Williams, L.R., and Varon, S., Morphological response of axotomized septal neurons to nerve growth factor, J. Comp. Neurol., [In Press], 1988.

Gage, F.H., Chen, S.H., Buzsaki, G., and Armstrong, D.M., Experimental approaches to age-related cognitive impair-

ments, <u>Neurobiol</u>. <u>Aging</u>, [In Press], 1988.

Higgins, G.A., Lewis, D.A., Bahmanyar, S., Goldgaber, D., Gajdusek, D.C., Young, W.G., Morrison, J.H., and Wilson, M.C., Differential regulation of amyloid beta-protein messenger RNA expression within neuronal subpopulations of the hippocampal formation in Alzheimer's Disease, <u>Proc</u>. <u>Natl</u>. <u>Acad</u>. <u>Sci</u>. (<u>USA</u>), 85:1297-1301, 1988.

Keyser, K., Karten, H.J., Katz, B., and Bohn, M.C., Catecholaminergic horizontal and amacrine cells in the ferret retina. <u>J</u>. <u>Neurosci</u>., 7:3996-4004, 1987.

Keyser, K.T., Hughes, T.E., Whiting, P.J., Lindstrom, J.M., and Karten, H.J., Cholinoceptive neurons in the retina of the chick: an immunohistochemical study of the nicotinic acetylcholine receptors. <u>Visual</u> <u>Neuroscience</u>. [In Press], 1988.

Lemere, C.A., Wurtz, C., and Livingston, R.B., Whole-brain mapping: strategies for the construction of "nested" computerized atlases, <u>Neurosci</u>. <u>Abstracts</u>, 13:146.19, 1987.

Lewis, D.A., Campbell, M.J., Terry, R.D., and Morrison, J.H., The laminar and regional distributions of neurofibrillary tangles and neuritic plaques in Alzheimer's Disease: A quantitative study of visual and auditory cortices, <u>J</u>. <u>Neuroscience</u>, 7:1799-1808, 1987.

Lewis, D.A., Higgins, G.A., Young, W.G., Goldgaber, D., Gajdusek, D.C., Wilson, M.C., and Morrison, J.H., The distribution of amyloid beta-protein messenger RNA in human cerebral cortex: Relationship to neurofibrillary tangles and neuritic plaques, <u>Proc</u>. <u>Natl</u>. <u>Acad</u>. <u>Sci</u>. (<u>USA</u>), 85:1691-1695, 1988.

Toga, A.W., and Arnicar, T.L., Digital image reconstruction for the study of brain structure and function, <u>Journal</u> <u>Neurosci</u>. <u>Methods</u>, 20:7-21, 1987.

Toga, A.W., and Arnicar-Sulze, T.L., Three dimensional reconstruction of brain physiology, <u>Innovation</u> <u>et</u> <u>Technologie</u> <u>en</u> <u>Biologie</u> <u>et</u> <u>Medecine</u>, 8(1):92-103, 1986.

Toga, A.W., Arnicar, T.L., and Samaie, M., Three dimensional reconstruction and display of subcortical seizure processes, <u>Neurosci</u>. <u>Abstracts</u>, 12:111, 1986.

Toga, A.W., Samaie, M., Arnicar-Sulze, T.L., and Studt, J.W., Digital rat brain: A computerized stereotaxic atlas, <u>Neurosci</u>. <u>Abstracts</u>, 13:529, 1987.

140

END

DATE

9-88

DTIC